Smjernice za usporedbu i procjenu elemenata motora s unutarnjim izgaranjem u svrhu poboljšanja buke i vibracija

Vizir, Valentina

UNIVERSITY OF ZAGREB
FACULTY OF MECHANICAL ENGINEERING AND NAVAL ARCHITECTURE

MASTER'S THESIS

Valentina Vizir

Zagreb, May 2019

UNIVERSITY OF ZAGREB
FACULTY OF MECHANICAL ENGINEERING AND NAVAL ARCHITECTURE

Guidelines and benchmarking for engine components to achieve high quality NVH performance of the internal combustion engine

Mentor:

Izv. prof. dr. sc. Darko Kozarac, dipl. ing.

Student:

Valentina Vizir

Zagreb, May 2019

Izjavljujem da sam ovaj rad izradila samostalno koristeći znanja stečena tijekom studija i navedenu literaturu.

I hereby declare that I have done this thesis using knowledge and skills gained during my studies and using specified scientific literature.

ACKNOWLEDGES

I would like to offer my special thanks to *MPhil Nikola Naranča* from AVL-AST d.o.o. for providing me with this great opportunity.

I would also like to express my very great appreciation to *Msc Mehdi Mehrgou* from AVL List GmbH for his valuable and constructive suggestions during the development of this thesis.

I am particularly grateful for the advices and assistance given by *mag. ing. mech. Borna Kovarik* from AVL-AST d.o.o. His willingness to give his time so generously has been very much appreciated.

I also thank all my colleagues from AVL-AST d.o.o. and AVL List GmbH for all advices and support.

My deep gratitude goes to my thesis supervisor *izv. prof. dr. sc. Darko Kozarac* for his guidance and all valuable lessons during my studies.

My sincere thanks also go to all my *friends* for the spiritual support during writing this thesis and my life in general.

Finally, last but most important… I am immensely grateful to my *family* for their selfless love and sacrifice; and to my *boyfriend* for always being there for me.

Thank you so much!

"…od vsega srca fala!"

Valentina Vizir

SVEUČILIŠTE U ZAGREBU
FAKULTET STROJARSTVA I BRODOGRADNJE
Središnje povjerenstvo za završne i diplomske ispite
Povjerenstvo za diplomske ispite studija strojarstva za smjerove:
procesno-energetski, konstrukcijski, brodostrojarski i inženjersko modeliranje i računalne simulacije

Sveučilište u Zagrebu Fakultet strojarstva i brodogradnje	
Datum	Prilog
Klasa:	
Ur. broj:	

DIPLOMSKI ZADATAK

Student: **Valentina Vizir** Mat. br.: 0035195074

Naslov rada na hrvatskom jeziku: **Smjernice za usporedbu i procjenu elemenata motora s unutarnjim izgaranjem u svrhu poboljšanja buke i vibracija**

Naslov rada na engleskom jeziku: **Guidelines and benchmarking of the internal combustion engine components for enhancement of NVH performance**

Opis zadatka:

Design and production of the NVH effective engines requires significant effort in the development process. The engineering work required to achieve acceptable NVH performance starts already at the early stage of design and engine development. Vibration and noise radiation from the particular engine components need to be reduced at the early stage of development even if some uncertainness or non-availability of the other engine components exists. Also, in the early development stage the full range of the excitation (gas pressure load, valve train and timing drive loads) is often not available. The main objective of this master thesis is to define proper guidelines for components design that will provide good engine NVH behavior (as a full assembly). In particular, the work includes cascading of the global engine targets to component targets. This will be demonstrated on the validated multibody dynamic model.

Based on the above, in this study it is necessary to:

1. Study the literature and publications related to NVH performance of modern engine designs and their main components (e.g. crankcase, oil pan, covers, etc.).
2. Benchmarking of the engines with the same engine design and excitations to understand engine to engine differences in NVH and to be able to interpret the engine excitations in terms of frequency content.
3. Find a suitable simulation methodology (forced response FEM analysis) of engine parts at early stage, considering also replacement of the "white noise" excitation with the more realistic excitation.
4. Evaluation of the results and cascading of the global engine targets to components targets.

During thesis preparation one must comply with the rules for preparation of the Master thesis.
It is necessary to list all literature used and received assistance.

Zadatak zadan:	Datum predaje rada:	Predviđeni datum obrane:
7. ožujka 2019.	9. svibnja 2019.	15., 16. i 17. svibnja 2019.

Zadatak zadao: Predsjednica Povjerenstva:

izv. prof. dr. sc. Darko Kozarac Prof. dr. sc. Tanja Jurčević Lulić

CONTENTS

LIST OF FIGURES

LIST OF TABLES

LIST OF SYMBOLS AND UNITS

Symbol	Unit	Description
A_j	m^2	area of element
A_{tot}	m^2	total area
L	dB	velocity/acceleration amplitude in logarithmic scale
F_{rec}	N	reciprocating force
F_{rot}	N	centrifugal force
a	m/s or m/s^2	amplitude of signal
a_i	m/s	velocity amplitude at node
a_0	m/s or m/s^2	reference value of signal
$\bar{a}$	m/s	average velocity amplitude on an element
f_c	Hz	centre frequency of the band
f_l	Hz	lower frequency of the band
f_u	Hz	upper frequency of the band
m_{rec}	kg	reciprocating mass
m_{rot}	kg	rotating mass
r	m	radial distance of conrod bearing from crankshaft centerline
v	m/s	velocity amplitude
v_0	m/s	reference value of velocity amplitude
α	degrees	crankshaft angle relative to TDC
ω	rad/s	angular velocity

LIST OF ABBREVIATIONS

DOF	Degree of Freedom
FE	Finite Element
FFT	Fast Fourier Transformation
I4	Inline 4
NVH	Noise, Vibration, Harshness
TDC	Top Dead Center
V6	Vee 6

SAŽETAK

Osim manje potrošnje goriva i velike snage, udobnost u vožnji vrlo je važan zahtjev kod kupnje vozila. Budući da je motor s unutarnjim izgaranjem jedan od glavnih izvora buke i vibracija u vozilima, analiza buke i vibracija predstavlja velik izazov u razvoju motora s unutarnjim izgaranjem.

Cilj ovog rada je odrediti odgovarajuću metodu koja bi omogućila predviđanje vibracija pojedinih komponenata motora s unutarnjim izgaranjem na početku razvoja prije nego što je poznata konstrukcija cijelog motora. Time bi se smanjili troškovi i vrijeme potrebno za razvoj motora s unutarnjim izgaranjem.

Analizirana su tri prednabijena redna trocilindarska Otto motora. Pojedini dijelovi motora (usisna grana, uljno korito i poklopac glave motora) analizirani su u trećinsko-oktavnom pojasu od 800 Hz do 3150 Hz (frekvencijsko područje od 708 Hz do 3548 Hz). Prvo je potrebno definirati odgovarajuće rubne uvjete koji bi zamijenili utjecaj opterećenja koje se prenosi iz bloka motora preko vijčanog spoja na određenu komponentu motora. Rubni uvjeti su definirani u obliku ubrzanja. Nakon toga, različiti tipovi krivulja ubrzanja primjenjuju se u čvorovima na mjestima vijčanog spoja promatrane komponente s ostatkom strukture. Na kraju, rezultati su uspoređeni na temelju raspodjele vibracija po površini strukture i ovisno o tome koliko pojedina komponenta pridonosi ukupnim vibracijama motora s unutarnjim izgaranjem.

Ključne riječi: Buka, vibracije, uzbuda, odziv, ubrzanje

ABSTRACT

Lower fuel consumption and high power, together with the increased driving comfort, represent some of the most important customer demands. Since internal combustion engine represents one of the biggest contributors to the overall noise and vibration levels, a special attention should be given to the NVH (noise, vibration, harshness) analysis. The objective of this study is to define a method for predicting the NVH performance of the engine components at early stages of engine development before they are coupled to the full engine assembly. As a result, the whole development process would be less time and money consuming.

The study is conducted for three gasoline turbocharged inline 3-cylinder engines. Engine components (intake manifold, oil pan and cam cover) are analyzed in mid and high frequency domain for 3rd octave band 800 Hz up to 3rd octave band 3150 Hz (from 708 Hz to 3548 Hz). The first step is to define the adequate boundary conditions that will replace the impact of the forces generated in the engine block and transmitted through the bolts to the observed component. Boundary conditions are defined in the form of enforced motions (accelerations). After that, different types of acceleration curves are applied as excitations at the bolt locations in the forced frequency response analysis. Finally, structure response is evaluated in 3rd octave bands based on the distribution of the surface velocities and the contribution of the observed component to the overall noise radiation level.

Key words: NVH, excitation, engine, response, acceleration

PROŠIRENI SAŽETAK

Ovaj rad izrađen je u suradnji s tvrtkama AVL - AST d.o.o. iz Zagreba i AVL List GmbH iz Graza.

Cilj ovog rada je pronaći odgovarajuću metodu koja bi omogućila predviđanje vibracija pojedinih elemenata motora s unutarnjim izgaranjem na samom početku razvoja. Dakle, potrebno je odrediti odgovarajuće i jednostavne rubne uvjete koji bi zamijenili utjecaj cjelokupne strukture na promatrani dio. Budući da bi se time cjelokupan proces analize buke i vibracija ubrzao, ujedno bi se smanjili troškovi i vrijeme potrebno za razvoj motora s unutarnjim izgaranjem.

Zahtjevi kupaca uvelike određuju smjer razvoja motora s unutarnjim izgaranjem. Želja za manjom potrošnjom goriva, većom snagom i udobnošću u vožnji dovodi do potrebe za optimiranjem buke i vibracija u vozilima. Posebnu pažnju potrebno je posvetiti motoru s unutarnjim izgaranjem koji je jedan od glavnih izvora buke i vibracija u vozilima. Razina emisije buke mijenja se ovisno o komponentama motora i njihovom položaju u sklopu. Drugim riječima, komponente motora koje su spojene na krutu strukturu emitiraju manju razinu buke. Budući da se u području oko glavnih ležajeva u bloku motora prenose reakcijske sile koje uzrokuju vibracije motora, to je područje definirano kao kritično. Također, komponente izrađene od velikih ravnih površina (npr. poklopci, uljno korito) sklone su vibracijama uslijed čega dolazi do značajnih emisija buke. Frekvencijski odziv takvih komponenata može se smanjiti ukrućivanjem strukture, tj. dodavanjem rebara.

S druge strane, uravnoteženost motora s unutarnjim izgaranjem također utječe na ukupnu razinu buke i vibracije. Naime, kod motora kod kojih postoji neuravnoteženost sila inercija uslijed oscilirajućih masa ili neuravnoteženost momenata savijanja uslijed spomenutih sila inercije može se primijetiti da je ukupna razina vibracija i emisije buke veća nego kod uravnoteženih motora.

U ovom radu analizirana su tri prednabijena redna trocilindarska Otto motora (motor A, B i C) te su proučavane tri kritične komponente – usisna grana, uljno korito i poklopac glave motora. Analiza je provedena u srednje i visoko frekvencijskom području (708 Hz – 3548 Hz), a rezultati su uspoređivani u trećinsko-oktavnom pojasu.

Prvi korak je određivanje rubnih uvjeta. Rubni uvjeti predstavljaju odziv na mjestima vijaka promatranih komponenti na sile koje se javljaju u radu motora – sile plinova, sile inercije i sile u razvodnom mehanizmu. Rad motora simuliran je u programskom paketu *AVL Excite Power*

Unit. U ovom slučaju, rubni uvjeti su definirani u obliku ubrzanja u čvorovima na mjestu vijaka. Budući da se pretpostavlja da su ubrzanja u smjeru rotacijskih stupnjeva slobode zanemariva, u obzir su uzeta ubrzanja samo u smjeru translacijskih stupnjeva slobode.

Sljedeći korak sastoji se od pojednostavljenja rubnih uvjeta, tj. krivulja ubrzanja. Na početku se odredi prosječna vrijednost ubrzanja u svim čvorovima na mjestima vijaka. Nakon toga, definiraju se različite jednostavnije krivulje trenda kojima se zamjenjuje, još uvijek složena, krivulja prosječnih ubrzanja.

Primjer pojednostavljenja krivulje ubrzanja za usisnu granu A u smjeru osi *x* prikazan je na slici 1. Usisna grana A spaja se sa šest vijaka na glavu motora. Plava krivulja prikazuje prosječnu vrijednost ubrzanja na mjestima svih šest vijaka u smjeru osi x. Isprekidane linije predstavljaju različite krivulje trenda koje se kasnije primjenjuju kao uzbude na mjestima vijaka.

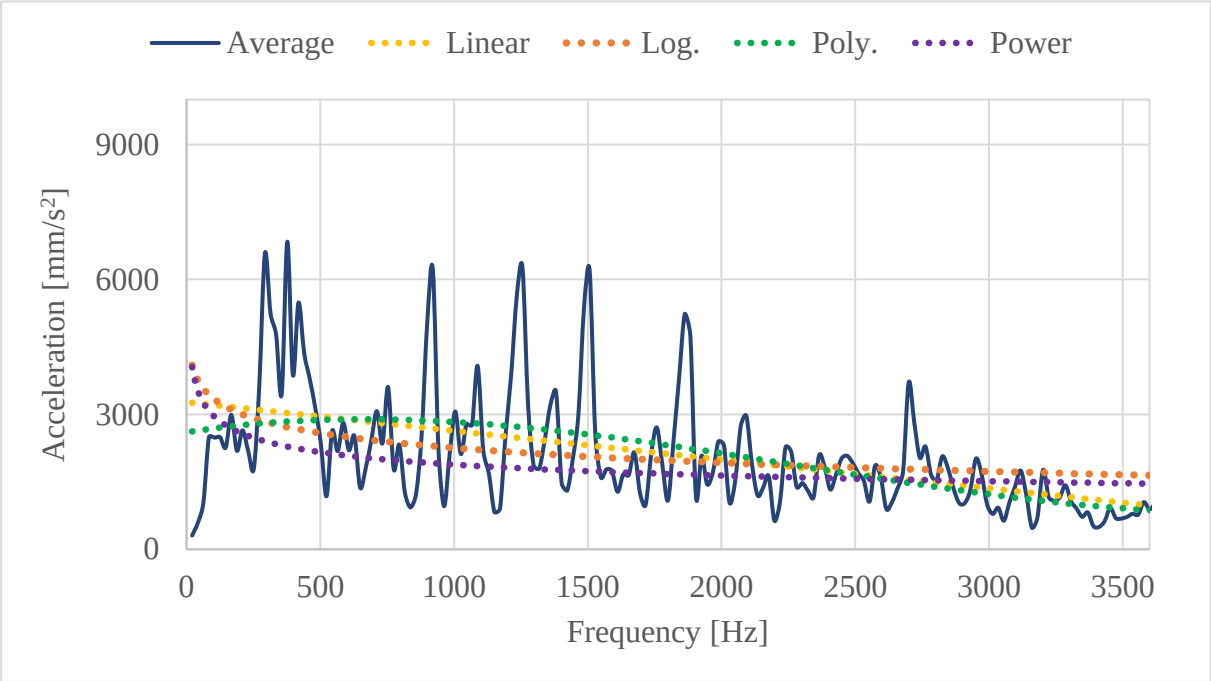

Slika 1. Krivulja prosječnog ubrzanja i krivulje trenda za translaciju u smjeru osi x za usisnu granu A.

Treći korak je analiza prisilnih vibracija u programskom paketu *MSC Nastran*. Različite vrste prethodno prikazanih krivulja ubrzanja primjenjuju se kao uzbude na mjestima vijaka. Na temelju rezultata za usisnu granu A, linearna krivulja ubrzanja definirana je kao najprihvatljivija.

Posljednji korak čini usporedba odziva strukture na osnovnu uzbudu (generiranu u programskom paketu *AVL Excite Power Unit*) i odziva na pojednostavljene uzbude. Rezultati

se uspoređuju u trećinsko-oktavnom pojasu, posebno za svaki pojas od 800 Hz do 3150 Hz. Usporedba se provodi na temelju sljedeća dva kriterija:

1. AVL-ov kriterij dozvoljenih odstupanja odziva strukture, definiran u tablici 1, i

Tablica 1. Kriterij dozvoljenih odstupanja odziva strukture

Razlika između odziva na osnovnu uzbudu i odziva na pojednostavljene uzbude	≤ 3.5 dB	prihvatljivo
	3.5 – 4.5 dB	granično
	≥ 4.5 dB	nije prihvatljivo

2. Slikovnog prikaza raspodjele brzina u čvorovima na površini strukture.

AVL-ov kriterij dozvoljenih odstupanja odziva strukture definira razliku u iznosu integrala brzine po površini strukture uslijed osnovne uzbude i pojednostavljenih tipova uzbude. Integral brzine po površini strukture daje podatak o tome koliko pojedini element motora doprinosi ukupnoj razini vibracija tog motora. Prema kriteriju, dozvoljeno je odstupanje do 3.5 dB u odnosu na osnovni udio.

Primjer usporedbe odziva strukture na osnovnu uzbudu i odziva na linearnu uzbudu za usisnu granu A prikazan je na slici 2. Ljubičasta krivulja prikazuje odziv na osnovnu uzbudu u frekvencijskom području od 708 Hz do 3548 Hz. Također, odziv na osnovnu uzbudu prikazan je i u trećinsko-oktavnom pojasu od frekvencije 800 Hz do 3150 Hz. Isto tako prikazan je i odziv na linearnu uzbudu (narančasta krivulja).

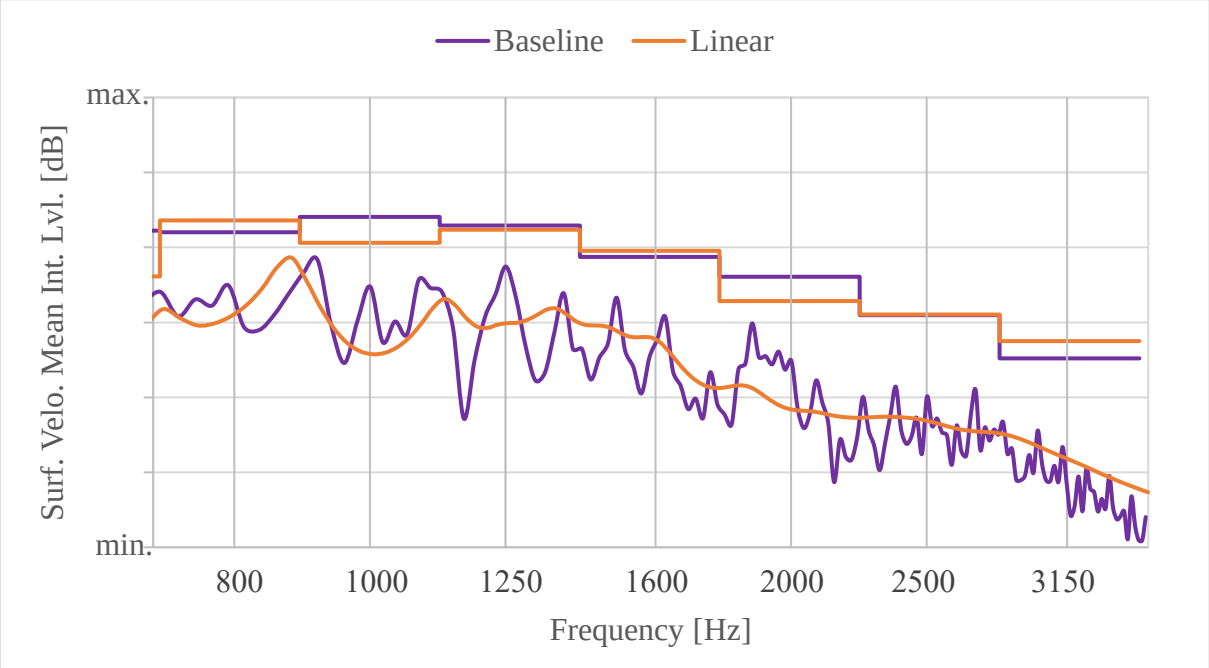

Slika 2. Usporedba odziva na osnovnu uzbudu i odziva na linearnu uzbudu za usisnu granu A.

Slikovni prikaz raspodjele brzina u čvorovima na površini opisuje raspodjelu vibracija na promatranom elementu motora. Vibracije koje nastaju kao odziv na pojednostavljene uzbude moraju imati istu/vrlo sličnu raspodjelu i intenzitet kao i vibracije koje su posljedica osnovne uzbude. Na slici 3 prikazana je usporedba brzina u čvorovima na površini usisne grane A za frekvencijsko područje od 1413 Hz do 1778 Hz (trećinsko-oktavni pojas 1600 Hz). Na slici se može primjetiti da je raspodjela vibracija po površini usisne grane A vrlo slična u oba slučaja – u slučaju osnovne i linearne uzbude. Osim raspodjele, intenzitet vibracija se također podudara u oba slučaja. Jedina zamjetnija razlika je označena na slici, ali, unatoč tome, odziv na linearnu uzbudu može se definirati kao prihvatljiv unutar promatranog frekvencijskog područja.

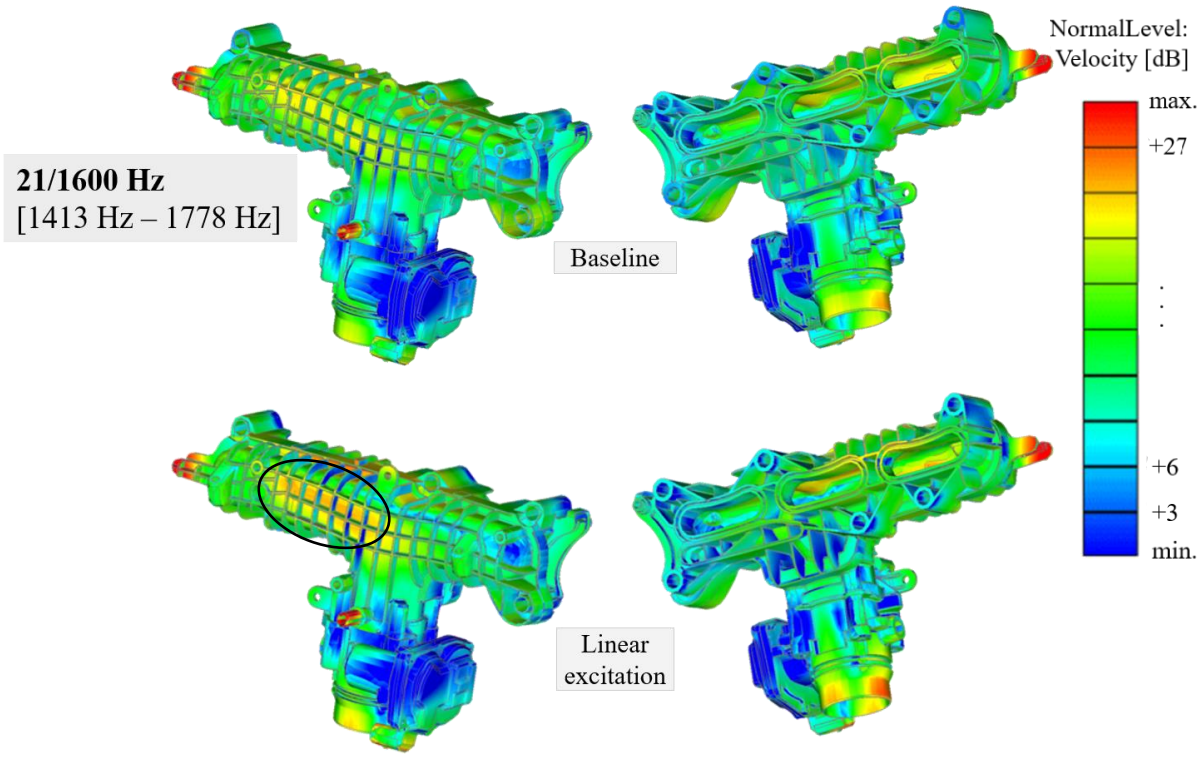

Slika 3. Usporedba brzina u čvorovima na površini usisne grane A za frekvencijsko područje od 1413 Hz do 1778 Hz za osnovnu i linearnu uzbudu.

Analiza se na jednak način provodi za sve ostale proučavane komponente motora.

Na temelju usporedbe rezultata, zaključeno je da je kod svake od promatranih komponenti pojava vibracija različita. Vibracije koje se javljaju na usisnoj grani ovise o konstrukciji usisne grane te stoga nije moguće pronaći vrstu krivulje uzbude koja bi mogla dobro opisati ponašanje svake usisne grane.

Analiza pojave vibracija na uljnom koritu pokazala je da se vibracije uljnog korita ne mogu predvidjeti kada se primjenjuju jednostavne krivulje uzbude. Naime, sva tri promatrana

uljna korita spajaju opterećen donji dio motora (blok ili kućište radilice) s mjenjačkom kutijom. Stoga, uljno korito predstavlja vrlo važnu strukturnu komponentu motora s unutarnjim izgaranjem čija se složena uzbuda ne može zamijeniti jednostavnijom.

Pojava vibracija na poklopcu glave motora može se relativno dobro predvidjeti za oba promatrana poklopca kada se primjenjuju jednostavni rubni uvjeti. Razlog tome je vrlo slična konstrukcija poklopaca glave motora i mjesta spajanja na glavu motora.

Također, treba spomenuti da veliki utjecaj na cjelokupne vibracije u sustavu imaju i sile koje su uzrokovane djelovanjem razvodnog mehanizma i neuravnoteženi momenti savijanja uslijed inercijskih sila. Sile uzrokovane djelovanjem razvodnog mehanizma značajno utječu na visokim frekvencijama. S druge strane, neuravnoteženi momenti savijanja uslijed inercijskih sila inercije povećavaju nivo vibracija u motoru s unutarnjim izgaranjem.

1. INTRODUCTION

1.1. Motivation

Vehicle development is a very complex process. At this moment, NVH behaviour of the engine components is observed when the engine design process is almost over. This could be very problematic in terms of time consumption and costs if some engine parts do not have acceptable NVH performance. When and if that occurs, the whole engine design process must be repeated until an acceptable design is achieved. Consequently, that prolongs the time needed to design an engine. Longer design time leads to the higher costs that should be avoided. Therefore, it is necessary to establish a proper boundary conditions of an observed engine component which could successfully replace the behaviour and impact of the engine assembly on that specific component. In other words, the NVH behaviour of the engine components should be successfully assumed at the early stages of design.

So far, the assessment of the NVH behaviour of engine components at the early stages of engine design is done by using a white noise excitation in forced frequency response analysis. White noise excitation is defined as a constant excitation value over the whole frequency range. Therefore, it is not frequency depended and does not consider the change of dynamic excitation amplitude with the frequency. For this reason, this type of analysis gives rough and unreal assessment.

The objective of this thesis is to find a method that should give us a better representation of the NVH behaviour of engine parts at the early stages of design. This includes finding a better and suitable, but simple type of excitation and analyzing the needed complexity of studied component to achieve a satisfying response. As a result, the engine design process would be simplified and less time consuming.

1.2. NVH Analysis

Together with the high power and low fuel consumption as the most important requirements when buying a vehicle, buyers also want their car and driving to be comfortable without excessive noise and vibrations. This leads to the one of the most important tasks of the automotive engineers - NVH analysis. NVH is an abbreviation meaning noise, vibration and harshness and the main goal of the NVH analysis is to provide a good engine performance without any unexpected and uncommon noises and vibrations. While noise and vibration can

be measured, harshness is subjective and depends on the person. Harshness can be described as an overall driving impression. NVH analysis is a process that, not only carries out at the end of the design process, but also should be considered during the whole development stage.

It is important to design a part in a way that will not serve to appearance of a resonance, but a structural design focused on avoiding resonances is not sufficient to assure an acceptable sound level and superior sound quality. Since the overall engine noise level is not caused by structural resonances but rather by the response of the engine structure under forced response excitation, this leads to a whole new area that should be explored [1].

1.2.1. Development stage

The first step in a design process of an engine is a target setting by benchmarking process where NVH performance of the best competitor engines is to be known [2]. Benchmarking objects, i.e., competitors' engines are determined based on the similar design, weight and performances as the future developed engine. The whole benchmarking process is carried out to determine what are good, poor and realistic designs [3]. Based on the performed benchmarking process, targets for newly developed engines are being set. The process consists of setting targets not only for the whole engine as an assembly, but also for different engine components. Therefore, direction of engine development is determined by target setting.

1.2.2. NVH classification

According to [4], vehicle NVH can be classified in several ways. One of the classifications of the vehicle NVH is on interior and exterior vehicle NVH. Interior NVH includes noise and vibrations that affect passengers in the vehicle cabin. On the other side, the exterior NVH deals with the noise radiated by the vehicle. The other classification separates vehicle NVH based on different excitation sources. Road surface conditions and environmental impact belong to the external excitation sources.

On the contrary, internal excitation sources include forces that derive from an engine - powertrain and drivetrain forces, then tire and wheel imbalance, brake forces, etc. [4] However, the target of this thesis is the NVH analysis of an engine, therefore only excitations that affect engine NVH will be discussed later.

Furthermore, two different types of engine noise must be mentioned. Structure-borne noise is the sound that propagates through the structure of an engine causing a vibration of the surface. On the other side, air-borne noise is the sound that is transmitted through the acoustic

medium, i.e., air. Accordingly, structure-borne noise travels from engine through engine mounts, chassis and car body to vehicle cabin, while air-borne noise travels from the engine compartment through the firewall to the cabin.

1.2.3. Engine components NVH performance

According to [5], the biggest contributors to the overall engine noise are sumps, covers and intake manifolds, i.e., large flexible surfaces. Not only they contribute to the overall noise level by noise radiation (air-borne noise), but also increase vibration level because of the vibrations transferred from engine block (structure-borne noise). Because of that, these components must be isolated from the engine block vibrations.

Oil pan has no direct excitation applied on it, but it suffers from vibrations transferred from cylinder block. It represents a large exposed area and radiates a lot of noise. There are two methods for decreasing oil pan noise radiation. The first one is to lower engine block vibrations that can be achieved by stiffening the block. The second method consists of local stiffening of the oil pan.

Another engine component with large exposed area and no direct excitation is the valve cover. Valve cover suffers from vibrations transferred from cylinder head (structure-borne noise) and noise that propagates through the valve cover (air-borne noise). Valve cover noise level can be lowered by stiffening the cover by using the metal shields at the area where camshafts are [6].

A huge influence to the overall engine noise and vibration level has engine bottom end design. Analyses have shown that stiffening of the engine bottom end, engine noise and vibrations can be significantly reduced [7]. The most critical part is the area near the main bearings and crankcase. Hence, different design variations, shown in the Figure 1, were examined.

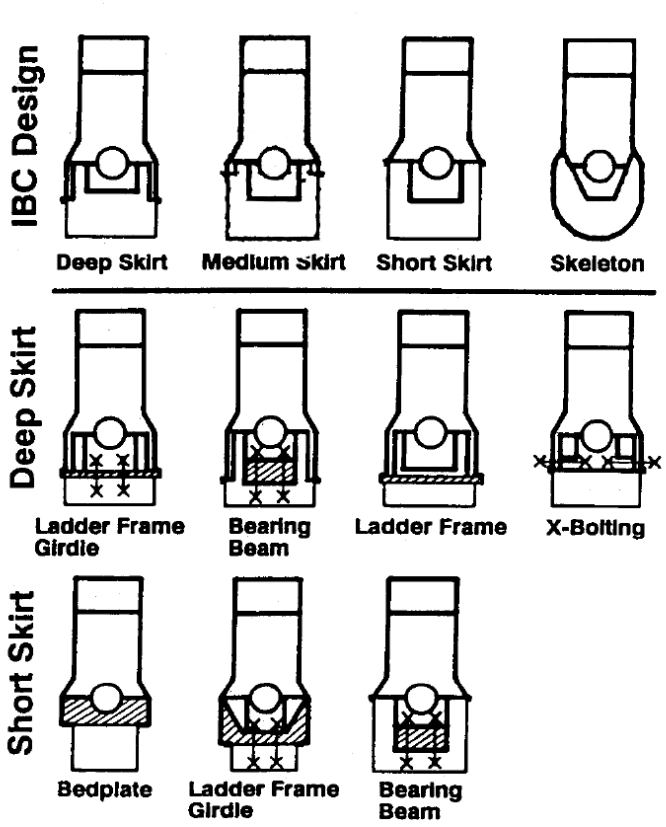

Figure 1. Different bottom end designs [7]

It was discovered that engine design with bearing beam or bedplate increases the stiffness comparing to a design with individual bearing caps [6].

Besides of the previously described impact of the engine bottom end design, a major influence on NVH behaviour have crankshaft material and cranktrain dynamics. According to [8], a stiff crankshaft is essential for good NVH performances. There are large forces transmitted through the main bearings, therefore it is important that area near the main bearings is of sufficient stiffness. Stiffer crankshaft deforms less which results in smaller bending moments transmitted to the surrounding area. Likewise, vibrations at front and rear crankshaft side are lower. Furthermore, forged steel crankshafts have better NVH performances than cast iron crankshafts.

Crankcase material also has a significant effect on the powertrain NVH performance. Aluminium crankcases itself do not have sufficient stiffness, so corresponding stiffening methods must be executed during the design stage. This primarily refers to preventing a vibration transfer to the critical areas where a significant noise is usually generated, i.e. oil pan and crankcase sidewalls.

As mentioned before, engine component must be designed in order to avoid appearance of the resonance. This means designing a component with higher resonant frequencies, i.e. eigenfrequencies, where the dynamic excitation amplitude is lower. Given that, special attention must be paid to the frequency of the first bending mode of the engine block and transmission, the frequency of the first torsion and bending mode of the crankshaft and the frequency of the bending modes of the engine mounting brackets [9]. Another thing that should be considered is the location of engine auxiliary devices. They must be attached to the places where low vibrations occur and places with higher stiffness.

Cylinder block and head, as the biggest engine components, must be carefully designed because they have a major role in transmission and attenuation of the vibrations generated within the engine. The following Figure 2 shows a noise and vibration transfer paths within the engine.

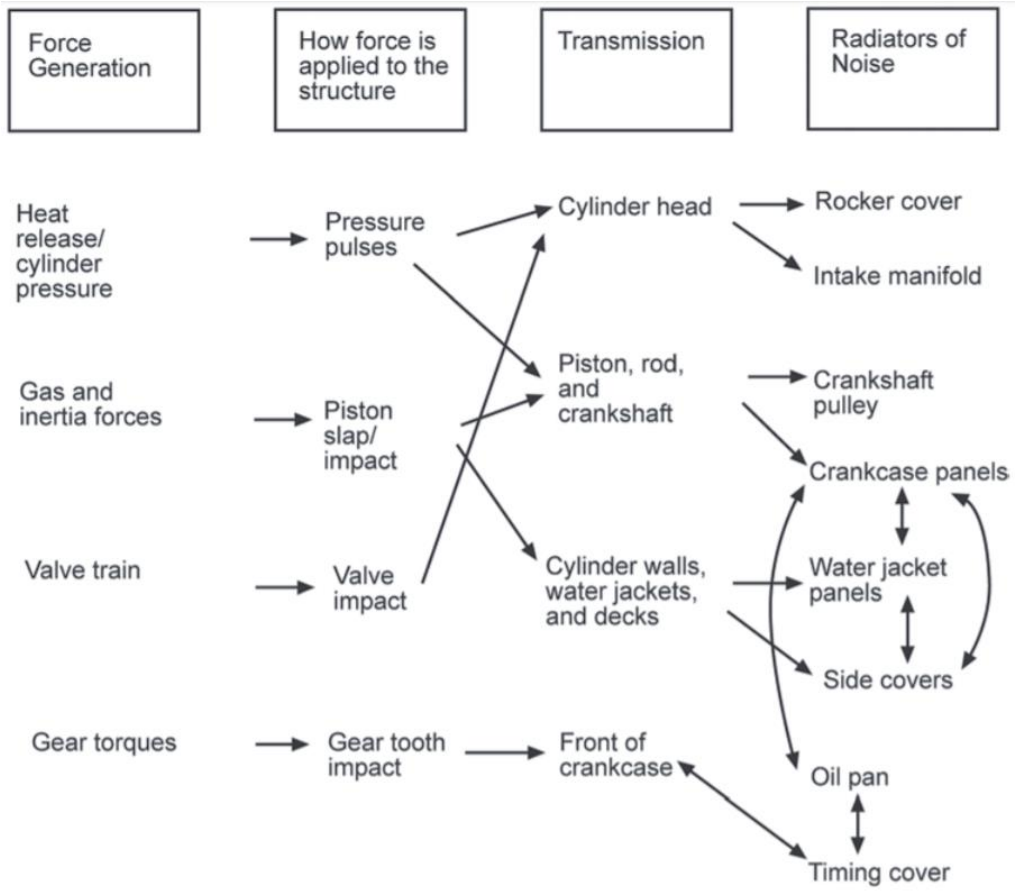

Figure 2. Engine noise generation, transfer and radiation [10]

Since large flat panel surfaces radiate a lot of noise, a cylinder block must be designed in order to avoid that. That is achieved by curving the surface or adding ribs. Cylinder block material also contributes to the overall NVH behaviour.

Cylinder blocks made from gray cast iron have higher stiffness, but also higher mass. That is why cylinder blocks from aluminium alloys are often used. Compared with the gray cast iron block, aluminium alloy block weights 40 - 50 percent less. The main disadvantages of the aluminium alloys are lower stiffness, high temperature creep relaxation and poor wear characteristics. Because of the poor wear characteristics, special inserts for cylinder wall must be defined. Lower stiffness results in lower critical frequencies meaning that resonance will occur at lower frequencies. Therefore, aluminium alloy components must be designed in order to achieve higher stiffness which implies adding more ribs to the structure [10].

1.2.4. Engine balance and configuration impact on NVH

The main source of the vehicle noise and vibrations is powertrain. During the combustion process, high forces are being generated in the cylinders. These forces, shown in Figure 3 are the result of gas pressure forces and inertia forces of rotating and reciprocating masses. The total force acting on the piston, F, is a result of gas pressure and inertia forces. Force acting on the conrod, F_c, varies with the crank angle. F_r is a radial force acting on the main bearings, while F_t is a tangential force that rotates the crankshaft.

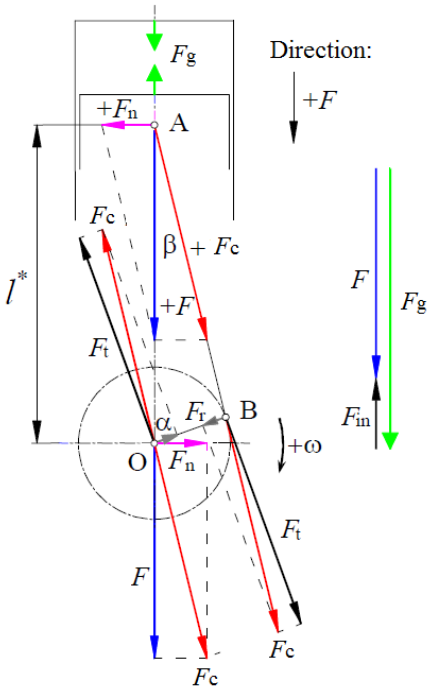

Figure 3. Cylinder forces [11]

Unbalance of the mentioned forces within the engine leads to the unwanted engine motions show in the Figure 4.

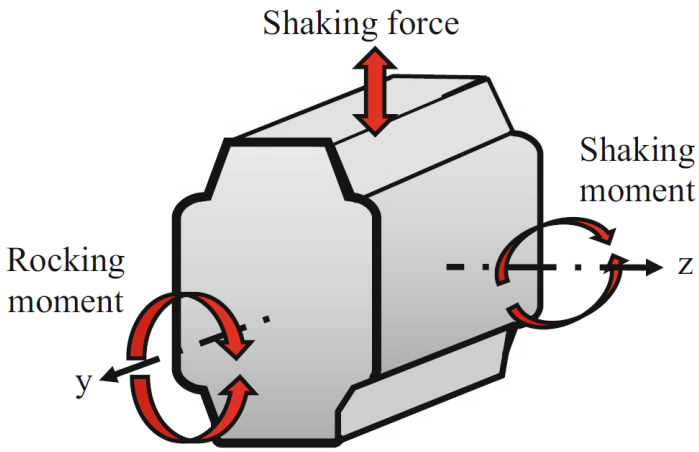

Figure 4. Excitation of engine block [5]

The cylinder gas pressure has a major influence on the overall noise and vibration level. High peak cylinder gas pressure and high pressure rise rates generate high excitation forces and rapid variations of forces transmitted to the engine block structure [8]. Gas pressure forces are balanced within the cylinder, but the pressure varies with the crank angle causing a torque fluctuation. These cannot be balanced and are transmitted through engine mounts to the vehicle. Thus, engine mounts must be designed in order to minimize that transmission.

Rotating masses include crank throw mass and one portion of the crankshaft mass. Rotating masses generate a centrifugal force calculated as

$$F_{\mathrm{rot}} = -m_{\mathrm{rot}} r \omega^2, \tag{1}$$

where:

m_{rot} - rotating mass,

r - radial distance of conrod bearing from crankshaft centerline,

ω - angular velocity.

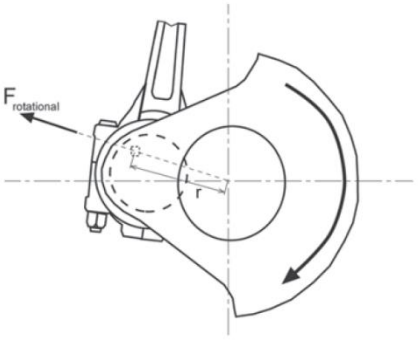

Figure 5. Summary of centrifugal force calculation [12]

The resulting rotational force, according to Figure 5, acts outward from the crankshaft centerline and it can be counterbalanced by adding an additional mass to the crankshaft section opposite of the crank throw [11].

On the other hand, reciprocating masses consist of the piston, piston pin and rings mass, but also the upper portion of the conrod mass [11]. As well as the torque fluctuations, inertia forces of reciprocating masses are the main cause of the engine vibrations since they cannot be completely balanced. The reciprocating forces can be calculated according to

$$F_{rec} = -m_{rec} r\omega^2 (A_1 cos\alpha + A_2 cos2\alpha + A_4 cos4\alpha + A_6 cos6\alpha \dots), \quad (2)$$

where:

m_{rec} - reciprocating mass,

r - radial distance of conrod bearing from crankshaft centerline,

ω - angular velocity of crankshaft,

α - crank angle relative to TDC [11].

The frequency of engine vibrations varies with the engine speed, thus specific frequencies, called vibration orders, can be determined. These frequencies define a number of events that occur per one crankshaft rotation. Therefore, the values in the brackets represent first-order, second-order, fourth-order, etc. inertia forces, but only the first two are being taken into the consideration (higher orders are quite smaller). For analyzing the crankshaft balance, star diagrams are being used. Figure 6 shows how does the star diagram of 1st and 2nd order for some inline engines look like.

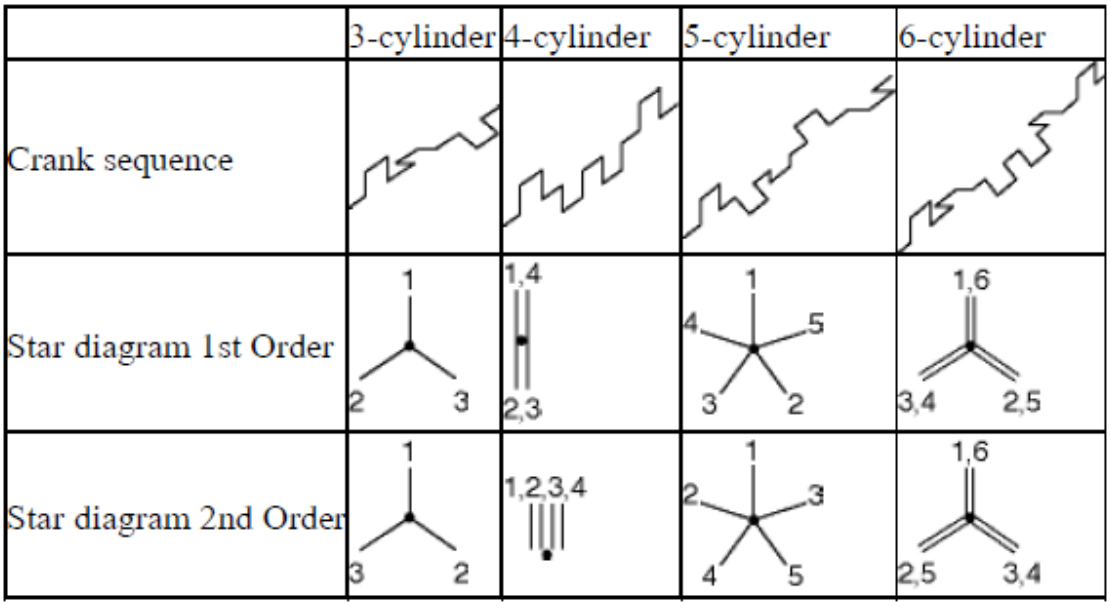

Figure 6. Star diagram of the 1st and 2nd order inertia forces [13]

Usually, only 50 % of first-order inertia forces can be balanced with counterweights, while special balancershafts (each rotates in one direction, twice the speed of the crankshaft) are used to balance a second-order inertia forces. Engine balance depends on the number of cylinders and firing order. A few examples of unbalanced inertia forces and moments for different (four-stroke) engine configurations are shown in the Figure 7.

z	Crankshaft form for 4-stroke engines	Firing interval δ	Firing order	Inertia forces rot	Inertia forces osc I	Inertia forces osc II	Inertia moments rot	Inertia moments osc I	Inertia moments osc II
1		720°	1	F_{mR}	F_{moI}	F_{moII}	0	0	0
2	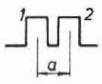	360°	1-2	$2\ F_{mR}$	$2\ F_{moI}$	$2\ F_{moII}$	0	0	0
3	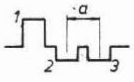	240°	1-2-3	0	0	0	$1.732\ F_{mR}\cdot a$	$1.732\ F_{moI}\cdot a$	$1.732\ F_{moII}\cdot a$
4	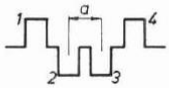	180°	1-3-4-2 1-2-4-3	0	0	$4\ F_{moII}$	0	0	0
5	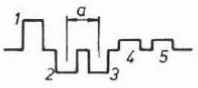	144°	1-2-4-5-3	0	0	0	$0.449\ F_{mR}\cdot a$	$0.449\ F_{moI}\cdot a$	$4.98\ F_{moII}\cdot a$
6	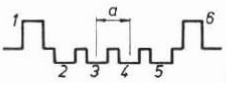	120°	1-5-3-6-2-4 1-4-2-6-3-5 1-3-5-6-4-2	0	0	0	0	0	0

Figure 7. 1st and 2nd order unbalanced inertia forces and moments for different engine configurations [14]

1.2.5. Comparison between vibration performance of I-4 and V-6 engine

An example showing how engine configuration affects vibrations will be shown. According to [15], a study that shows a difference in vibration performance of the four-cylinder and six-cylinder gasoline engine has been carried out. The specifications of selected engines are shown in the Table 1. Comparison of engine data [15]

Table 1. Comparison of engine data [15]

	Inline 4-cylinder gasoline engine	**Vee 6-cylinder gasoline engine**
Swept-volume [l]	2.0	2.0
Firing order	1-3-4-2	1-5-3-6-2-4
Bore [mm]	86	70
Stroke [mm]	86	86
Conrod length [mm]	143.5	143.5
Piston material	aluminium alloy	aluminium alloy
Piston mass [g]	372	303
Conrod material	steel	steel
Conrod mass [g]	647	647

Shaking force produced by the two mentioned engines was calculated. When analyzing an inline four-cylinder engine, one can notice that first-order inertia forces are balanced, but there is an imbalance in second-order inertia forces since they simultaneously reach their maximum [11]. On the other hand, V6 engine produces no shaking force. This means that there are considerable vibrations that affect engine mounts in I4 engine. Also, the study has shown that there are less torque fluctuations in the V6 than in the I4 engine which explains why V6 is usually referred as ’smooth’ [15]. Figure 8 shows the difference in performance of an I4 and V6 engine.

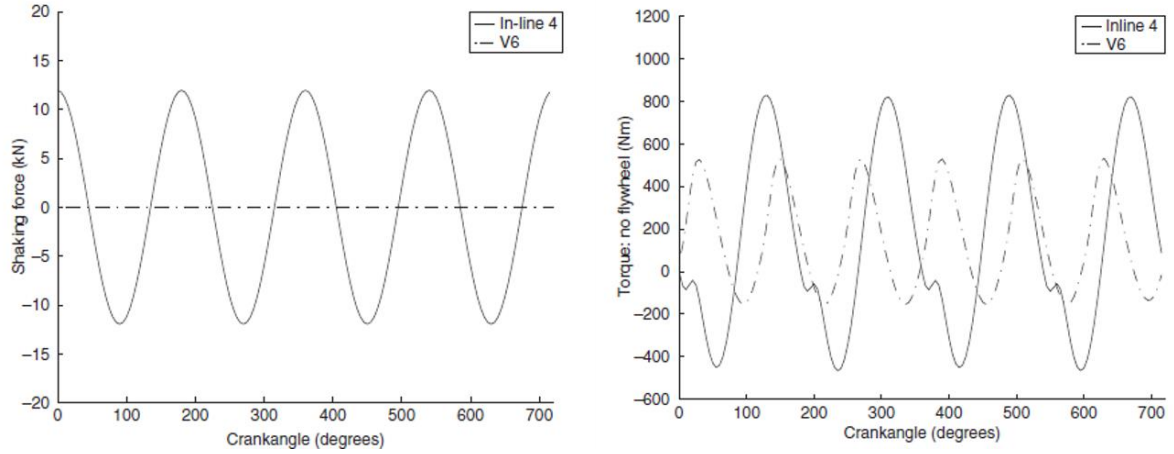

Figure 8. Difference in shaking force and torque fluctuations between I-4 and V-6 engine [15]

1.2.6. Acoustic materials

Moreover, noise and vibration levels also depend on types of materials that are being used. Among other well-known material properties, i.e. density, stiffness, hardness and elastic modulus, every material also has different acoustical characteristics. Acoustical characteristics depend on basic physical properties of the material [16]. So, using the right material noise and vibration levels can also be significantly reduced. Used materials can be classified into three categories:

1. sound absorbing materials,
2. sound barrier materials and
3. sound damping materials.

Sound absorbing materials are usually porous in order to trap the air within the pores and restrict its free flow [9]. The absorptivity is related to thickness and mounting method [16]. Sound barrier materials must block sound propagation from one area to another which ensures their nonporous and heavy structure [17]. Sound barrier materials used in automobiles are sheet metal, glass and loaded rubber sheets. Their effectiveness is defined by transmission loss. Damping materials are used to reduce the amplitude of vibration and sound radiation when a structure vibrates at its resonant frequency. It is achieved by transferring a vibration energy into heat [17]. Therefore, absorbers and barriers are used for airborne noise problems, while dampers are used for structure-borne noise problems [17].

1.2.7. The influence of CO_2 reduction on NVH behaviour

Climate changes represent the highest threat for the future of the human race. Well known greenhouse effect gets more and more dangerous with the increase of greenhouse gasses in the Earth's atmosphere. Since the main and the most dangerous contributor of the greenhouse gasses is CO_2, it is evidently that certain measures must be taken to decrease its presence in the atmosphere. Figure 9 shows that the fuel combustion for transport took one fourth of the overall greenhouse gas emission in European Union in 2016.

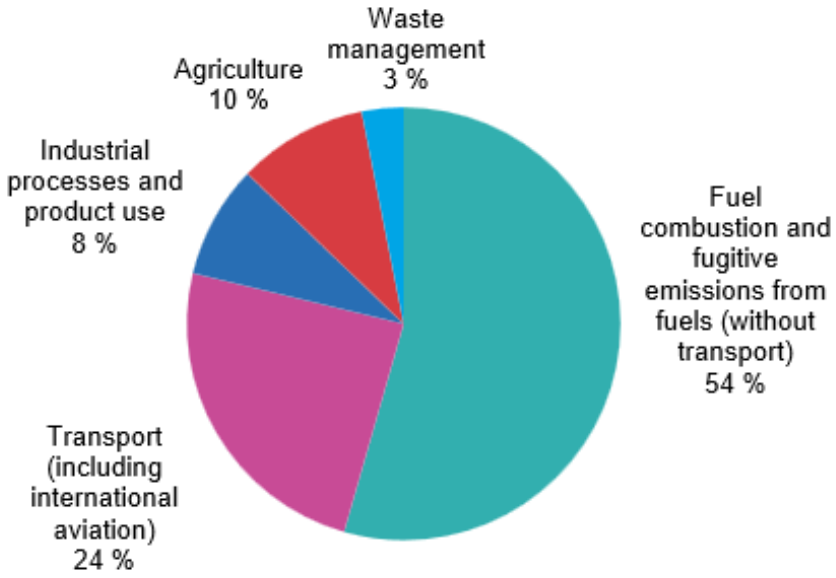

Figure 9. Greenhouse gas emissions, analysis by source sector, EU-28, 2016 [18]

According to [18], 76 % of that was caused by road traffic. Furthermore, 44 % of the transport greenhouse gas emissions was caused by passenger cars, while 19 % came from heavy-duty vehicles.

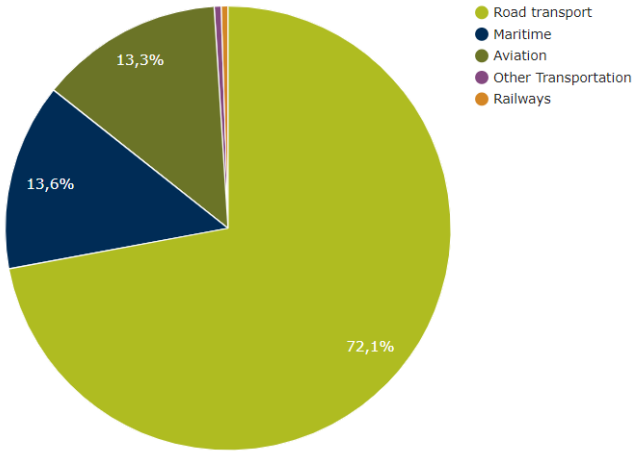

Figure 10. Share of transport greenhouse gas emissions, EU-28, 2016 [18]

With that in mind, special regulations must be set on the vehicle emissions in order to reduce the amount of the CO_2 emission.

Brandl [8] states that CO_2 reduction is currently one of the most important requirements for internal combustion engines and all other tasks must be adapted to it, so does the NVH analysis, as well.

As shown in the Figure 11, CO_2 reduction requires, among other things, reducing weight of a vehicle which, consequently, affects the increase in noise and vibration level.

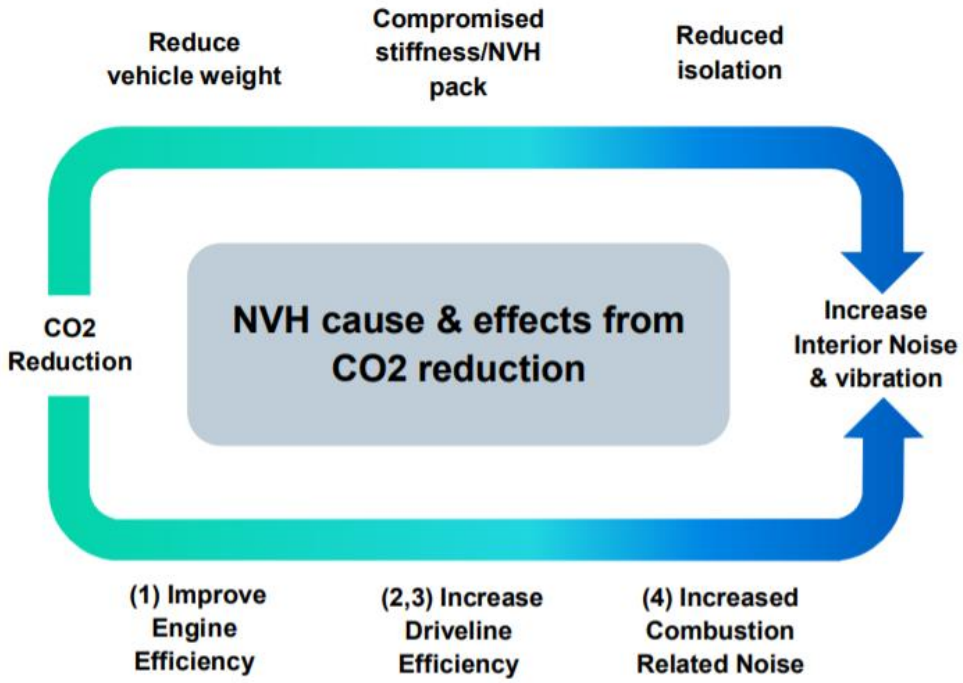

Figure 11. CO_2 reduction effect on NVH [19]

Weight reduction can be achieved by using light-weight materials and by using less material. But, using less material leads to a significant change in damping and stiffness. Furthermore, another way of reducing CO_2 is reducing fuel consumption. Both things lead to engine downsizing.

The main idea of the engine downsizing is to achieve the same engine performance (torque and power output), but with a smaller engine, i.e., decreased number of cylinders. Of course, that leads to a conclusion that, for the same structural behaviour, the engine with the lower number of cylinders will have higher cylinder pressures and hence, higher noise and vibration levels. Downsized engines have higher power to weight ratio, i.e., lower mass and less structural attenuation [4]. Engine downsizing leads also to an increase in speed irregularity [8].

Furthermore, sound characteristics of downsized engines also differ. AVL has developed an objective value for quantifying the sound quality of the engines called AVL Annoyance Index shown in the Figure 12 [8].

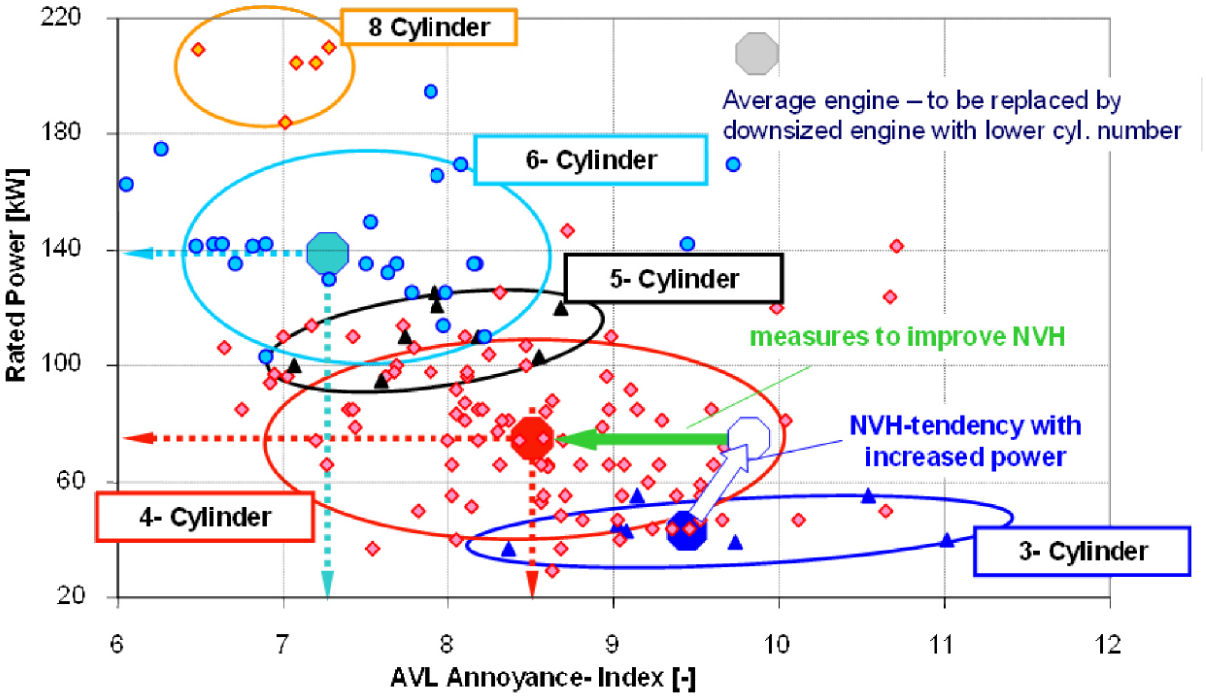

Figure 12. Annoyance index for different engines [8]

Sound quality significantly changes with the change of engine configuration and rated power. It can be noticed that, for the same rated power, the annoyance index increases with the decrease of the cylinder number.

2. MODEL DESCRIPTION

The study is carried out for three gasoline turbocharged engines, with the same configuration - inline 3-cylinder engines, at their rated speed. Engine, named engine A, is chosen as a reference engine and was studied first. The other two engines will be referred to as engine B and engine C. Also, the main characteristics of the studied engines are given as a ratio of the engine B or C characteristics to the reference engine characteristics (engine A). The characteristics are shown in Table 2.

Table 2. Characteristics of the studied engines

	Engine A	**Engine B**	**Engine C**
Bore [mm]	1	0.92	1
Stroke [mm]	1	0.94	1.02
Cylinder No.	3	3	3
Peak firing pressure [bar]	1	0.92	0.94
Volume/cylinder [l]	1	0.82	1.02
Swept-volume [l]	1	0.81	1.01
Rated power [kW]	1	0.72	0.76
Rated speed [rpm]	1	1.1	1.2
Break mean effective pressure [bar]	1	0.82	0.68
Specific power [kW/l]	1	0.90	0.75
Maximum torque [Nm]	1	0.73	0.85
Maximum torque speed [rpm]	1	1.33	0.83
Firing order	1-3-2	1-2-3	1-2-3
Reciprocating mass [kg]	1	1.01	1.56
Conrod radius [mm]	1	0.94	1.02
Conrod length [mm]	1	0.97	1.05
Engine mass [kg]	1	0.98	0.93
Timing drive	Belt	Chain	Chain
Bedplate	Yes	Yes	No
Balancershaft	Yes	Yes	Yes
Engine configuration	Testbed	Vehicle	Vehicle

2.1. Excite Power Unit Simulation

The first step of this Thesis is to analyze the displacements, velocities and accelerations at the bolt locations of the components of interest. In order to do that, a simulation in AVL Excite Power Unit is run. After that, the results are analyzed with Impress Chart.

2.1.1. Engine A

Figure 13 shows Excite Power Unit model of the Engine A.

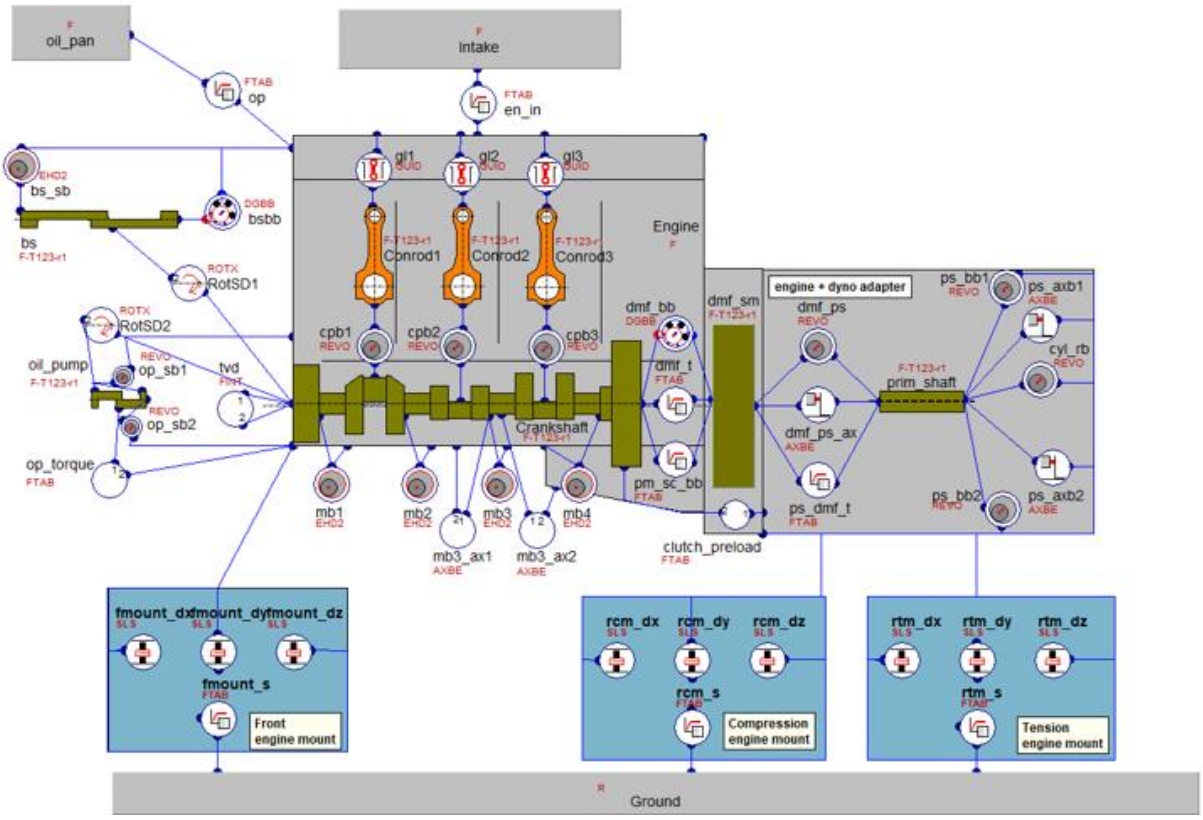

Figure 13. Engine A Excite Power Unit model

Powertrain excitation sources include following forces:

- gas cylinder pressure forces,
- cranktrain inertia loads,
- timing drive and valve train forces.

The powertrain excitation sources are the same for engines B and C as well.

2.2. Characteristics of studied parts

To be able to understand the difference in results, the main characteristics of the three studied components for three different engines are shown in the table. There is a difference in material, design, bolt number and bolt location between the studied components.

Table 3. Characteristics of engine components

			Material properties		
		Bolt No.	**Density** [kg/m^3]	**Young's modulus** [MPa]	**Poisson's ratio** [-]
Intake	**Intake A**	6	3670	8500	0.42
	Intake B	8	1400	8500	0.52
	Intake C	4	1410	6335	0.40
Oil pan	**Oil pan A**	20	2750	75000	0.33
	Oil pan B	19	2700	71000	0.31
	Oil pan C	20	2700	74500	0.33
Cam cover	**Cam cover A**	23	2750	75000	0.33
	Cam cover B	15	1400	8500	0.42
	Cam cover C	13	1480	7200	0.42

Furthermore, the cam cover A will not be studied in this Thesis. Cam cover A is made from an aluminium alloy. Due to the integrated camshaft bearing support, it represents a structural part. On the other hand, cam covers B and C are made from plastic material and only serve for covering the area above the valves and camshafts.

The study will be conducted in mid and high frequency domain (708 Hz - 3548 Hz) that includes seven 3rd octave bands. Engine A components will be observed first. Based on the obtained results and conclusions, the analysis will further be extended to engine B and engine C components.

3. EVALUATION CRITERIA

3.1. Surface integrals

Results are being evaluated as a difference in surface velocity mean integral levels. Evaluation is conducted in a one-third octave band. One-third octave band represents a special classification of the whole frequency range. The band is named after its centre frequency and it spreads over a defined range of frequencies.

One-third octave bands up to 4000 Hz are shown in Table 4.

Table 4. One third Octave Frequency Band

3rd octave No.	Centre Frequency	Lower Frequency	Upper Frequency
1	16	14.1	17.8
2	20	17.8	22.4
3	25	22.4	28.2
4	31.5	28.2	35.5
5	40	35.5	44.7
6	50	44.7	56.2
7	63	56.2	70.7
8	80	70.7	89.1
9	100	89.1	112
10	125	112	141
11	160	141	178
12	200	178	224
13	250	224	282
14	315	282	355
15	400	355	447
16	500	447	562
17	630	562	708
18	800	708	891
19	1000	891	1122
20	1250	1122	1413
21	1600	1413	1778
22	2000	1778	2239
23	2500	2239	2818
24	3150	2818	3548
25	4000	3548	4467

Evaluated range

The lower (f_l) and upper (f_u) frequencies of one band are related with the following equations with the centre (f_c) frequency:

$$f_l = \frac{f_c}{\sqrt[6]{2}}, \tag{3}$$

$$f_u = \sqrt[6]{2} f_c. \tag{4}$$

Mid and high frequency domain hereby includes 3rd octave bands from No. 18 to No. 24, i.e. frequency range from 708 Hz up to 3548 Hz. The results are being evaluated in that range since there is most radiated noise from the engine.

Velocity and acceleration amplitudes for single frequency can be calculated in logarithmic scale (L, [dB]) according to the equation:

$$L(f) = 20 \log_{10} \frac{a(f)}{a_0}, \tag{5}$$

where:

$a(f)$ - amplitude of signal,

a_0 - reference value.

AVL reference vales are shown in the Table 5.

Table 5. AVL reference values

a_0	SIGNAL
1E-5 mm/s	velocity
1E-3 mm/s^2	acceleration

Since the results are observed as a velocity levels in logarithmic scale throughout a defined frequency band, the equation (5) transfers to:

$$L_{\text{freq\_band}} = 20 \log_{10} \frac{\sqrt{\sum_{f_l}^{f_u} v^2(f)}}{v_0}. \tag{6}$$

Surface velocities are estimated based on the calculated surface integral level. There are two methods available:

1. Integral Mean and
2. Integral Normalized.

Integral Mean calculates surface integral level over the whole selected surface, while Integral Normalized calculates surface integral level over the determined reference area.

In this Thesis results were evaluated based on the Integral Mean. First, mean values on the surface patch must be calculated. Mean signal amplitude on a surface patch (element surface) with n_{patch} nodes is calculated according to:

$$ {}_j\bar{a} = \sqrt{\frac{\sum_{node\ i\ belonging\ to\ patch} a_i^2}{n_{patch}}}. \tag{7} $$

The mean level on a surface with area A_{tot}, that is made of N surface patches with areas $A_j, j = 1, \ldots, N$, is calculated by:

$$ {}_AL = 10\log_{10}\left(\frac{1}{a_0^2 A_{\mathrm{tot}}}\sum_{j=1}^{N_j} \bar{a}^2 A_{\mathrm{j}}\right), \tag{8} $$

where:

$\bar{a}$ - average velocity amplitude on an element,

A_{tot} - total area,

A_{j} - area of element,

a_0 - reference velocity.

3.2. Evaluation steps

Before comparing the results, evaluation criteria must be established. Results are compared and evaluated in 3rd octave bands according to the following criteria:

1. AVL benchmark acceptance criterion,
2. surface velocity plots.

AVL benchmark acceptance criterion defines the evaluation grades for comparing the surface mean integral velocity levels for each 3rd octave band separately. Calculation of the surface mean integral velocity levels gives only one value for each frequency, i.e. each 3rd octave band. Based on this, the contribution of the observed component in the overall noise radiation level in each 3rd octave band separately can be defined.

AVL benchmark acceptance criterion is shown in Table 6.

Table 6. Acceptance criterion

Difference between baseline and responses to simplified excitations	≤ 3.5 dB	acceptable
	3.5 – 4.5 dB	borderline
	≥ 4.5 dB	not acceptable

The second criterion is completely visual. It gives the information about shape of vibrations, i.e. distribution of surface velocities. Although surface mean integral velocity levels can be similar, there can be found a significant difference in the shape of vibrations. Therefore, during the evaluation based on the surface velocity plots one must ensure that surface velocity distribution over whole component area is similar. Also, the location of the monopole sources must coincide for both evaluated cases.

4. INTAKE MANIFOLD ANALYSIS

Three different intake manifolds are analyzed in this study. The basic properties of the observed components are shown in Table 7.

Table 7. Characteristics of intake manifolds

			Material properties		
		Bolt No.	**Density** [kg/m^3]	**Young's modulus** [MPa]	**Poisson's ratio** [-]
Engine A	**Intake A**	6	3670	8500	0.42
Engine B	**Intake B**	8	1400	8500	0.52
Engine C	**Intake C**	4	1410	6335	0.40

4.1. Intake manifold A

The first studied part is intake A shown in Figure 14. As can be noticed, it is connected to the cylinder head with 6 bolts.

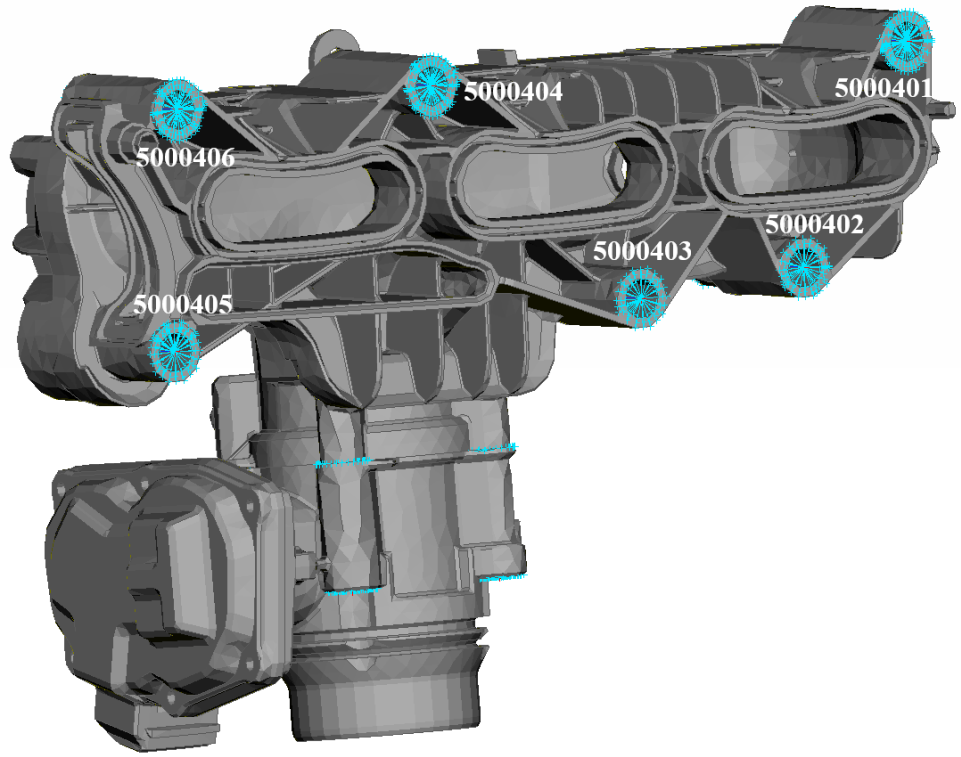

Figure 14. Intake manifold A bolt locations

4.1.1. Defining an excitation

The process of defining the excitation will be shown only for the intake manifold A. Excitation definition for all the other components undergoes the same process.

The first step is to analyze displacement, velocity and acceleration levels at the bolt locations in the frequency domain. With the assumption that results in direction of DOFs 4-6 do not contribute notably to the overall result, only results in direction of DOFs 1-3 will be observed. The results versus frequency are obtained using FFT in Impress Chart for the frequencies up to 3600 Hz. The results are given with the increment 1, i.e. each one fourth of the engine order. It should be kept in mind that displacement, velocity and acceleration are complex functions, but only their magnitude will be considered here.

The conclusion was obtained based on the results at all bolt locations but, to simplify, results only for one bolt location in direction of DOF 3 will be shown.

Displacement, velocity and acceleration versus time and frequency in direction of DOF 3 are shown at node 5000405 in the Figures 15, 16 and 17.

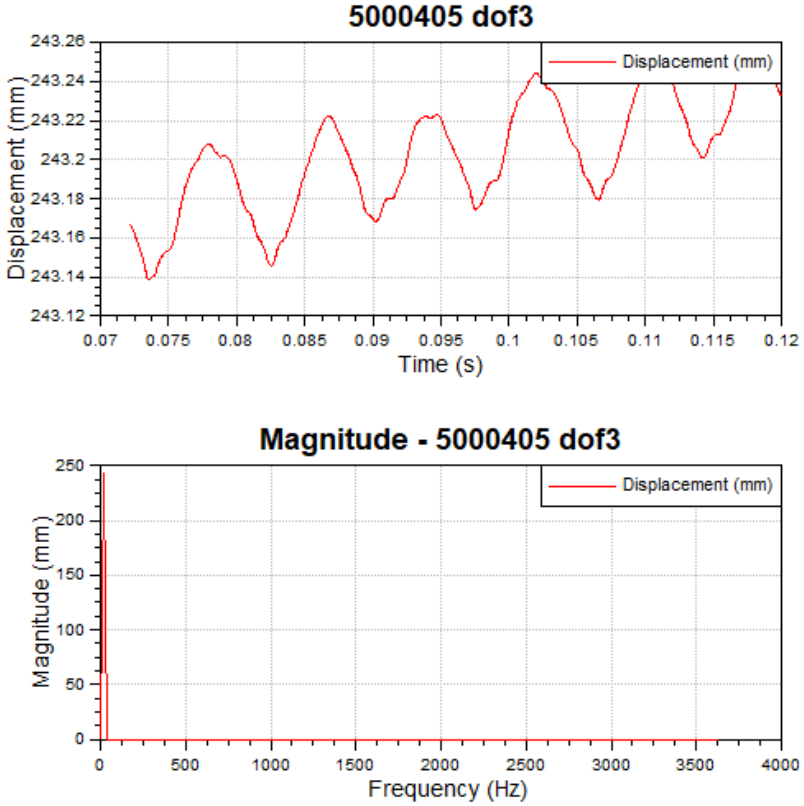

Figure 15. Displacement in direction of DOF 3 at node 5000405

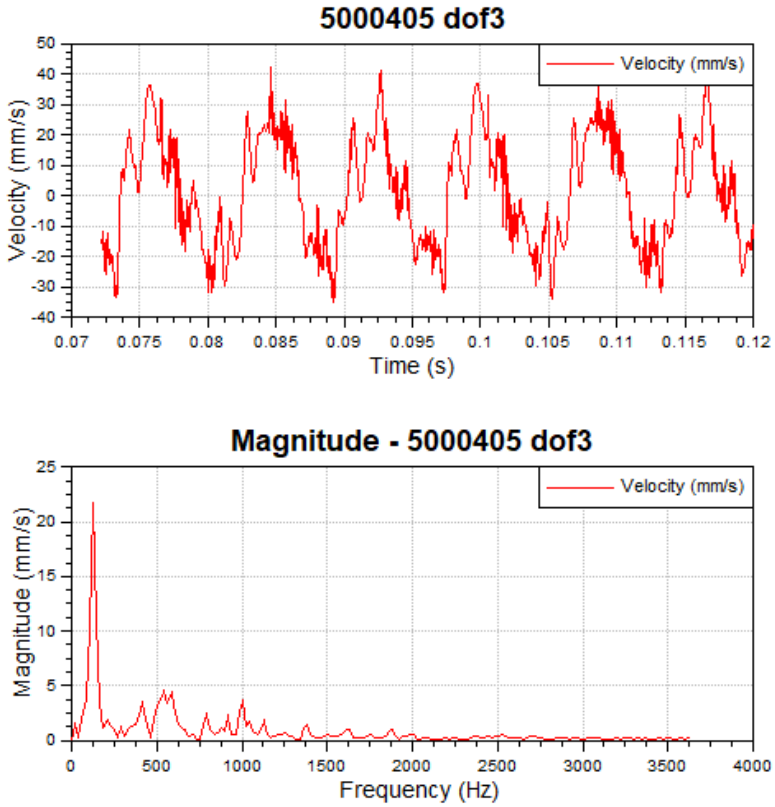

Figure 16. Velocity in direction of DOF 3 at node 5000405

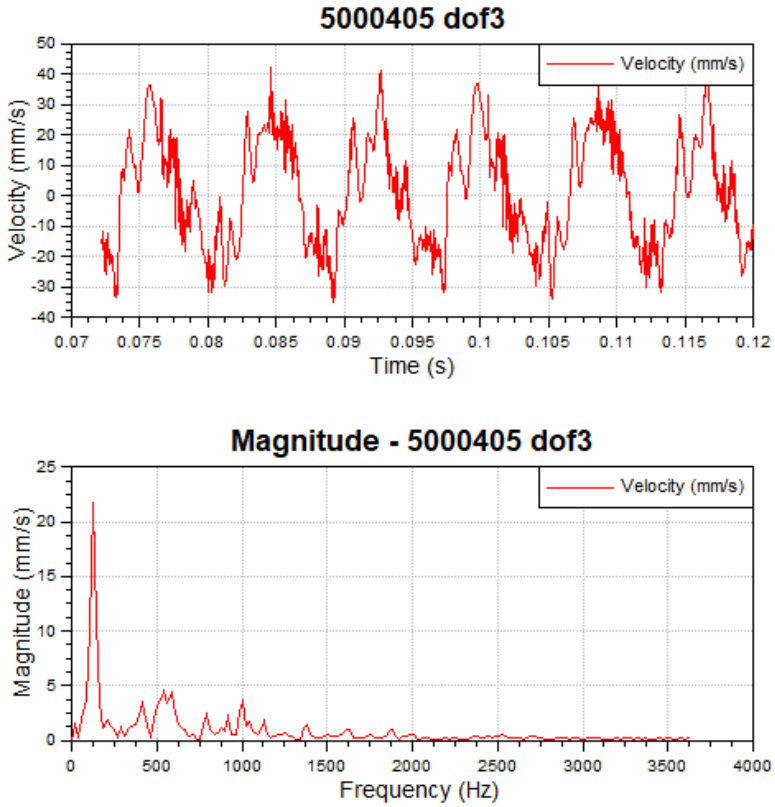

Figure 17. Acceleration in direction of DOF 3 at node 5000405

In order to better visualize the results versus frequency, semi-logarithmic plots (log-lin) were used.

Displacement versus frequency is shown in semi-logarithmic scale in Figure 18.

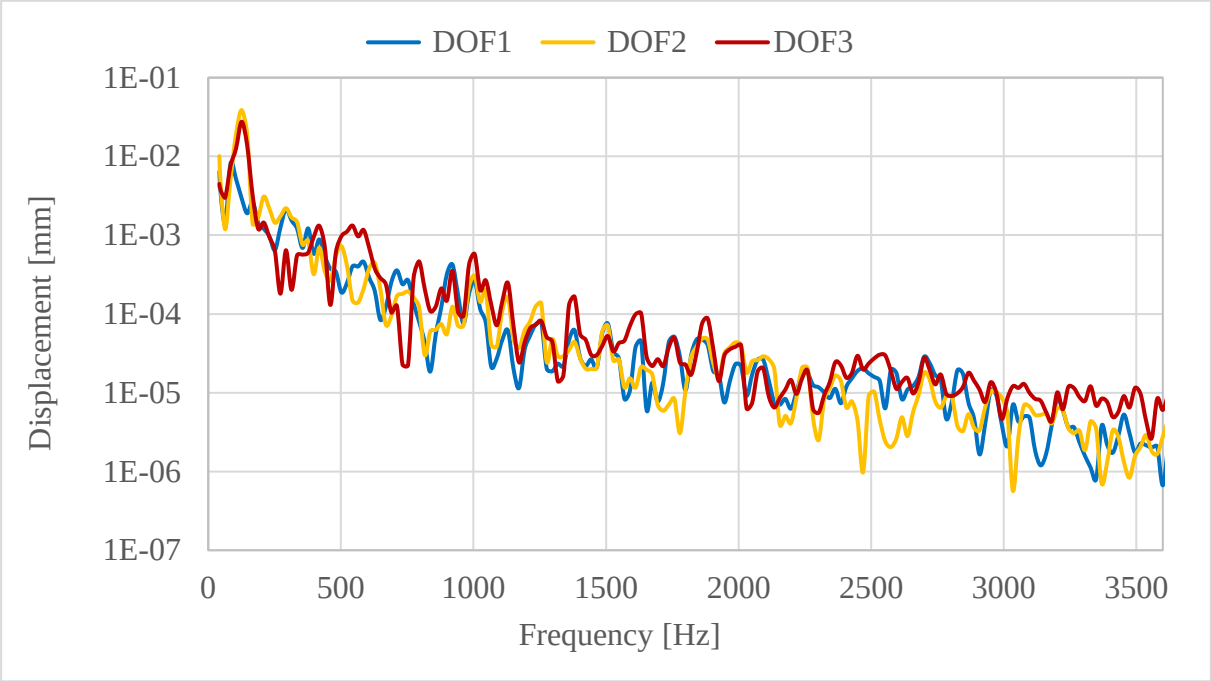

Figure 18. Displacement in frequency domain in semi-logarithmic scale at node 5000405

Velocity versus frequency is shown in semi-logarithmic scale in Figure 19.

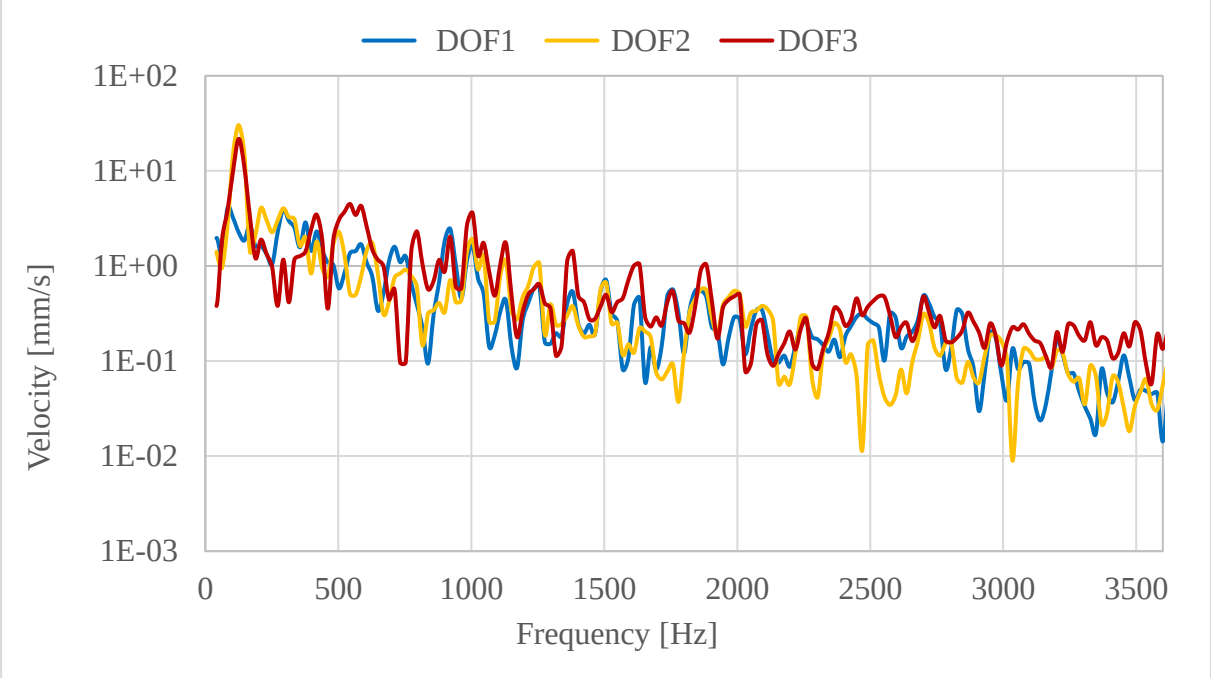

Figure 19. Velocity in frequency domain in semi-logarithmic scale at node 5000405

Acceleration versus frequency is shown in semi-logarithmic scale in Figure 20.

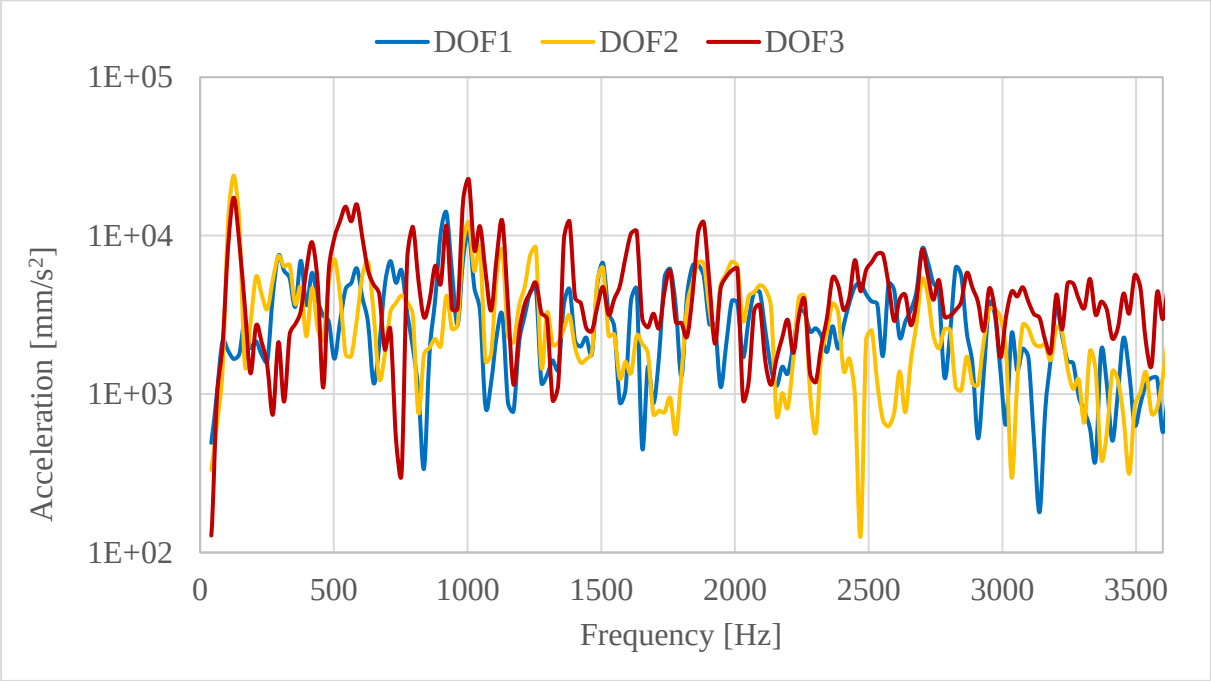

Figure 20. Acceleration in frequency domain in semi-logarithmic scale at node 5000405

Based on the curve behaviour, acceleration was chosen as an excitation. In other words, acceleration curve has the smallest gradient when averaged. Therefore, it is more likely that simplified acceleration curves (e.g. liner trendline or constant value curve) would yield better results than in the case of simplified displacement or velocity curves.

4.1.2. Simplifying the excitation

The real excitations at the bolt locations are very complicated. Each bolt has different values in direction of each DOF. For that reason, simplifying the excitations for each bolt location separately would still be very complicated. The simplification is thus extended to all bolt locations. That is, an averaged value of acceleration levels for all bolt locations (5000401 - 5000406) in direction of each translational DOF is calculated.

Figure 21 shows accelerations at each bolt location and an averaged acceleration in direction of DOF1.

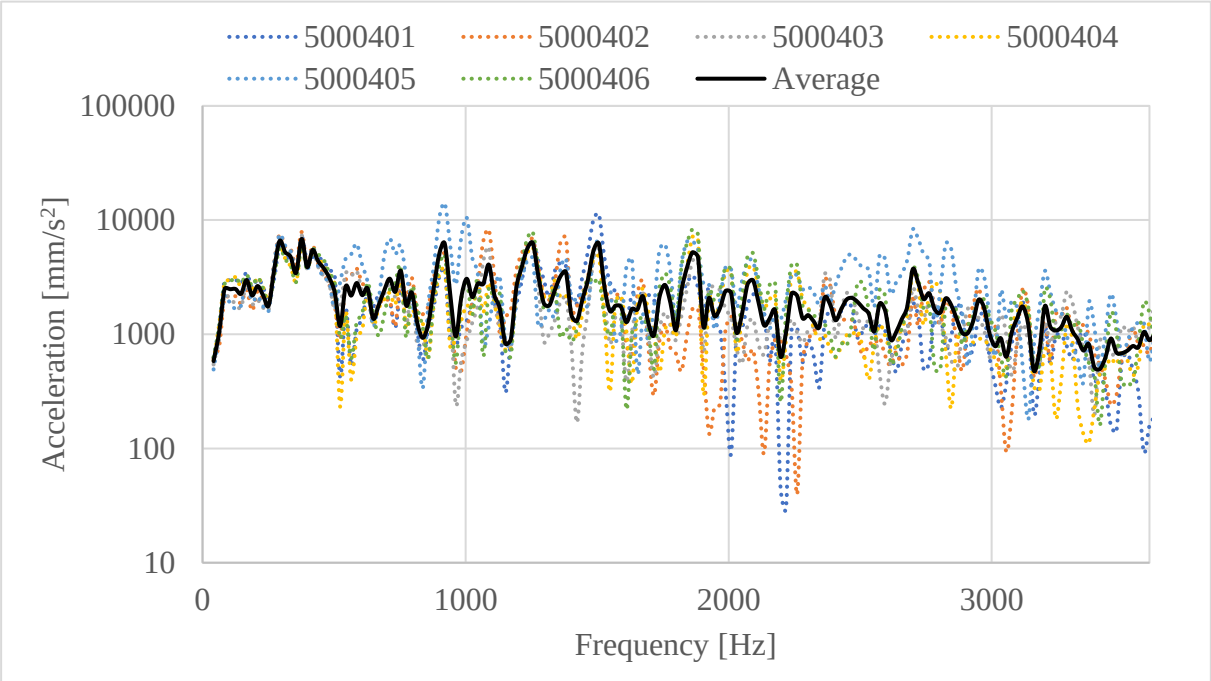

Figure 21. Averaged acceleration in direction of DOF 1

Figure 22 shows accelerations at each bolt location and an averaged acceleration in direction of DOF 2.

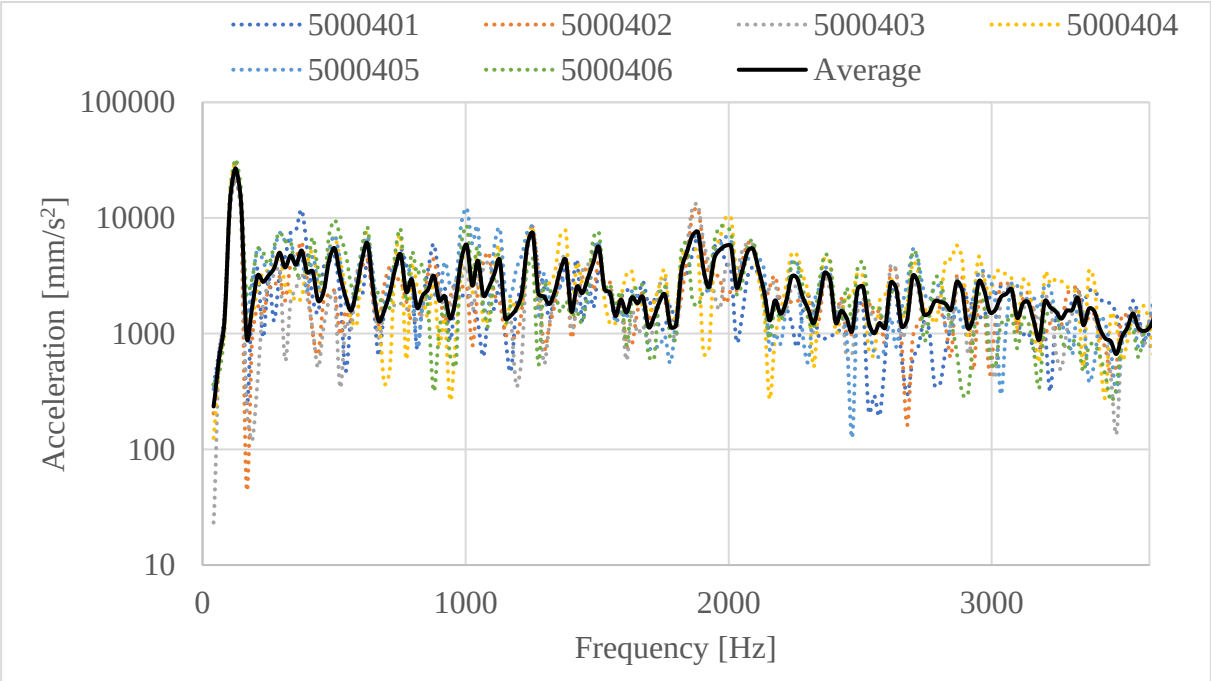

Figure 22. Averaged acceleration in direction of DOF 2

Figure 23 shows accelerations at each bolt location and an averaged acceleration in direction of DOF 3.

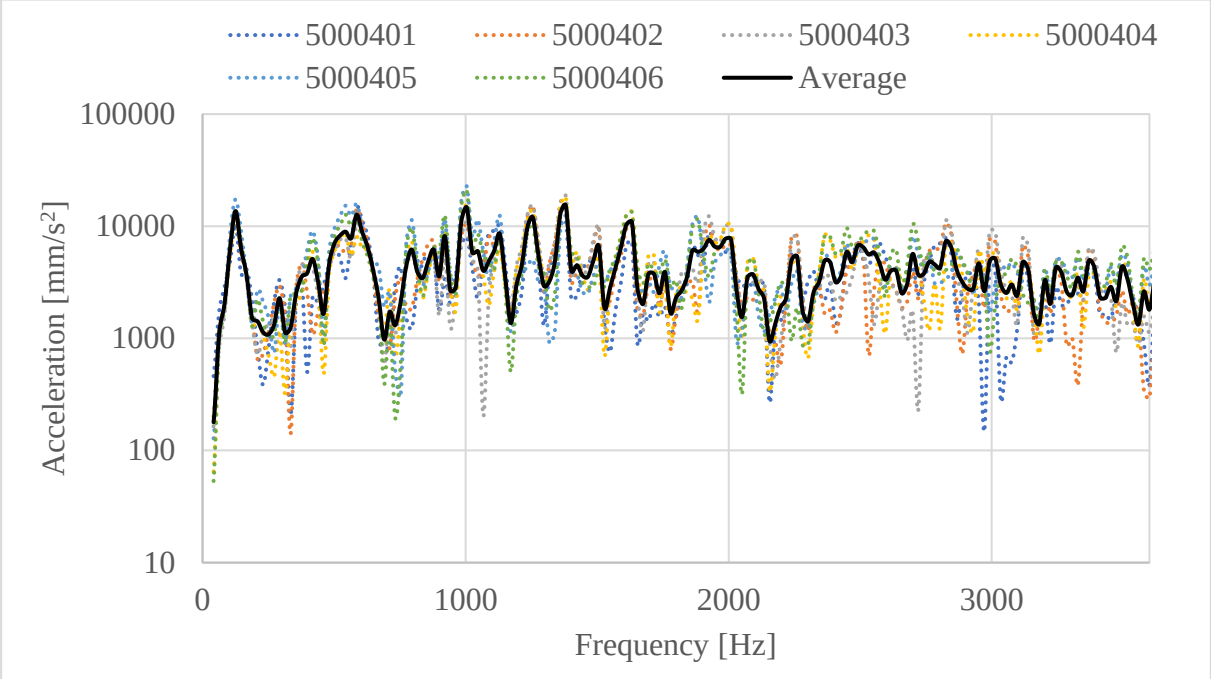

Figure 23. Averaged acceleration in direction of DOF 3

The averaged acceleration serves as the basis for further simplification. Different trendlines, which can be clearly described with the equations, are being generated based on the averaged acceleration.

Figure 24, Figure 25 and Figure 26 show linear, logarithmic, polynomial and power trendlines of the averaged acceleration in direction of each translational DOF.

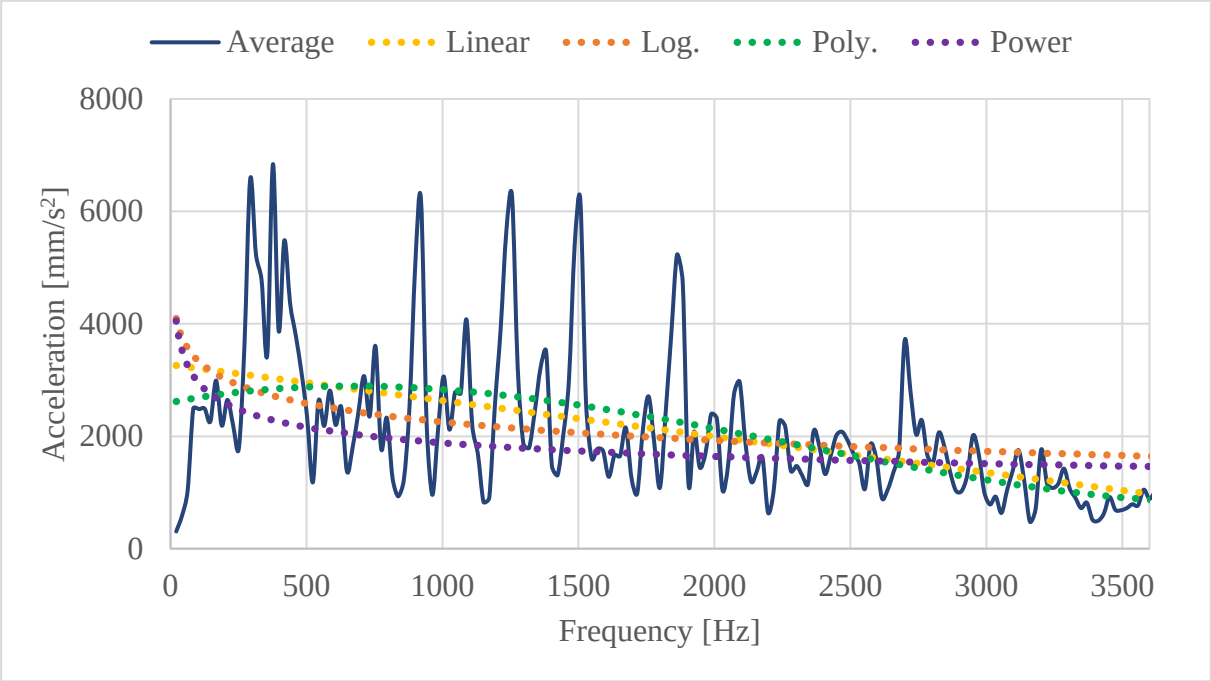

Figure 24. Averaged acceleration and trendlines in direction of DOF 1

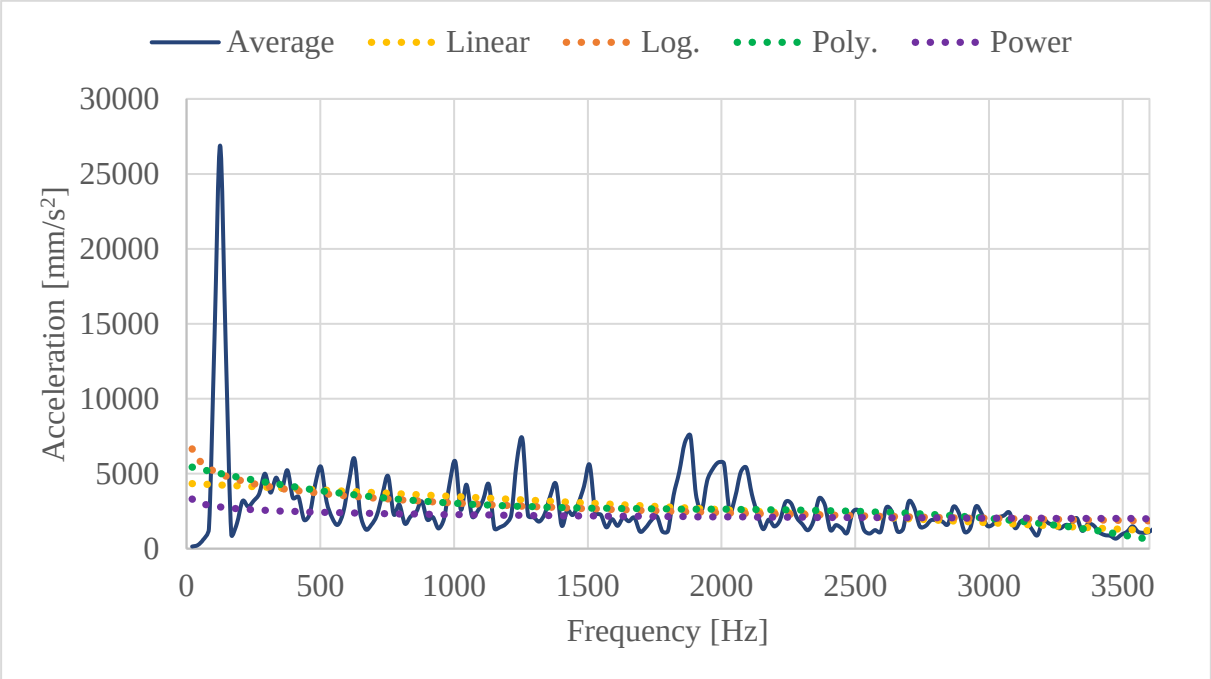

Figure 25. Averaged acceleration and trendlines in direction of DOF 2

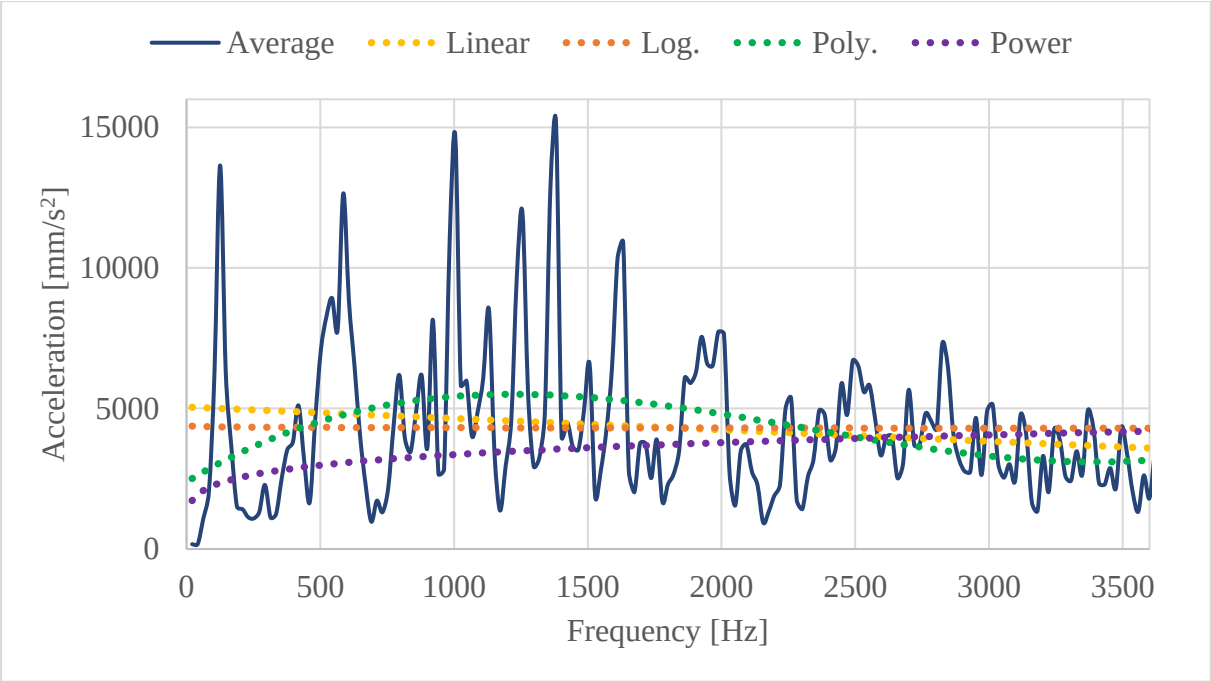

Figure 26. Averaged acceleration and trendlines in direction of DOF 3

4.1.3. Response to the baseline excitation

The next step is to evaluate the structure response to simplified excitations with the response to the baseline excitation generated by *AVL Excite* in module FE Analysis. *AVL Excite* writes an input file for *MSC Nastran* where Solution 111 (Modal Frequency Response) is performed. Data needed for generating the input file is shown in Figure 27.

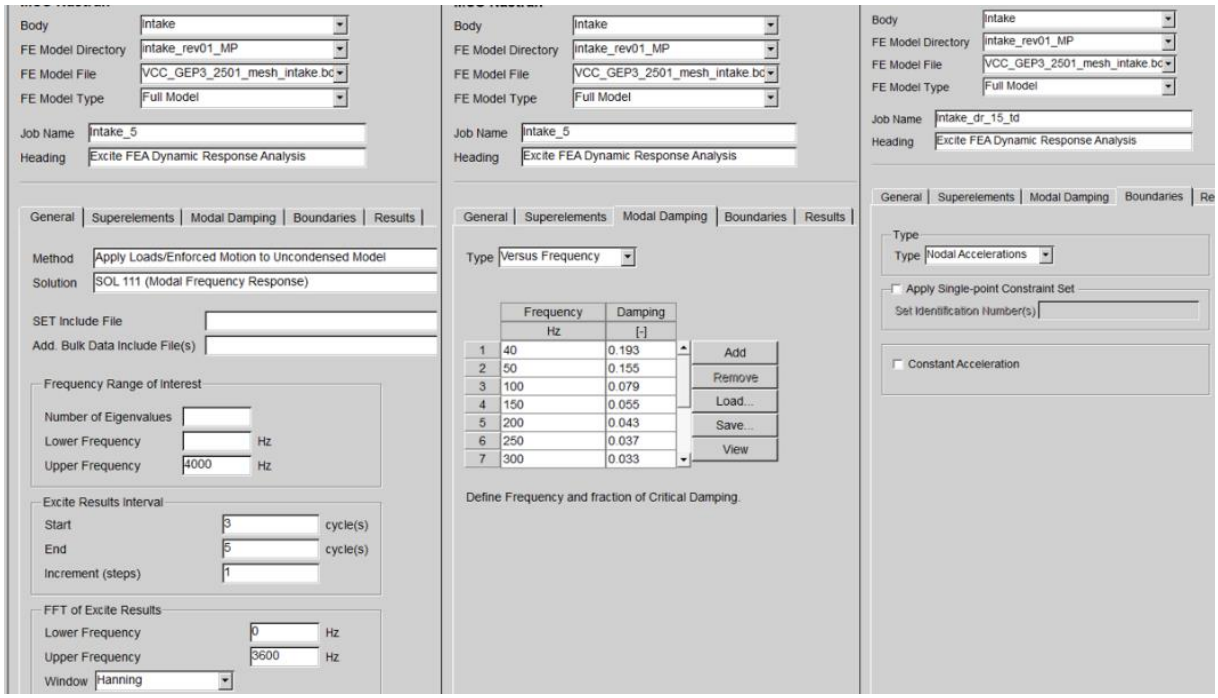

Figure 27. Data for Nastran input file

Example of *MSC Nastran* input file for performing Modal Frequency Response is shown in Appendix 1.

The response to the baseline excitation in narrow and 3rd octave band is shown in Figure 28.

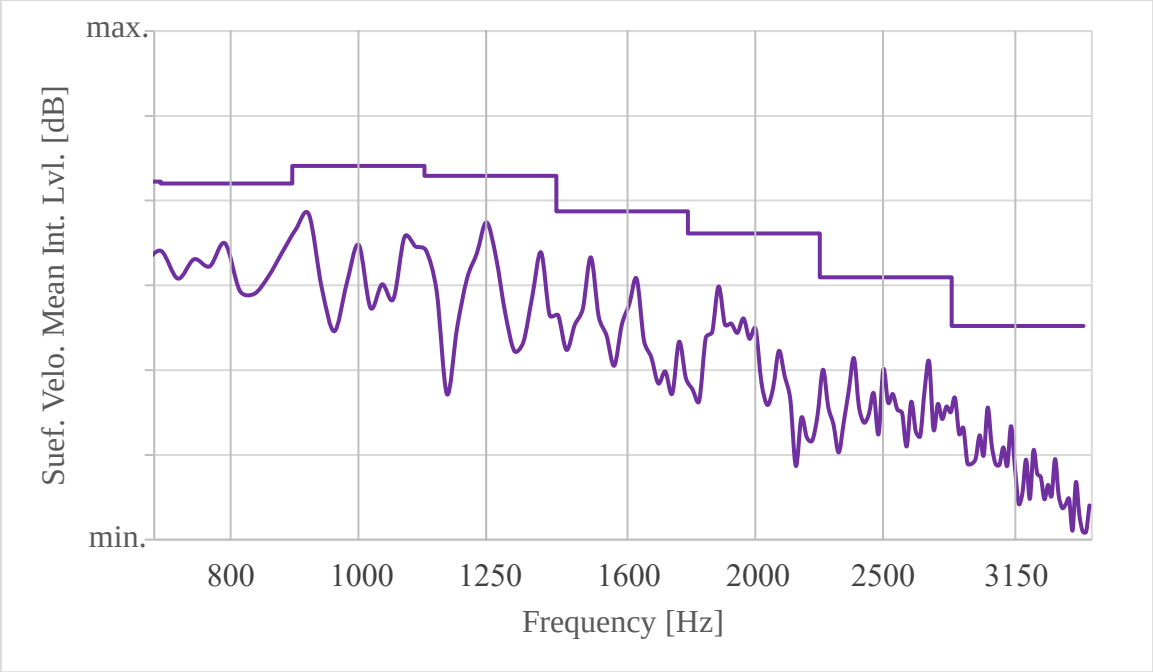

Figure 28. Response to the baseline excitation

4.1.3.1. Solution 111 (Modal Frequency Response) [20]

MSC Nastran SOL 111 (stands for Modal Frequency Response Analysis) represents a method for computing the frequency response of a structure. The method uses the mode shapes of the structure to reduce the size, uncouple the equations of motion (when modal or no damping is used), and make the numerical solution more efficient. Since the mode shapes are typically computed as part of the characterization of the structure, modal frequency response is a natural extension of normal modes analysis. The mode shapes are used to transform the problem in terms of the behaviour of the modes as opposed to the behavior of the grid points. In this uncoupled form, the equations of motion are written as a set of uncoupled single degree-of-freedom systems.

Forces can be in the form of applied forces and/or enforced motions (displacements, velocities or accelerations). A specific range of mode frequencies can be selected in analysis. Important is only that the modes whose resonant frequencies lie within the range of forcing frequencies are retained.

4.1.4. Surface velocity mean integral level evaluation

4.1.4.1. Simple comparison of responses to all excitation curves

Not all mentioned excitations will be shown here. Considering the accuracy of the results and curve complexity, the results will be presented only for average (base for all other curves) and linear excitation. Also, two special types of excitation (band and white noise excitation) will be explained later. Table 8 shows the absolute difference of structure response between simplified excitations and baseline excitation.

Table 8. Absolute difference of structure response between excitation curves

	AVERAGE	LINEAR	LOG.	POLY.	POWER
3rd octave band [Hz]	Difference in Surf. Velo. Mean Int. Lvl. [dB]				
800	0.3	1.6	0.6	1.9	1.8
1000	1.6	3.5	4.5	2.8	6.5
1250	2.4	0.5	1.3	0.5	3.1
1600	2.1	0.9	0.2	1.5	1.4
2000	0.8	3.2	3.5	2.2	4.6
2500	0.1	0.0	0.4	0.8	0.3
3150	2.7	2.3	3.7	2.8	3.5

≤ 3.5 dB	acceptable
3.5 – 4.5 dB	borderline
≥ 4.5 dB	not acceptable

4.1.4.2. Averaged excitation

As mentioned before, averaged excitation represents the first step of the analysis. Since all other excitations are based on it, it is very important that response to the averaged excitation is close to the baseline response. Averaged excitation in all three DOFs is shown in Figure 29.

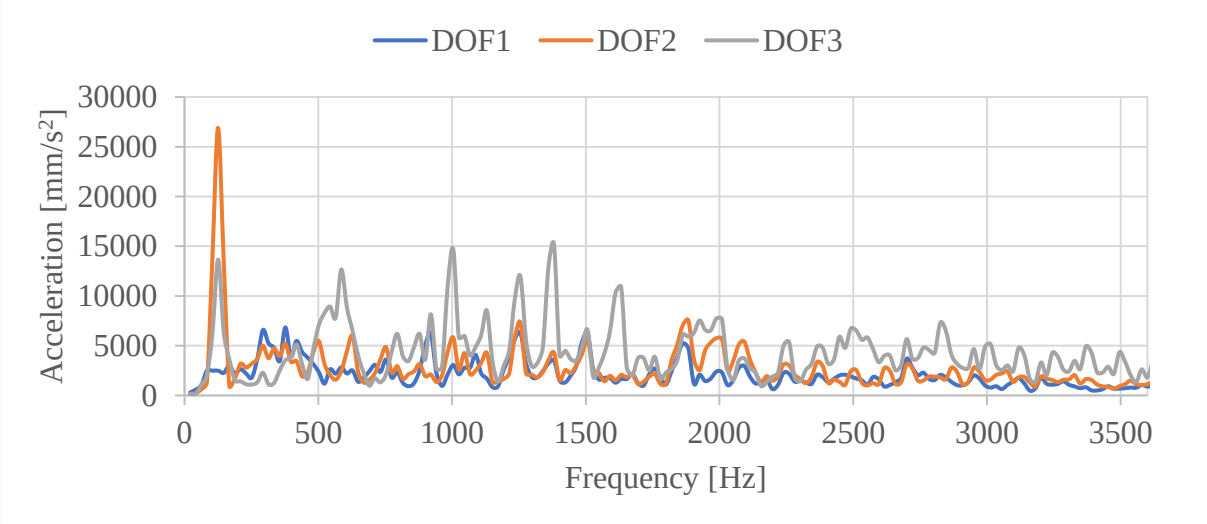

Figure 29. Averaged excitation

Response to the averaged excitation and comparison with the baseline response is shown in Figure 30.

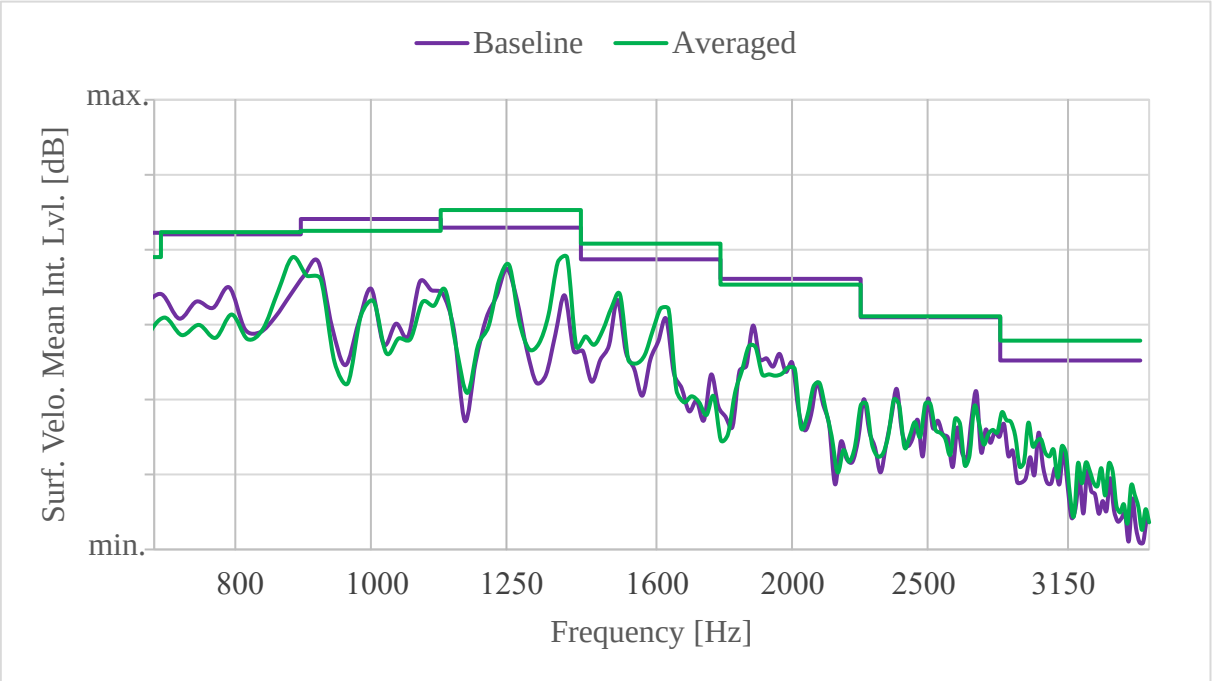

Figure 30. Structure response comparison between baseline and averaged excitation

Table 9 presents absolute difference of surface velocity mean integral level between baseline and averaged excitation. It can be noticed that structure response can still be well described with the averaged acceleration levels.

Table 9. Absolute difference of structure response between baseline and averaged excitation

3rd octave band [Hz]	Difference in Surf. Velo. Mean Int. Lvl. [dB]
800	0.3
1000	1.6
1250	2.4
1600	2.1
2000	0.8
2500	0.1
3150	2.7

4.1.4.3. Linear excitation

Averaged acceleration levels are further simplified by generating different simpler curves. The first step is finding a linear excitation. Linear excitation is defined as a linear trendline of the averaged acceleration levels at the bolt locations in DOFs 1-3. Linear excitation in all three DOFs is shown in Figure 31.

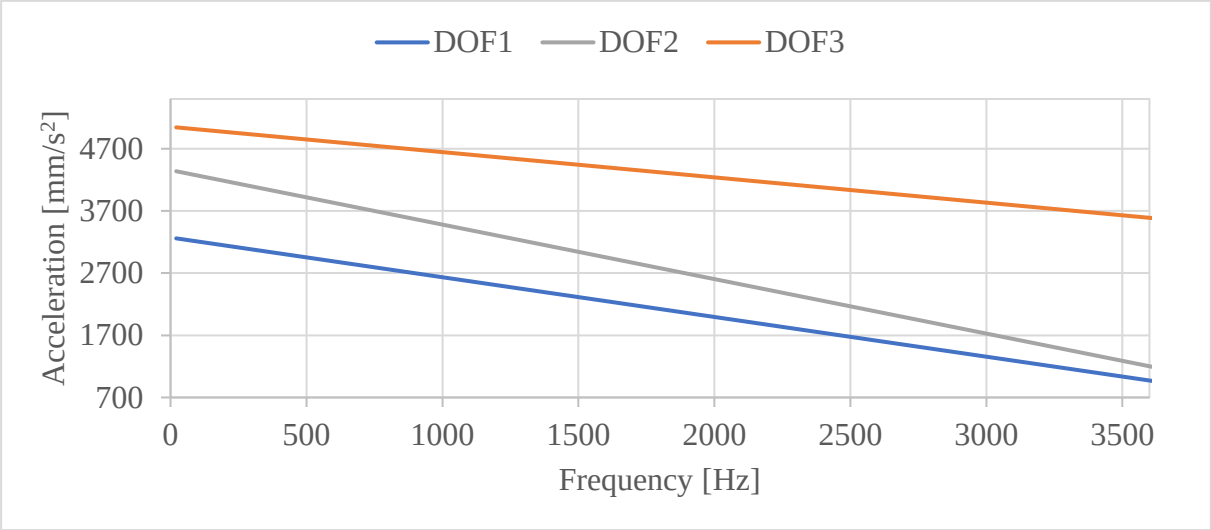

Figure 31. Linear excitation

Response to the linear excitation and comparison with the response to the baseline excitation is shown in Figure 32. Results are presented both in narrow and linear band.

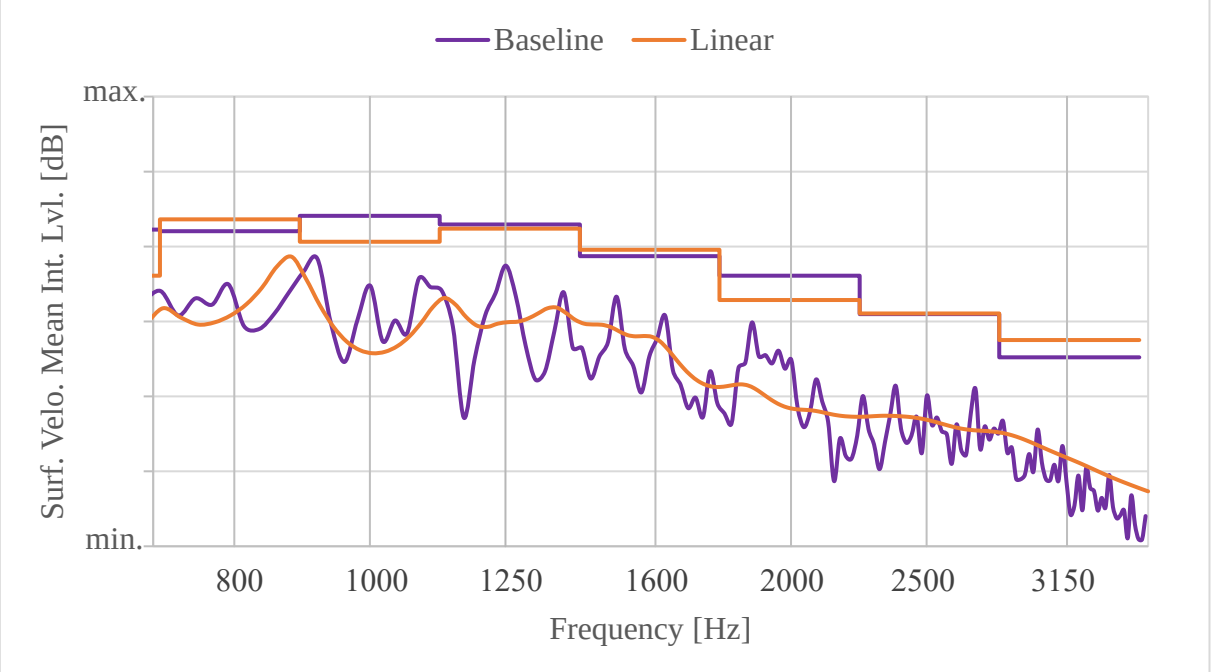

Figure 32. Structure response comparison between baseline and linear excitation

Table 10 presents absolute difference of surface velocity mean integral level between baseline and linear excitation.

Table 10. Absolute difference of structure response between baseline and linear excitation

3rd octave band [Hz]	Difference in Surf. Velo. Mean Int. Lvl. [dB]
800	1.6
1000	3.4
1250	0.6
1600	0.8
2000	3.3
2500	0.1
3150	2.3

Linear excitation is defined as acceptable in all observed 3rd octave bands.

4.1.4.4. White noise excitation

White noise excitation is a common type of excitation used at the beginning of the NVH analysis stage. It is characterized by a constant excitation value over the whole frequency range. When considering a known fact that dynamic excitation amplitude decreases with the frequency increase, it is obviously that this type of excitation is not quite realistic.

White noise excitation is hereby defined as a mean value of the averaged acceleration levels at the bolt locations in DOFs 1-3. White noise excitation in all three DOFs is shown in Figure 33.

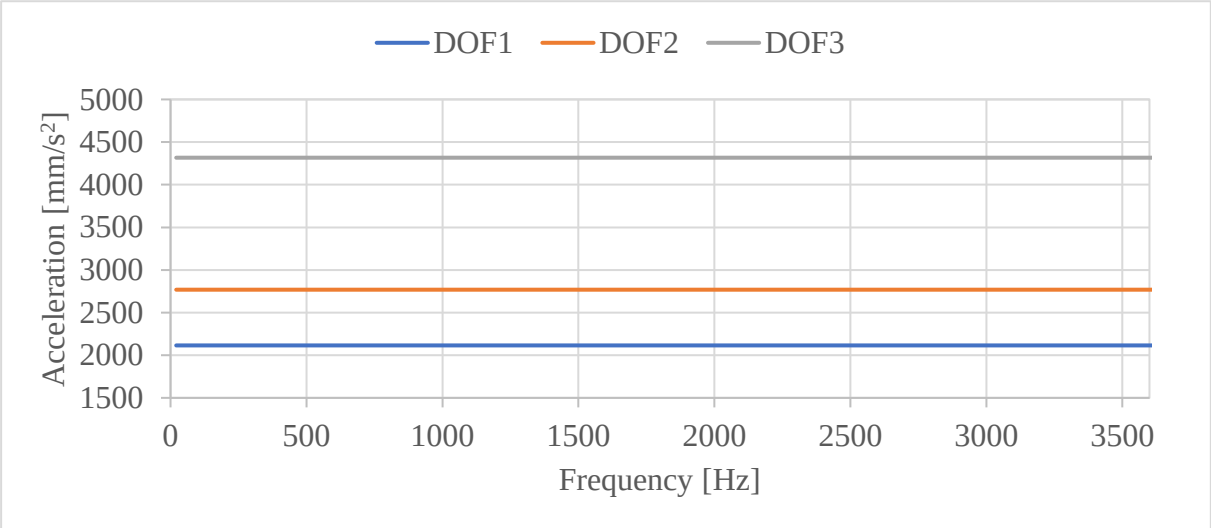

Figure 33. White noise excitation

Structure response to the white noise excitation and comparison with the baseline result is shown in Figure 34.

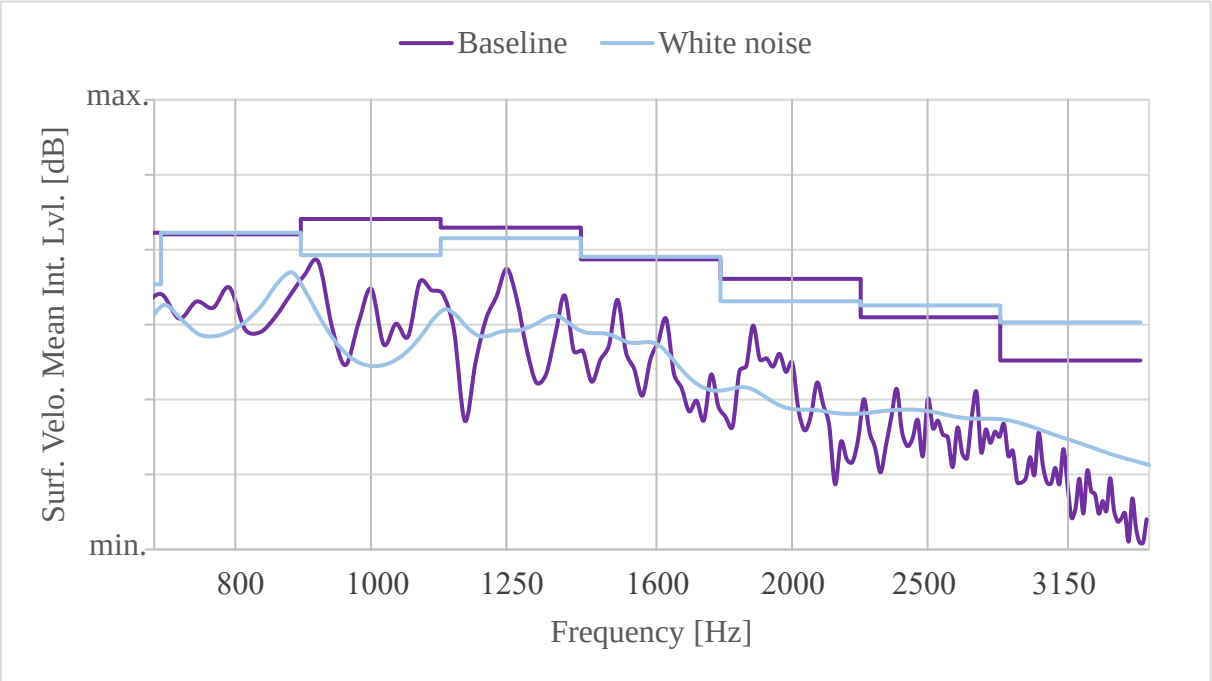

Figure 34. Structure response comparison between baseline and white noise excitation

Table 11 presents absolute difference of surface velocity mean integral level between baseline and white noise excitation. As assumed, white noise excitation generates too high structure response at higher frequencies.

Table 11. Absolute difference of structure response between baseline and white noise excitation

3rd octave band [Hz]	Difference in Surf. Velo. Mean Int. Lvl. [dB]
800	0.2
1000	4.8
1250	1.4
1600	0.3
2000	3.0
2500	1.6
3150	5.1

4.1.4.5. Band excitation

Band excitation is a special simplified excitation type. It can be defined as a white noise excitation that changes with the change of the 3rd octave band. The advantage of that type of excitation is taking into the consideration a structure behaviour within the narrower band which results in more accurate assumption of the structure response.

Band excitation for the intake manifold A is defined as the linear average of the averaged acceleration levels at the bolt locations in each 3rd octave band separately in direction of DOFs 1-3. Therefore, band excitation is constant in each band in the direction of observed DOFs. Band excitation in all three DOFs is shown in Figure 35.

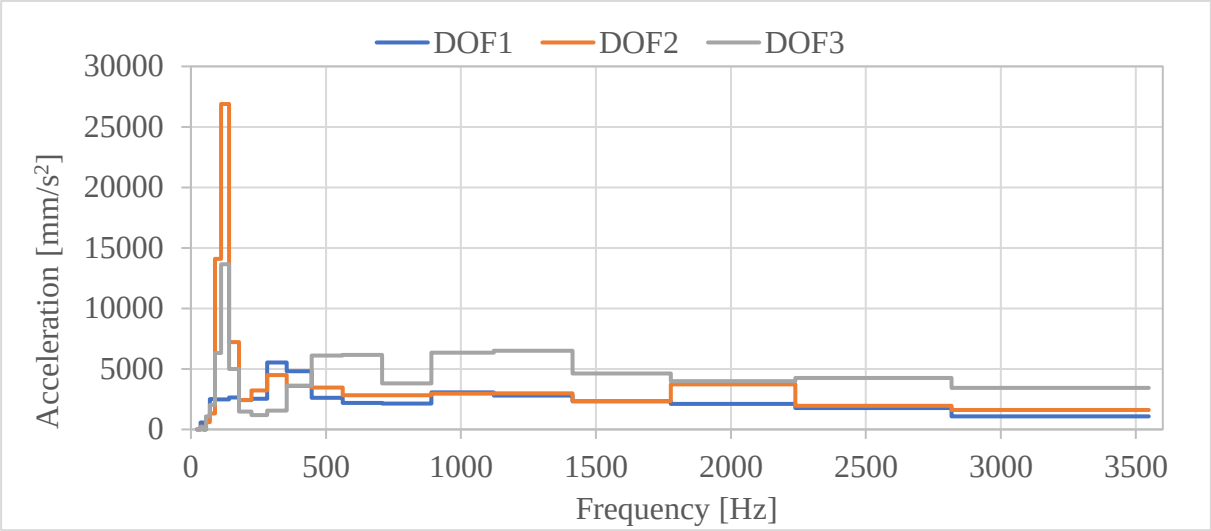

Figure 35. Band excitation

Response to the band excitation and comparison with the baseline result is shown in Figure 36. Table 12 presents absolute difference of surface velocity mean integral level between baseline and band excitation. Comparing the response with the response to a linear excitation shown in Table 10, it can be noticed that band excitation generates slightly more acceptable response than the linear excitation.

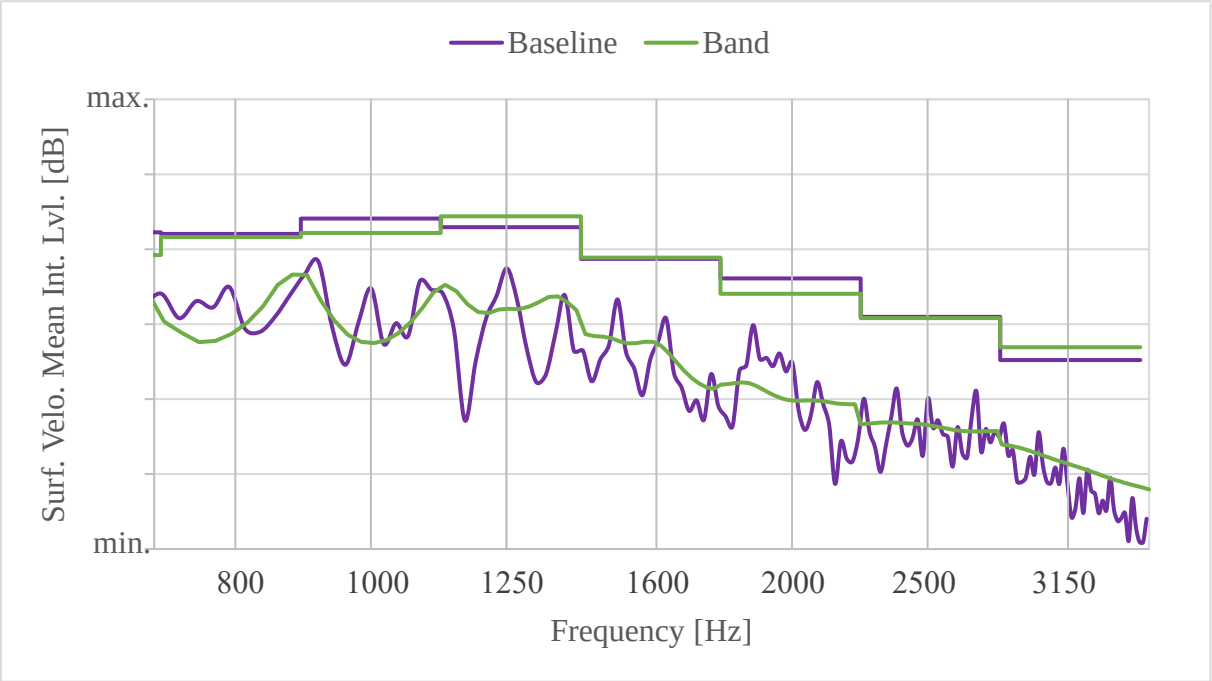

Figure 36. Structure response comparison between baseline and band excitation

Table 12. Absolute difference of structure response between baseline and band excitation

3rd octave band [Hz]	Difference in Surf. Velo. Mean Int. Lvl. [dB]
800	0.4
1000	1.9
1250	1.5
1600	0.2
2000	2.1
2500	0.2
3150	1.7

4.1.4.6. Overall comparison

Figure 37 shows the overall comparison of the structure response to defined excitation types. As can be noticed, linear and band excitations give the most acceptable results. Band excitation is more complex than the linear because it cannot be described with the simple equation for the whole frequency range. Furthermore, linear excitation could be simply scaled according to the difference in engine power (or other relevant characteristics) for observed engine components. Therefore, linear excitation is defined as the most acceptable.

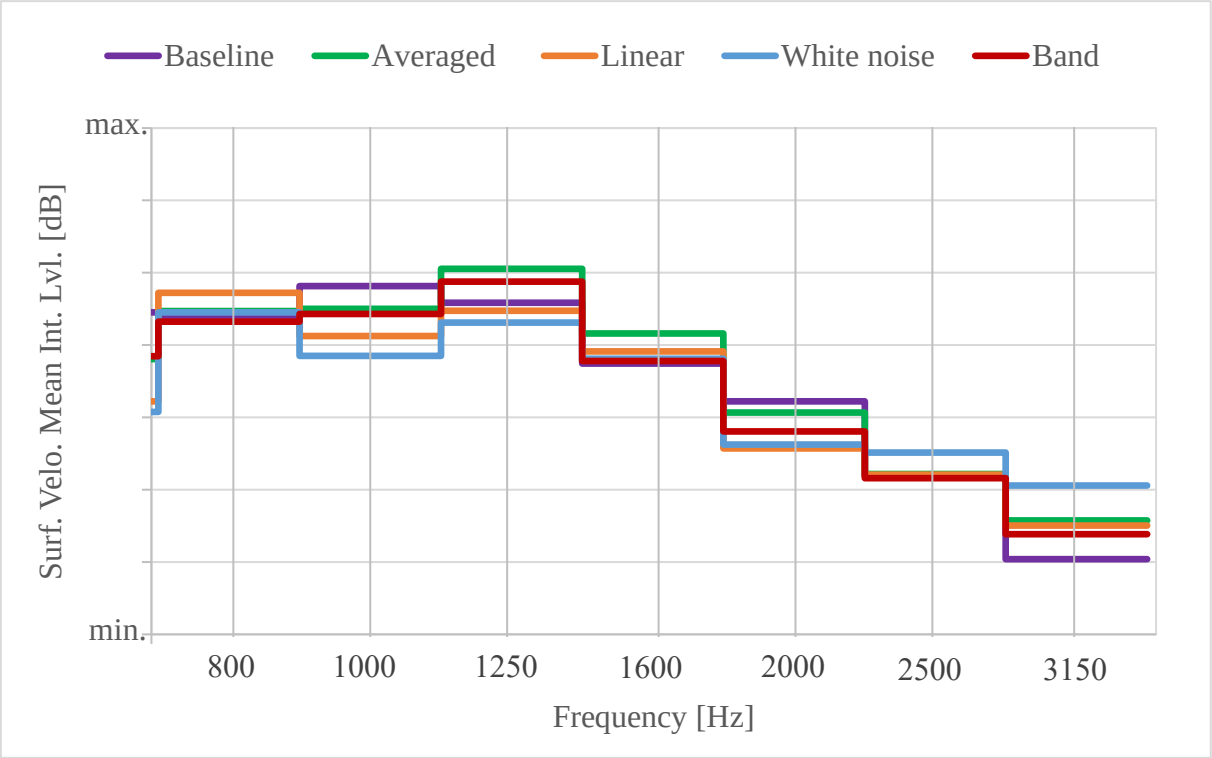

Figure 37. Overall comparison in 3rd octave bands

4.1.5. Surface velocity plots

Figures from Figure 38 to Figure 43 show surface normal velocity plots in 3rd octave bands with centre frequencies from 800 Hz to 3150 Hz. Areas with poor surface velocity distribution (when comparing with baseline) are marked. At the end, an overall excitation evaluation, based on both surface velocity plots and surface velocity mean integral levels evaluation, is presented. Linear excitation is defined as the most acceptable.

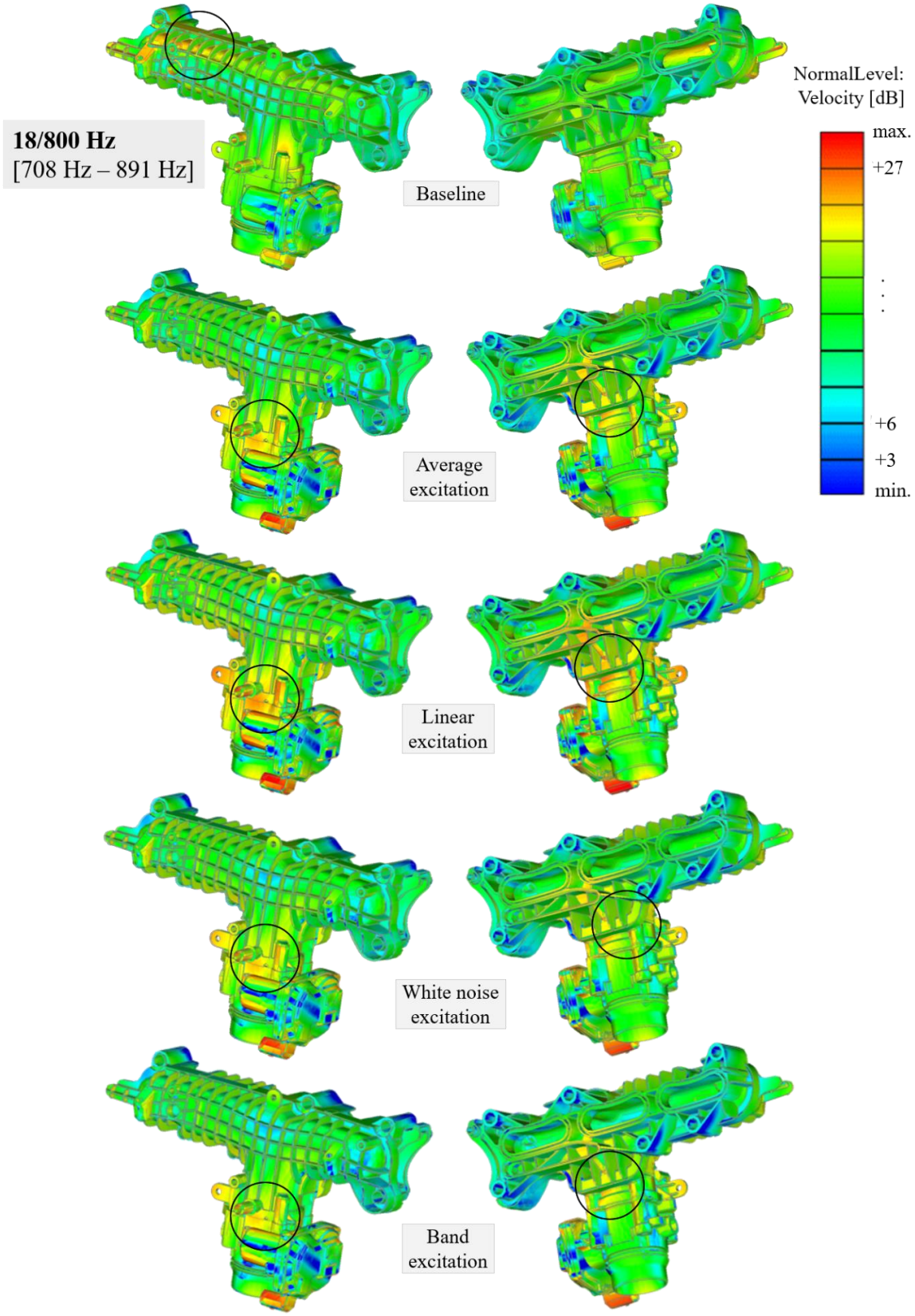

Figure 38. Structure response in form of normal velocity levels for 3rd octave band 800 Hz

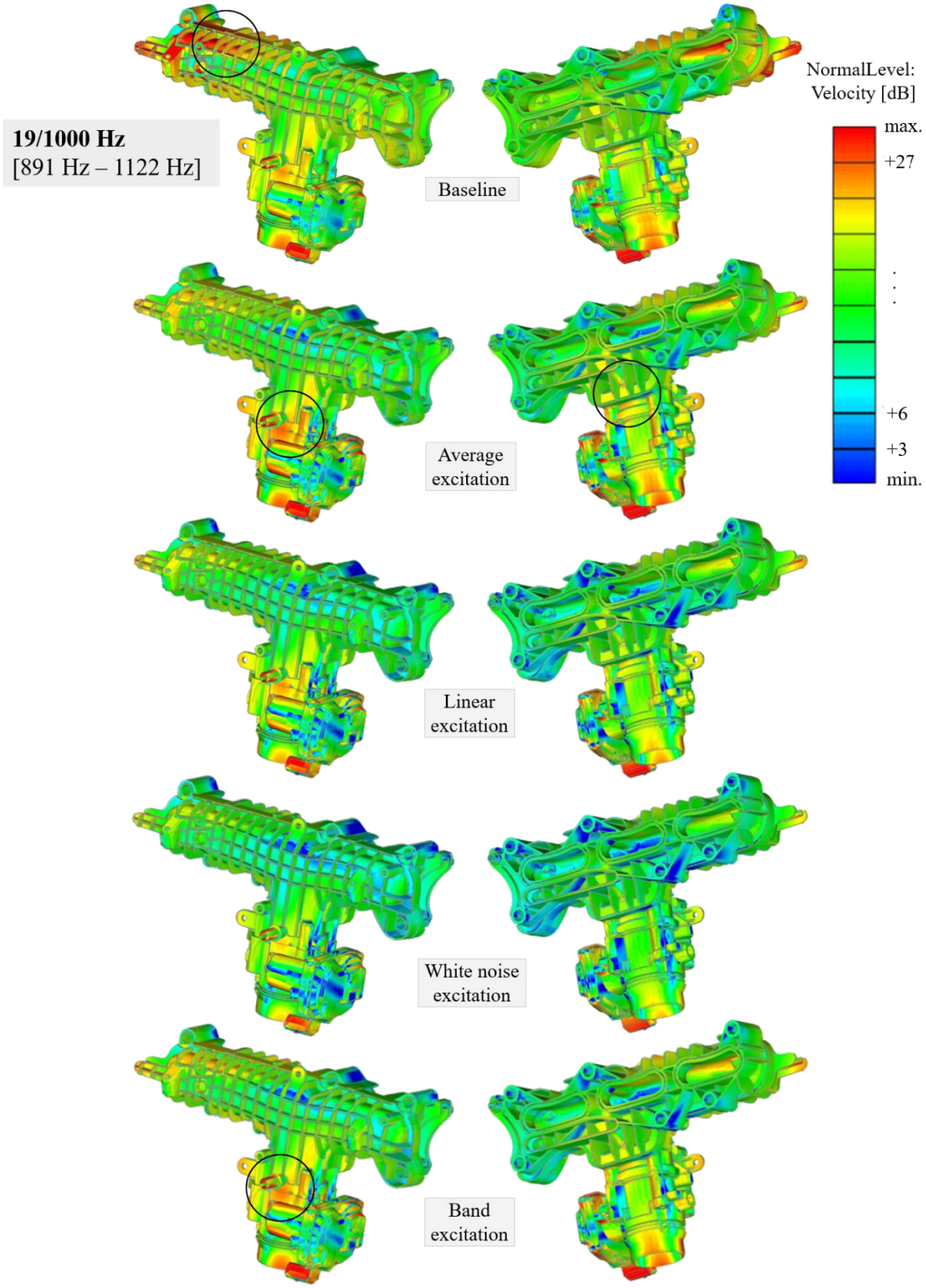

Figure 39. Structure response in form of normal velocity levels for 3rd octave band 1000 Hz

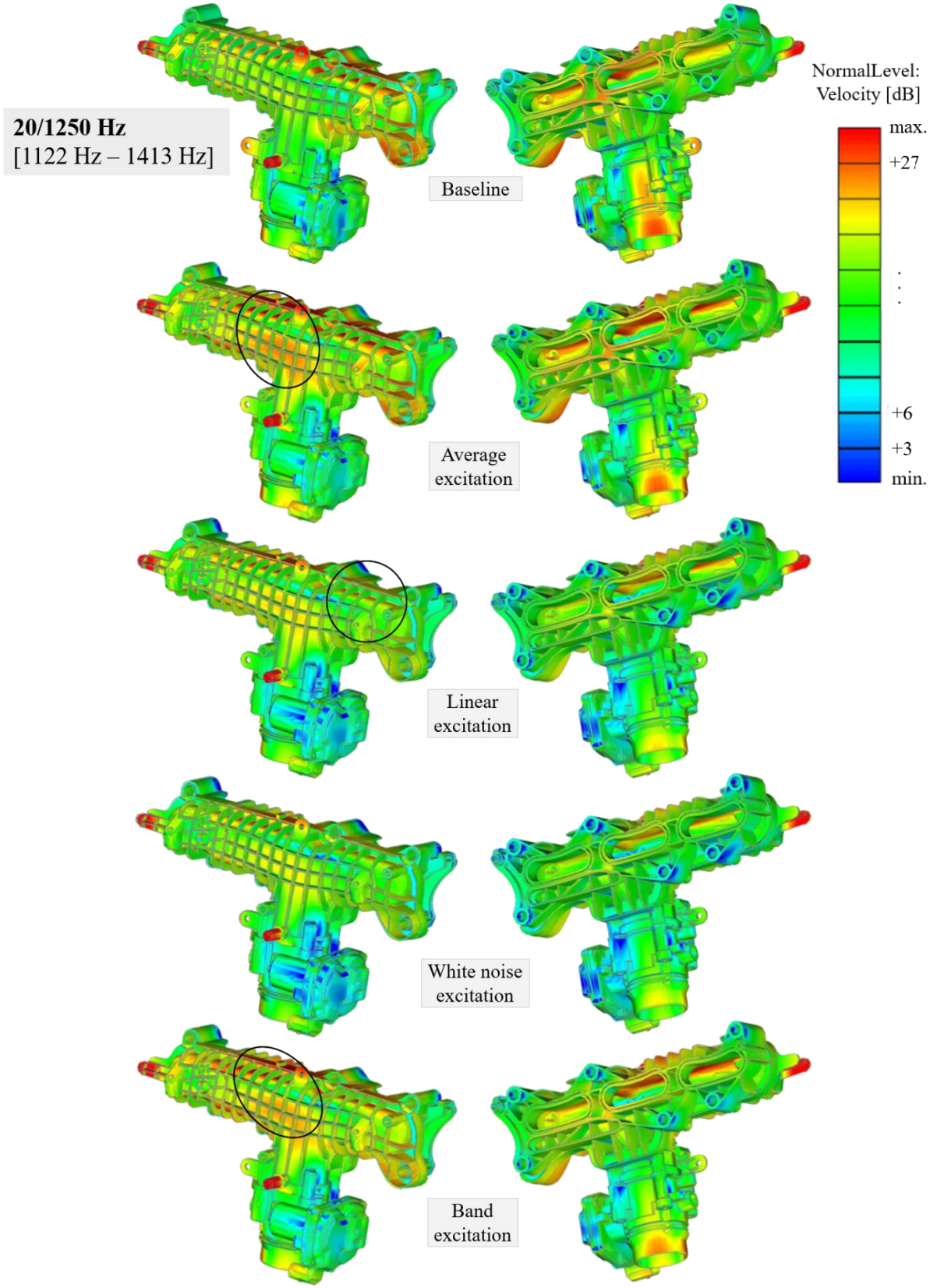

Figure 40. Structure response in form of normal velocity levels for 3rd octave band 1250 Hz

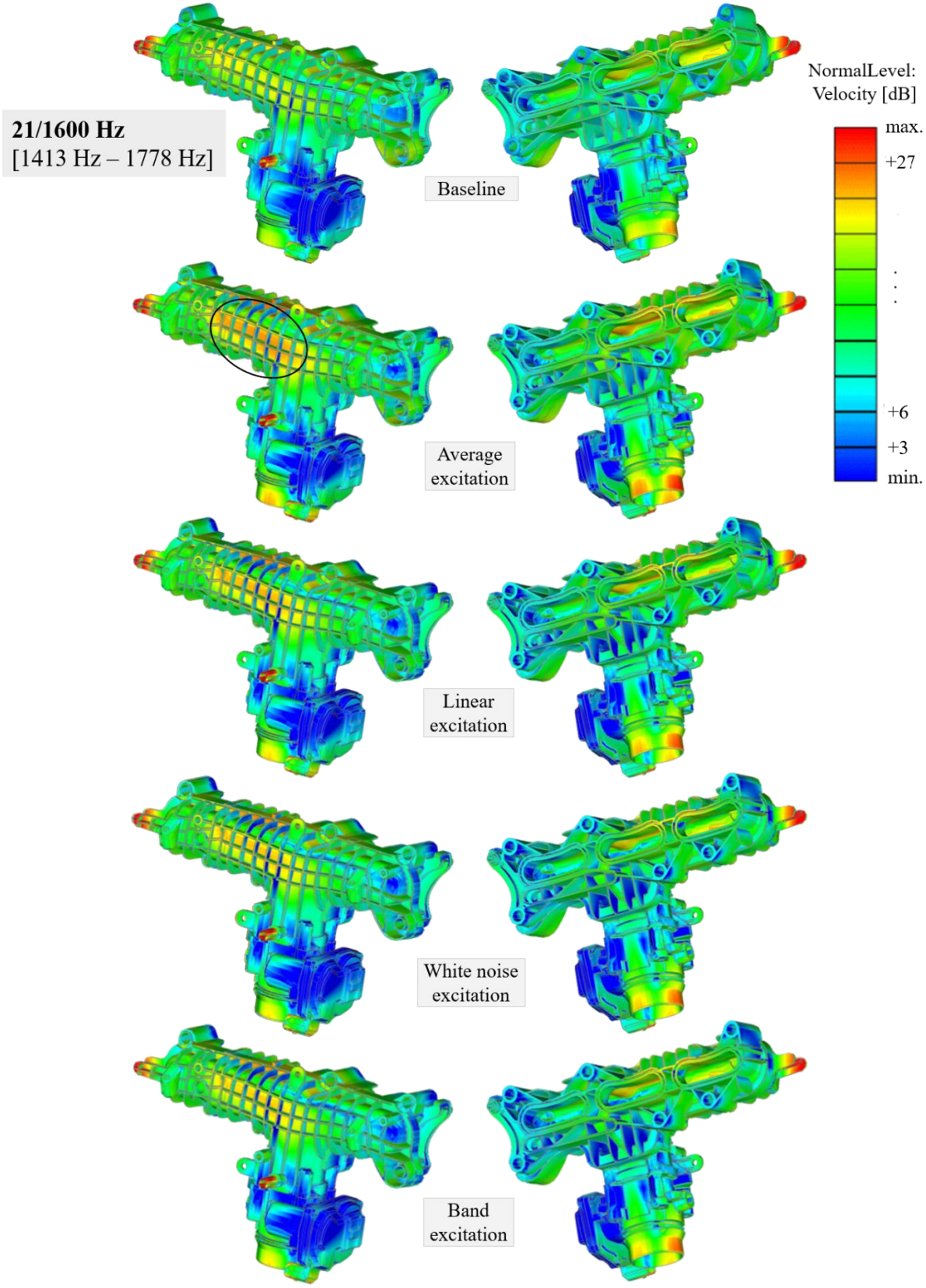

Figure 41. Structure response in form of normal velocity levels for 3rd octave band 1600 Hz

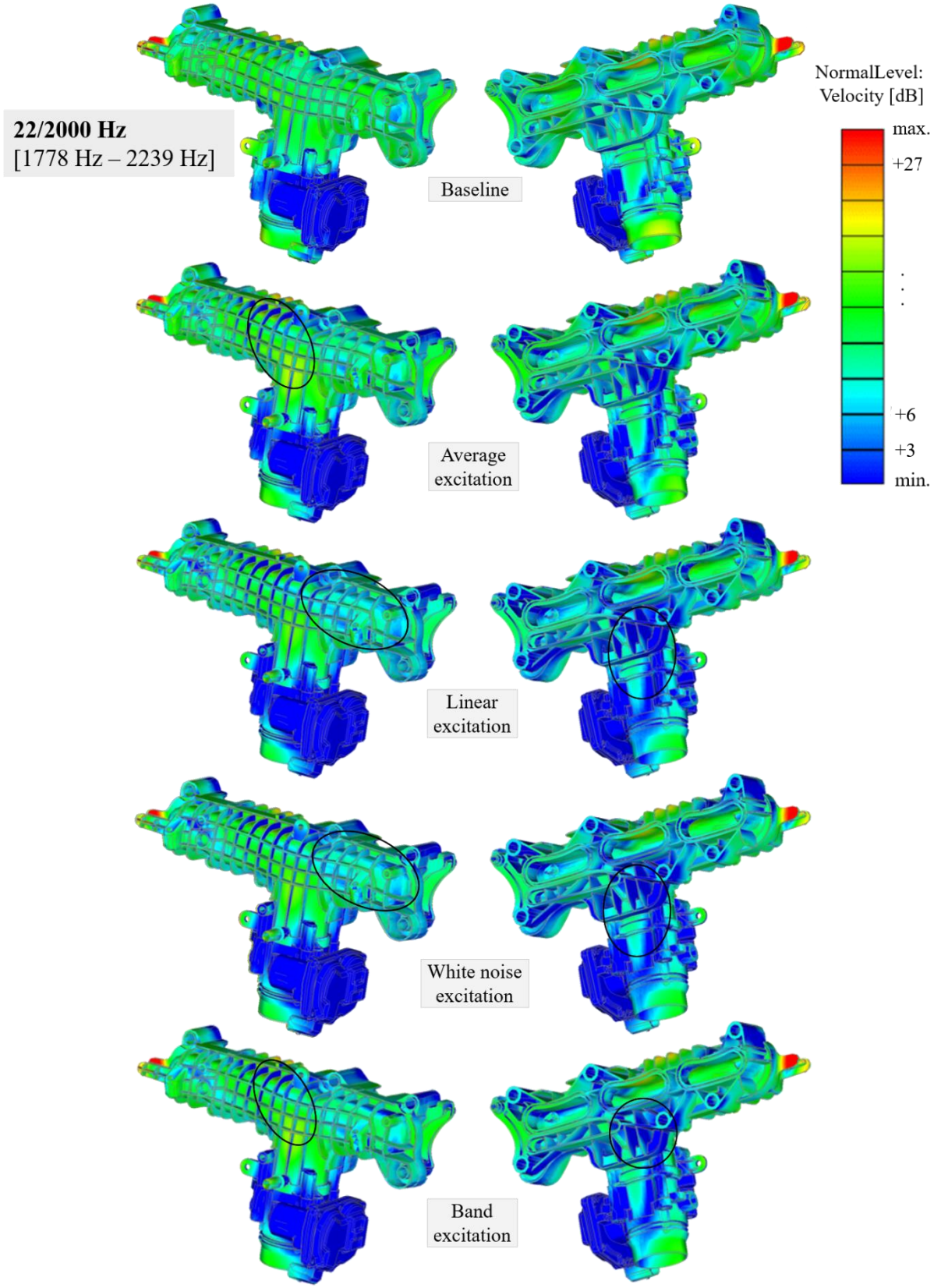

Figure 42. Structure response in form of normal velocity levels for 3rd octave band 2000 Hz

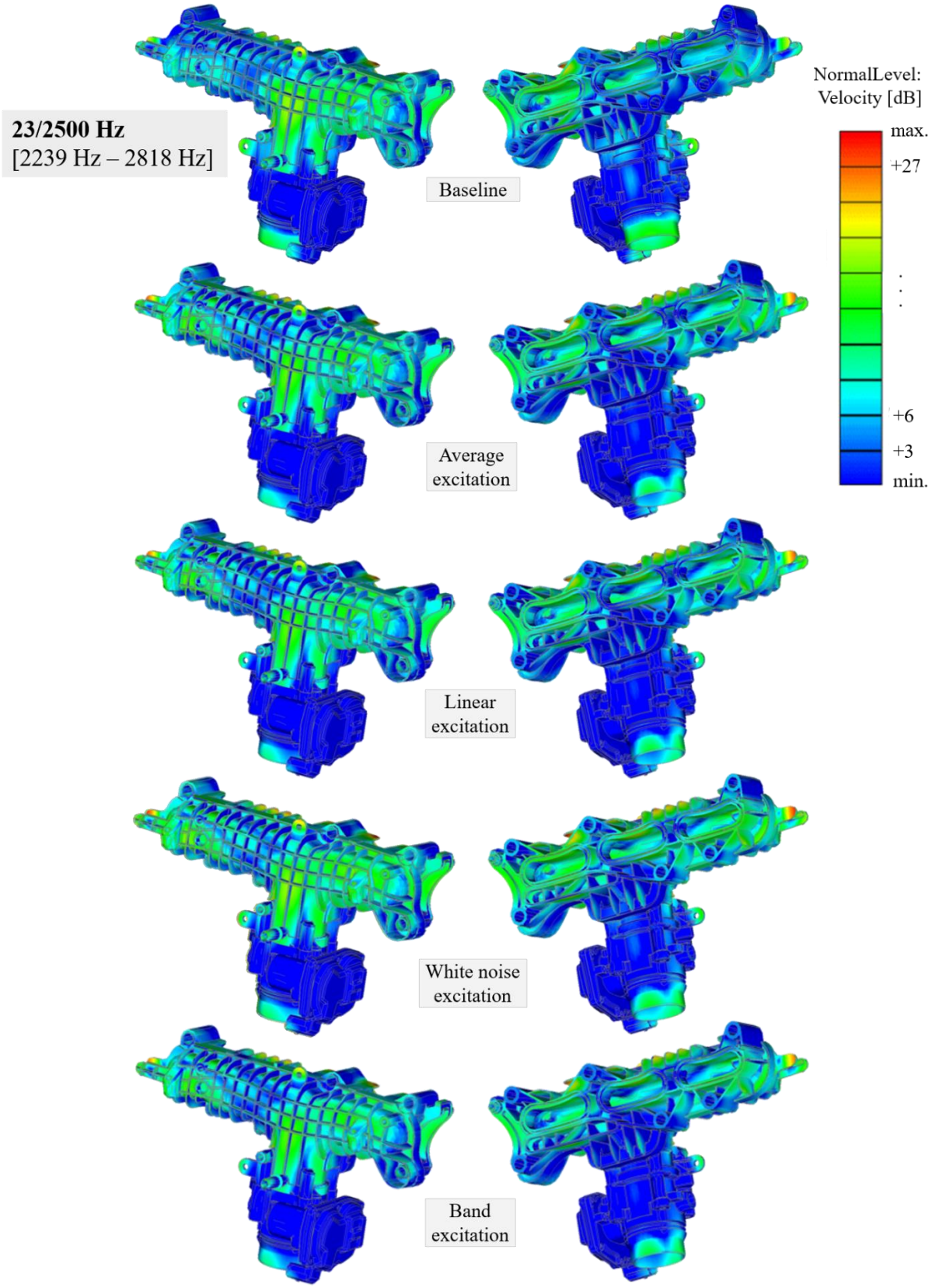

Figure 43. Structure response in form of normal velocity levels for 3rd octave band 2500 Hz

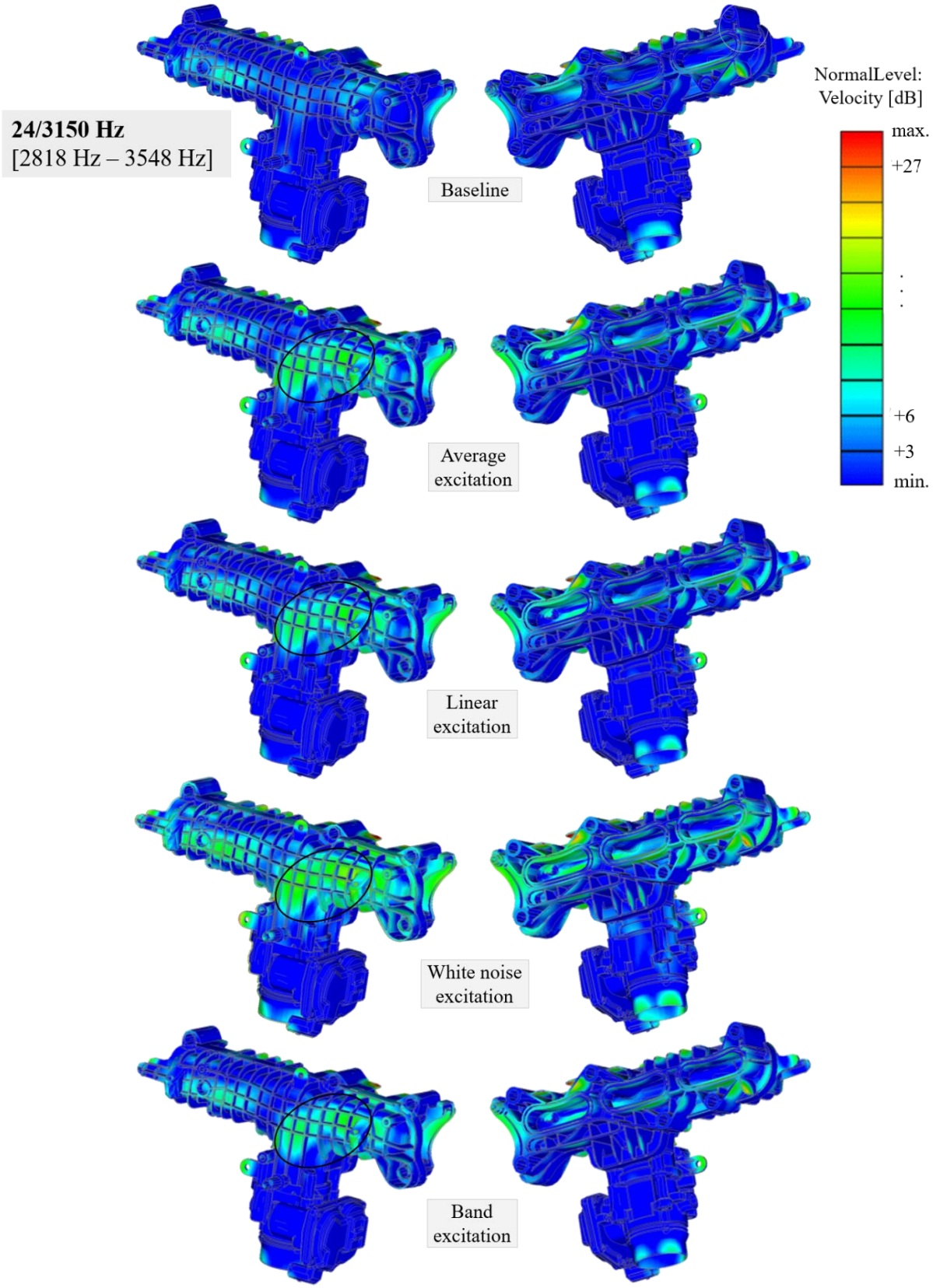

Figure 44. Structure response in form of normal velocity levels for 3rd octave band 3150 Hz

4.1.5.1. Surface velocity plots evaluation

1. **3rd octave band 18/800 Hz:** Area marked on the baseline result is described with none of the applied excitations. On the other hand, all excitations generate higher response at some other areas.

Based on the surface velocity plots and surface velocity mean integral level evaluation, structure response in considered 3rd octave band is borderline with all excitations.

2. **3rd octave band 19/1000 Hz:** Area marked on the baseline result is not described well with the applied excitations. On the other hand, average and band excitations generate higher response at other marked areas.

Based on the surface velocity plots and surface velocity mean integral level evaluation, structure response in considered 3rd octave band is acceptable with average, linear and band excitation, but not acceptable with white noise excitation.

3. **3rd octave band 20/1250 Hz:** Average and band excitation generate higher structure response at marked area than baseline. On the other hand, linear excitation generates lower response at marked area.

Based on the surface velocity plots and surface velocity mean integral level evaluation, structure response in considered 3rd octave band is borderline with average, white noise and band excitation, but acceptable with linear excitation.

4. **3rd octave band 21/1600 Hz:** All excitations generate higher structure response at marked area than baseline.

Based on the surface velocity plots and surface velocity mean integral level evaluation, structure response in considered 3rd octave band is acceptable with all excitations.

5. **3rd octave band 22/2000 Hz:** Average and band excitation generate higher structure response at marked area than baseline. On the other hand, linear and white noise excitation generate lower response at marked area.

Based on the surface velocity plots and surface velocity mean integral level evaluation, structure response in considered 3rd octave band is acceptable with all excitations.

6. **3rd octave band 23/2500 Hz:** All excitations generate structure response very similar to the baseline.

Based on the surface velocity plots and surface velocity mean integral level evaluation, structure response in considered 3rd octave band is acceptable with all excitations.

7. **3rd octave band 24/3150 Hz:** All excitations generate higher structure response at marked areas than baseline.

Based on the surface velocity plots and surface velocity mean integral level evaluation, structure response in considered 3rd octave band is acceptable with average, linear and band excitations, but not acceptable with white noise excitation.

4.2. Intake manifold B

Figure 45 shows a schematic representation of the intake manifold B. Intake manifold B is quite different than the intake manifold A. It consists of the plastic body and two metal brackets. Connection with the cylinder head is enabled by three bolts placed at the metal brackets and five bolts placed on the plastic body.

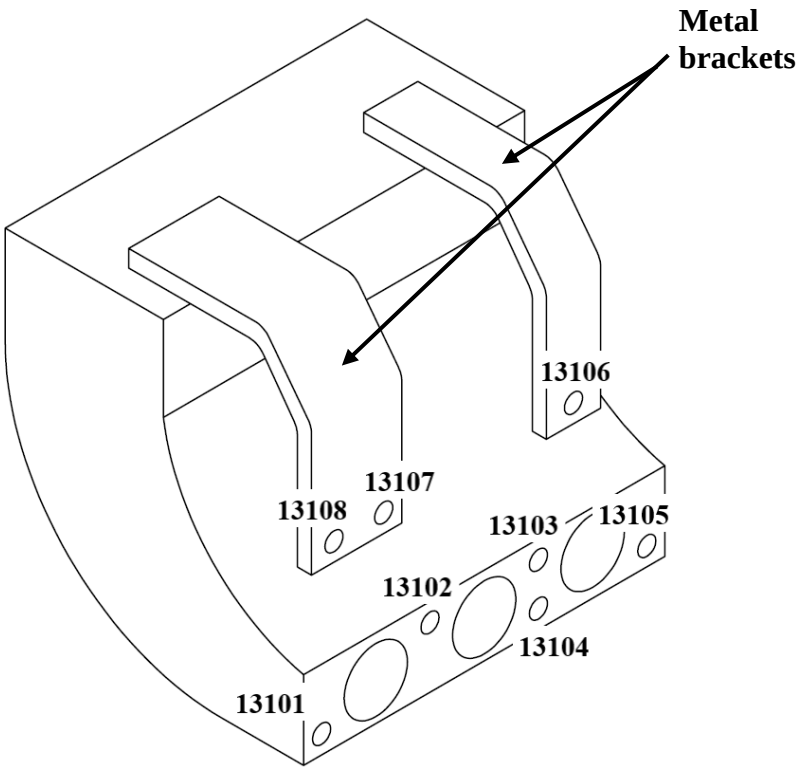

Figure 45. Schematic representation of the intake manifold B

4.2.1. Simplifying the excitation

After obtaining the acceleration values at the bolt locations, averaged value of acceleration levels for all bolt locations is calculated.

Figure 46 to Figure 48 show averaged acceleration values and some trendlines that will later be used as excitations.

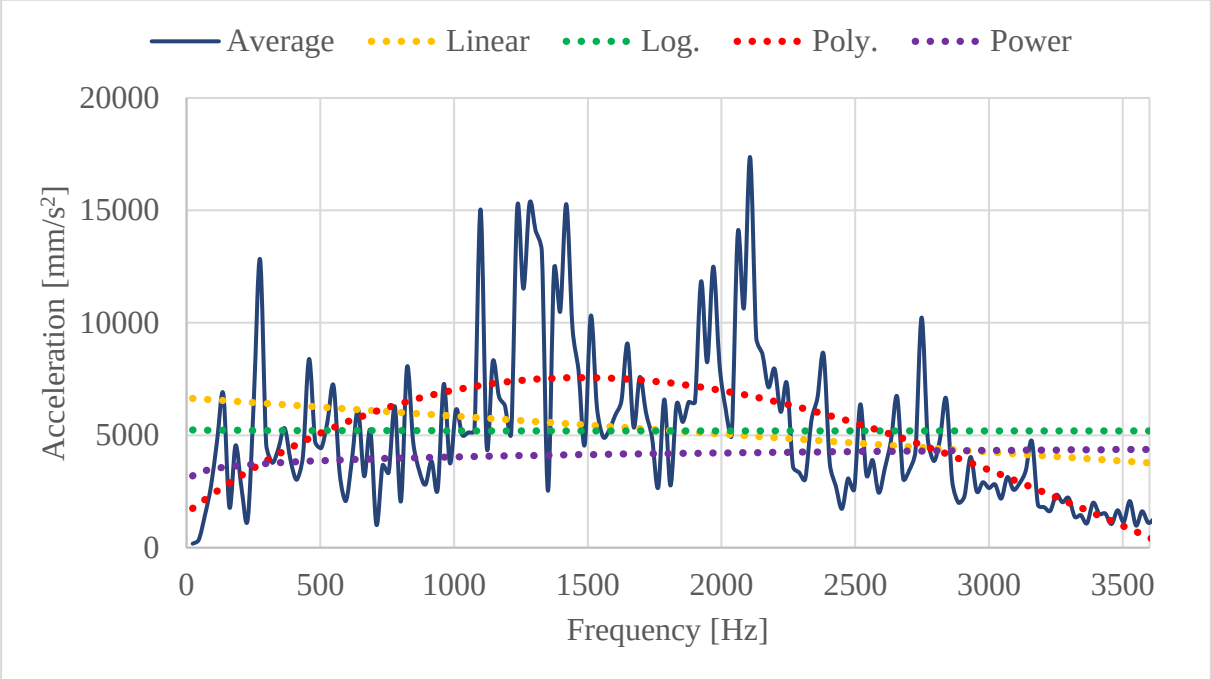

Figure 46. Averaged acceleration and trendlines in direction of DOF 1

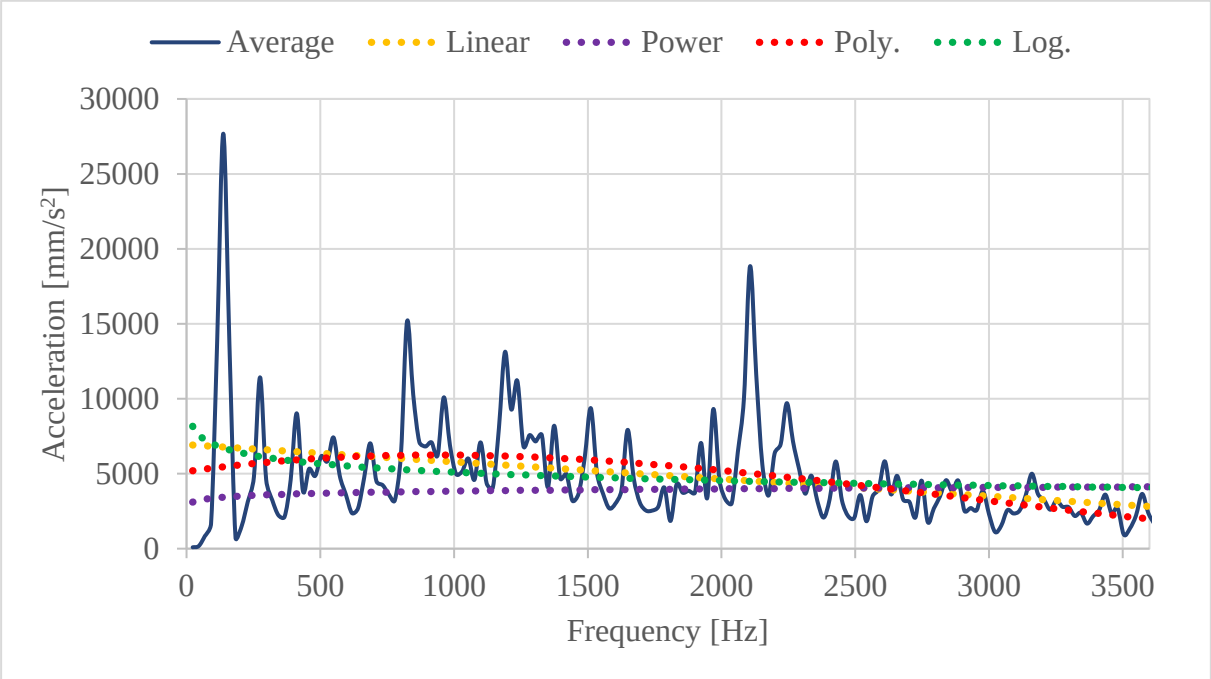

Figure 47. Averaged acceleration and trendlines in direction of DOF 2

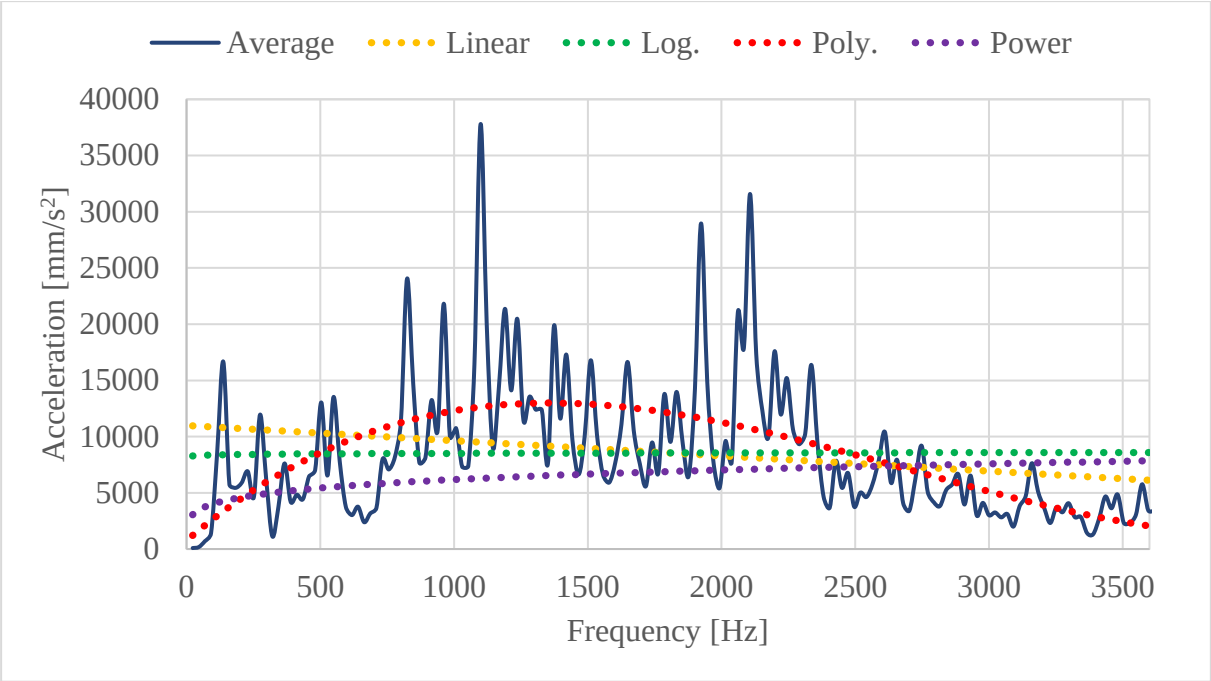

Figure 48. Averaged acceleration and trendlines in direction of DOF 3

4.2.2. Surface velocity mean integral level evaluation

4.2.2.1. Averaged excitation

First, response to the averaged excitation must be calculated, since it indicates if there is a problem with the excitation curve. Figure 49 presents difference between response to the baseline and averaged excitation.

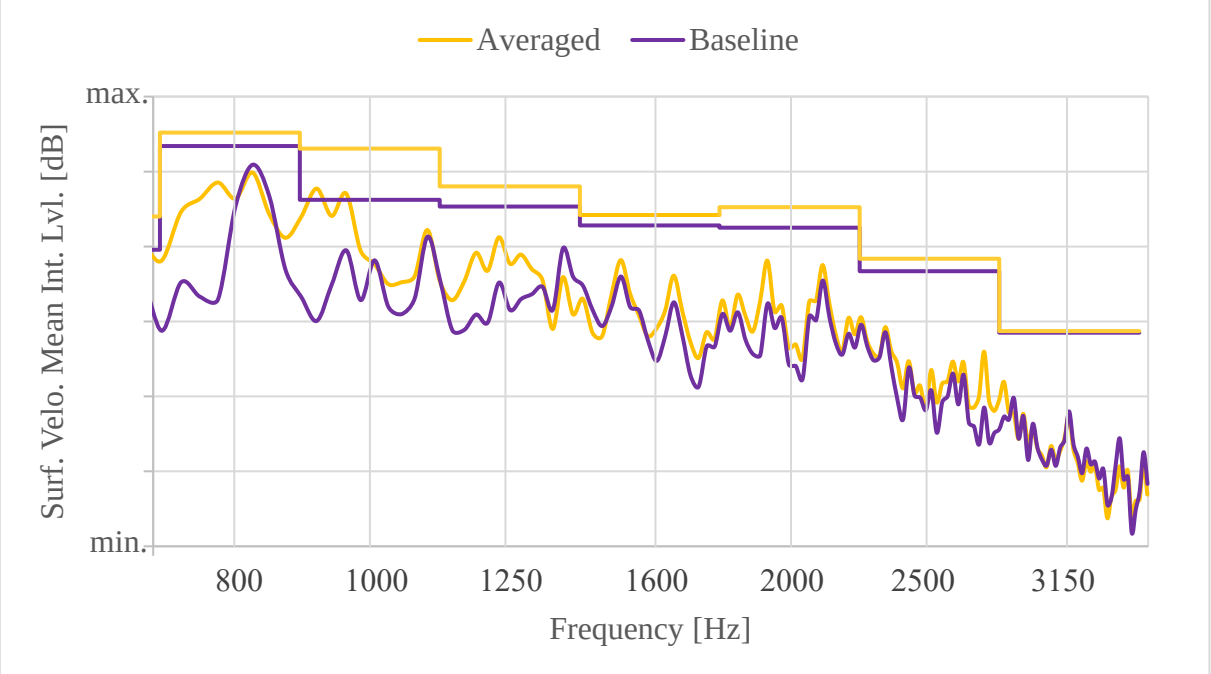

Figure 49. Structure response comparison between baseline and averaged excitation

Clearly, a structure response with averaged excitation is not acceptable in the 3rd octave band with the centre frequency 1000 Hz. Table 13 confirms the stated claim.

Table 13. Absolute difference of structure response between baseline and averaged excitation

3rd octave band [Hz]	Difference in Surf. Velo. Mean Int. Lvl. [dB]
800	1.8
1000	6.8
1250	2.7
1600	1.4
2000	2.7
2500	1.7
3150	0.2

4.2.2.2. Linear excitation

The second step represents exciting the component with the linear excitation.

Evaluation and comparison of the response to the linear excitation with the response to the baseline excitation is presented in Figure 50 and Table 14. It is notable that structure response is not acceptable in the 3rd octave band with the centre frequency 1000 Hz. Though, it was expected since the same 3rd octave band is determined as problematic already with the averaged excitation.

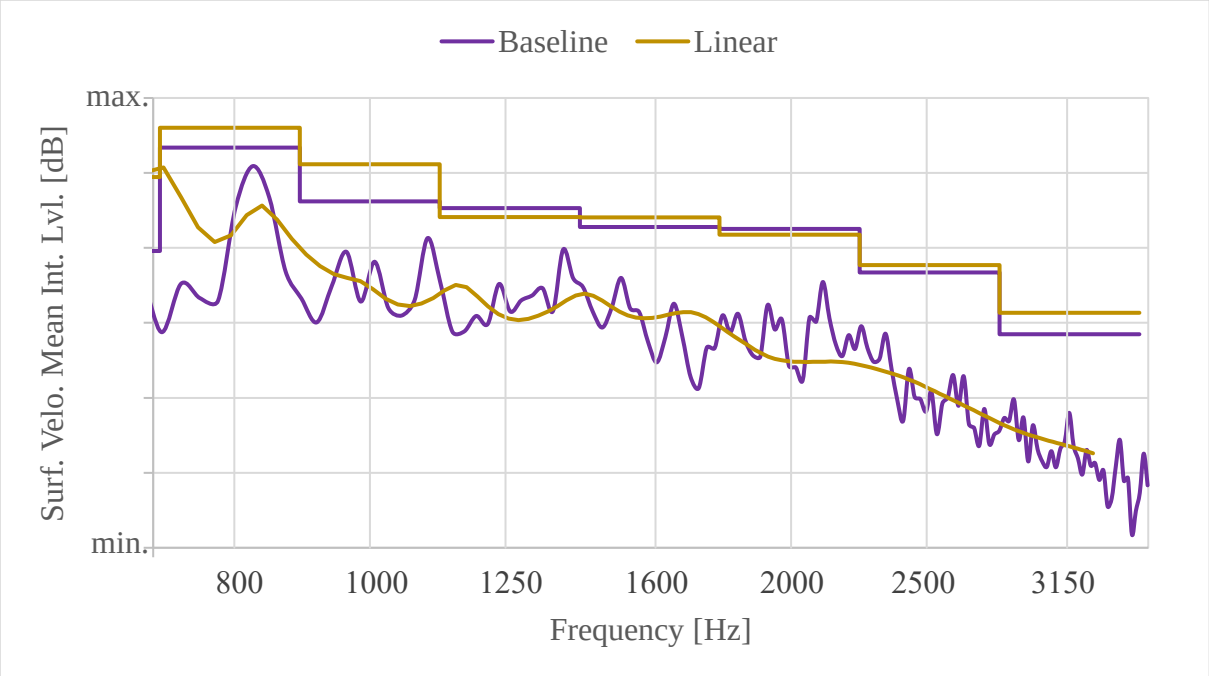

Figure 50. Structure response comparison between baseline and linear excitation

Table 14. Absolute difference of structure response between baseline and linear excitation

3rd octave band [Hz]	Difference in Surf. Velo. Mean Int. Lvl. [dB]
800	2.6
1000	4.9
1250	1.2
1600	1.3
2000	0.7
2500	1.0
3150	2.9

4.2.2.3. Evaluation

In order to increase the stiffness, the next step is to couple the intake manifold B to the cylinder head. After the analysis is conducted, it can be observed that the structure response remains the same. Therefore, the reason for the difference is not a surrounding structure stiffness. Since the structure response is not acceptable in the 3rd octave band with the centre frequency 1000 Hz already for the averaged excitation, it can be concluded that this is due to the component structure. The observed component is obviously very sensitive to averaging the excitations and neglecting the phase (only magnitude was taken into consideration). Consequently, an acceptable structure response cannot be expected with simplified excitations.

4.3. Intake manifold C

Since the characteristics of the intake manifold C are confidential, only a draft of the mentioned component is shown in Figure 51.

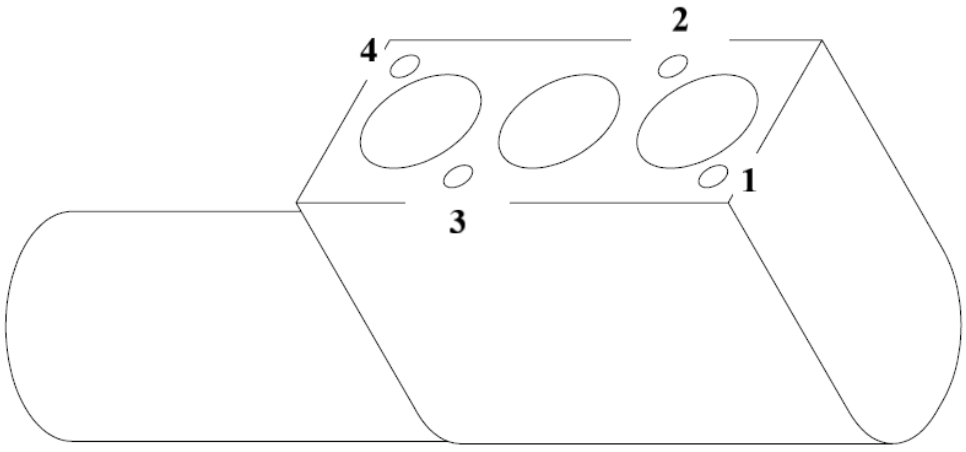

Figure 51. Schematic representation of the intake manifold C

4.3.1. Simplifying the excitation

Excitations are observed in direction of the three translational DOFs separately. Averaged acceleration values and trendlines used as excitations are displayed in Figure 52 to Figure 54.

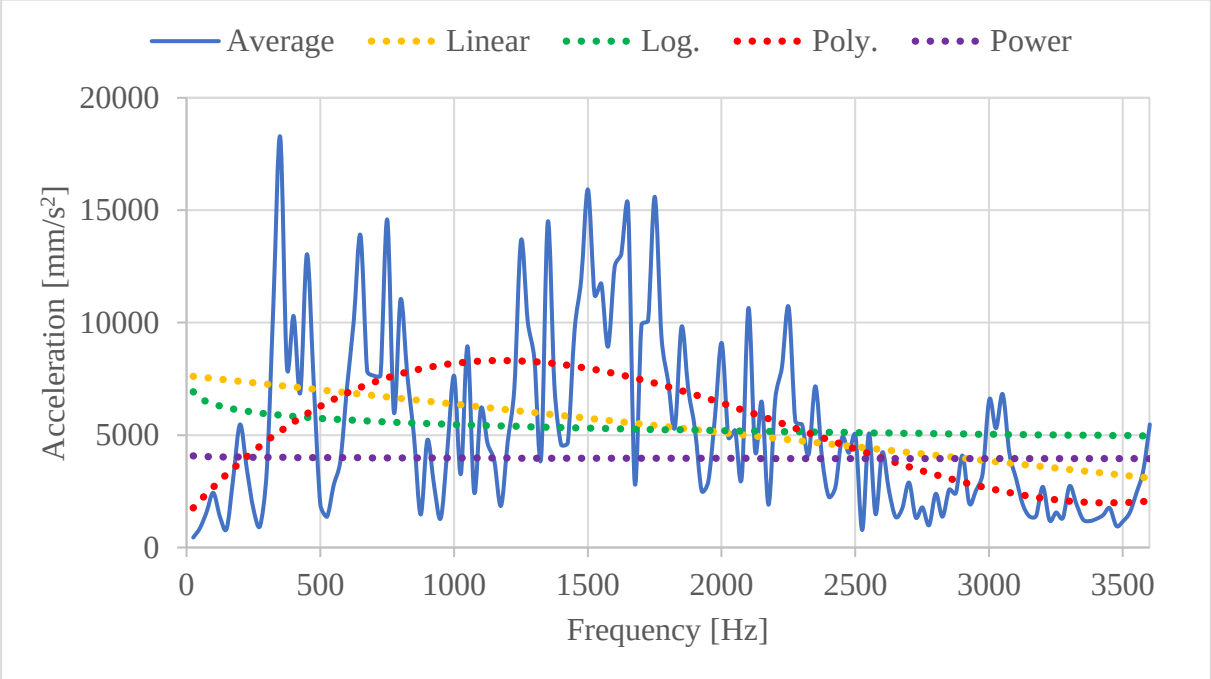

Figure 52. Averaged acceleration and trendlines in direction of DOF 1

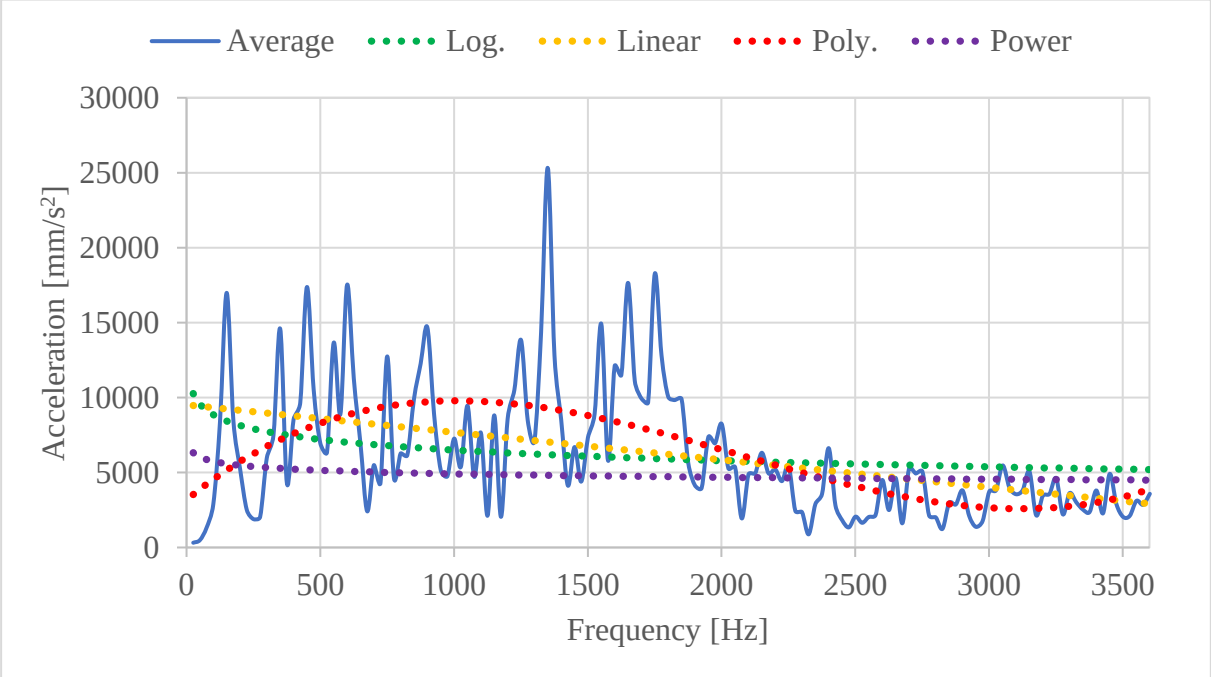

Figure 53. Averaged acceleration and trendlines in direction of DOF 2

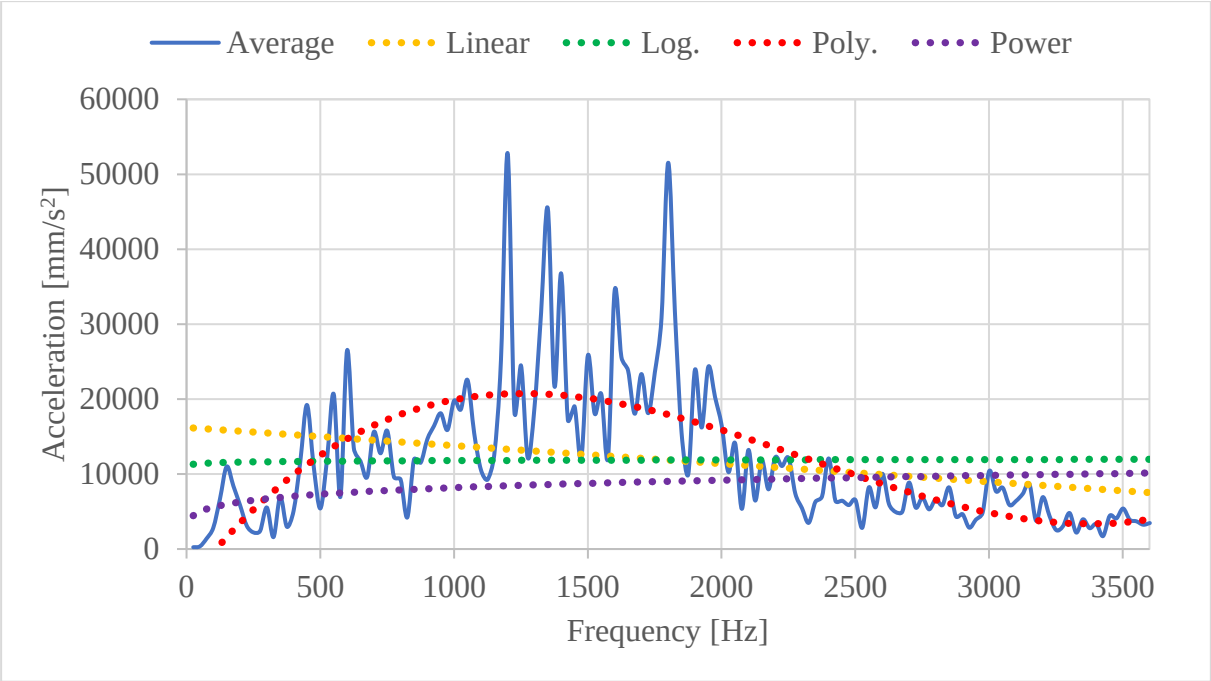

Figure 54. Averaged acceleration and trendlines in direction of DOF 3

4.3.2. Surface velocity mean integral level evaluation

4.3.2.1. Averaged excitation

The studied component is first excited with the previously showed averaged excitation at the four bolt locations in direction of three translational DOFs. Structure response is acceptable with the averaged excitation that is shown in Table 15.

Table 15. Structure response comparison between baseline and averaged excitation

3rd octave band [Hz]	Difference in Surf. Velo. Mean Int. Lvl. [dB]
800	2.7
1000	0.4
1250	1.8
1600	0.0
2000	1.0
2500	0.8
3150	0.5

4.3.2.2. Linear excitation

According to Table 16, response to a simplified linear excitation yields poor results.

Table 16. Absolute difference of structure response between baseline and linear excitation

3rd octave band [Hz]	Difference in Surf. Velo. Mean Int. Lvl. [dB]
800	2.8
1000	1.6
1250	6.9
1600	5.0
2000	5.2
2500	1.9
3150	3.5

4.3.2.3. Evaluation

The reason for not acceptable structure response lies in the poor linearization of the averaged excitation curve since the structure response with the averaged excitation is acceptable. According to Figure 52 to Figure 54, averaged excitation has high peaks in the frequency range from around 1000 Hz to around 2000 Hz. Linear trendline does not cover that range well and there is much less excitation applied than needed. This is in accordance with the poor structure response in 3rd octave bands with centre frequencies 1250, 1600 and 2000 Hz.

The improvement could be achieved if using a different simplified excitation, e. g. polynomial. Polynomial trendline describes the averaged excitation curve much better, thus, more acceptable results are expected. However, since this study is focused on the linear trendline, polynomial trendline will not be further discussed.

4.4. Conclusion

4.4.1. Influence of timing drive and inertia forces

Three engines with very similar peak firing pressures are studied. For that reason, a significant difference in the acceleration levels generated at the bolt locations, must be examined. Two possible reasons are being explored.

The first one includes the influence of the timing drive forces. The acceleration levels were compared for two load cases. One of them includes only gas pressure forces and inertia forces acting in the system while the other one includes gas pressure forces and inertia forces and

timing drive forces. The study of all three intake manifolds has shown that timing drive forces have a major impact at higher frequencies. This leads to the conclusion that timing drive design (belt/chain, pulleys) contributes to the overall noise and vibration levels, i.e. difference in the excitation level.

Influence of the timing drive forces on overall excitation level for intake A in direction of the DOF 3 is shown in Figure 55. Figure shows the difference between generated excitation levels when only gas pressure forces are acting in the system with the excitation levels when both gas pressure forces and timing drive forces are acting.

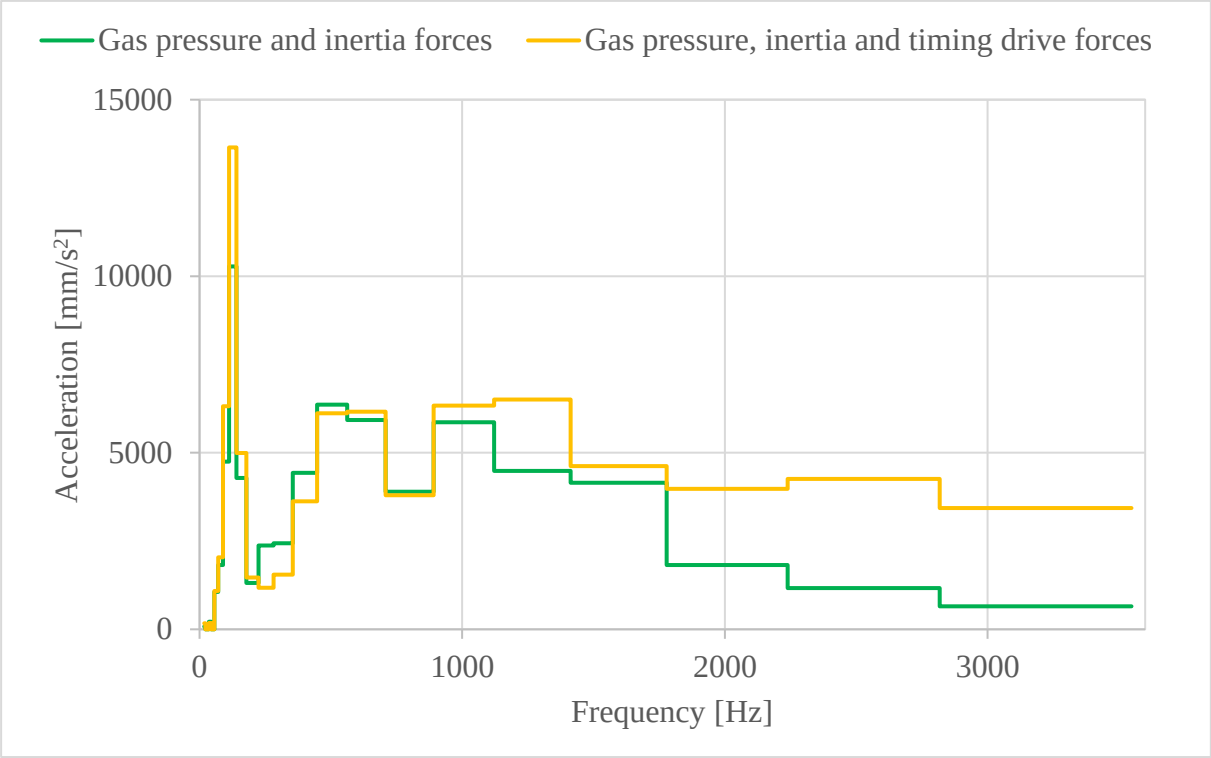

Figure 55. Intake A excitation level comparison in direction of DOF 3

Furthermore, higher unbalanced forces also lead to the higher overall structure response. There is the unbalance in the bending moments due to inertia forces of 3-cylinder engines. The unbalanced bending moments due to inertia forces of reciprocating masses of the three engines are studied. In this case, engine C has much higher unbalanced bending moments than other two engines. This is the result of higher reciprocating masses, but also higher distance between the cylinders. However, engine A is not relevant in this study because it is a testbed configuration (no gearbox). When comparing the excitation levels (response at the bolt locations) between engines B and C, it can be noticed that structure response of the engine C is

higher than the structure response of the engine B in the amount proportional to the difference in the bending moments.

Figure 56 presents the difference in sum of 1st and 2nd order unbalanced bending moments between engines B and C.

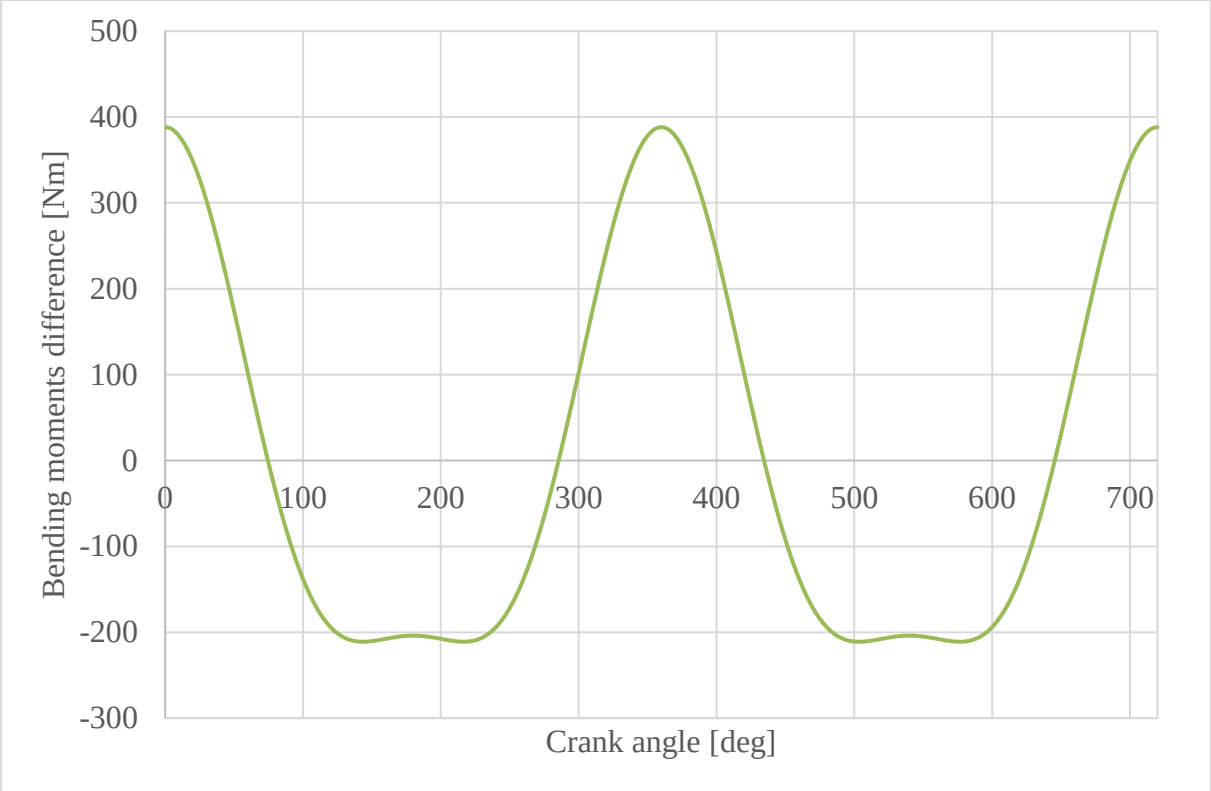

Figure 56. Difference in unbalanced bending moments due to inertia forces of reciprocating masses

5. OIL PAN ANALYSIS

Three different oil pans are analyzed in this study. The basic properties of the observed components are shown in Table 17.

Table 17. Characteristics of oil pans

			Material properties		
		Bolt No.	**Density** [kg/m^3]	**Young's modulus** [MPa]	**Poisson's ratio** [-]
Engine A	**Oil pan A**	20	2750	75000	0.33
Engine B	**Oil pan B**	19	2700	71000	0.31
Engine C	**Oil pan C**	20	2700	74500	0.33

5.1. Oil pan A

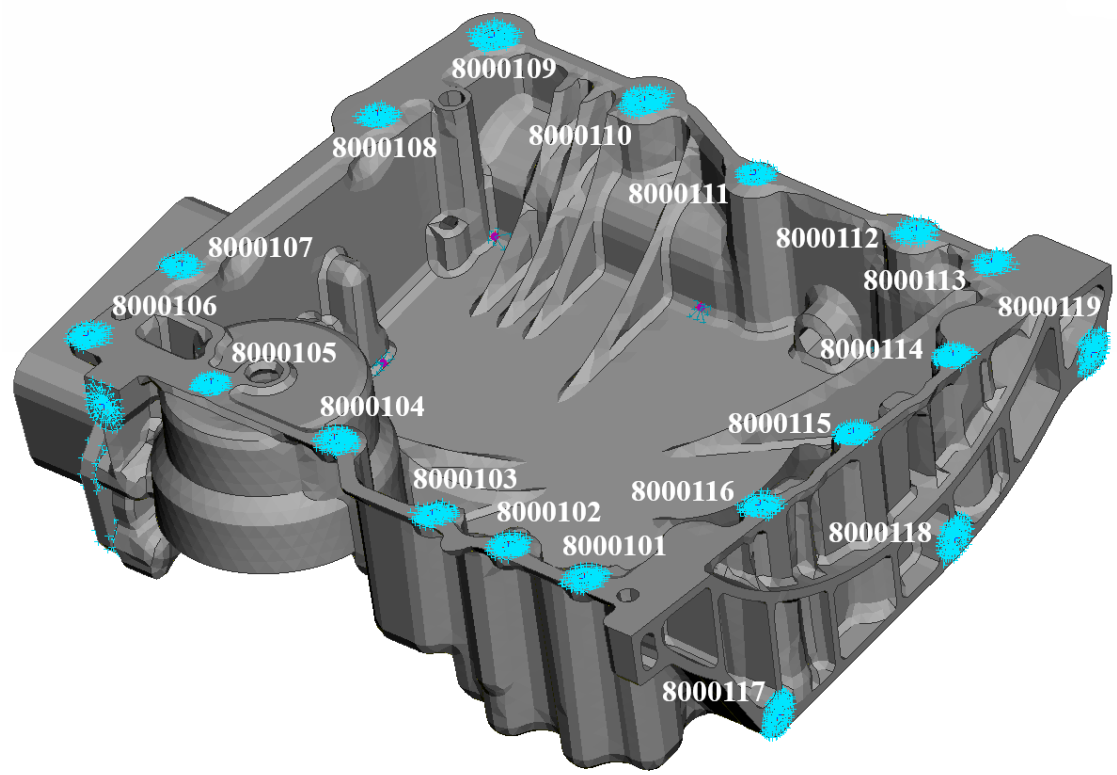

Figure 57. Oil pan A bolt locations

5.1.1. Simplifying of excitation

As can be noticed in Figure 57, oil pan A is coupled to the engine with 19 bolts in total. Of that, 16 bolts are used for connecting with bedplate, while the other 3 provide a connection with the bell housing. Therefore, the excitations will be analyzed separately for bolt locations 8000101-8000116 (later 1-16) and bolt locations 8000117-8000119 (later 17-19) in direction of each translational DOF.

Like before, only acceleration magnitude will be taken into the consideration (phase will be neglected for now).

Figures from Figure 58 to Figure 63 show linear, logarithmic, polynomial and power trendlines of the averaged acceleration levels in direction of each translational DOF.

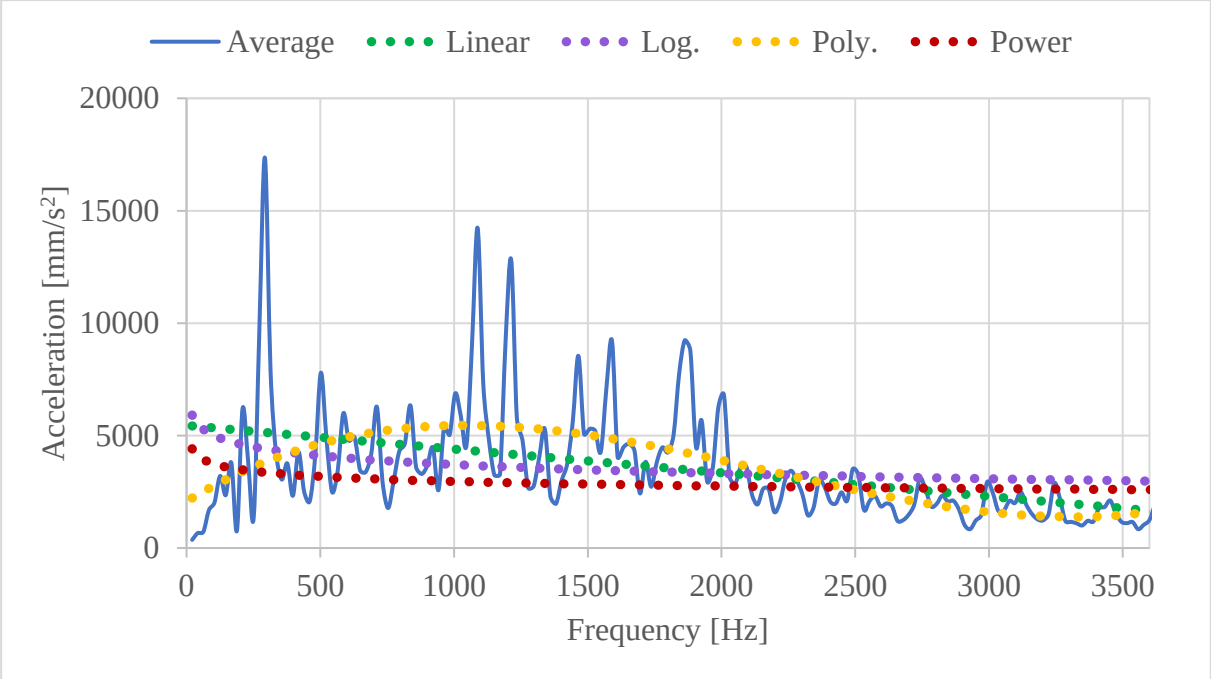

Figure 58. Averaged acceleration and trendlines in direction of DOF 1 for bolt locations 1-16

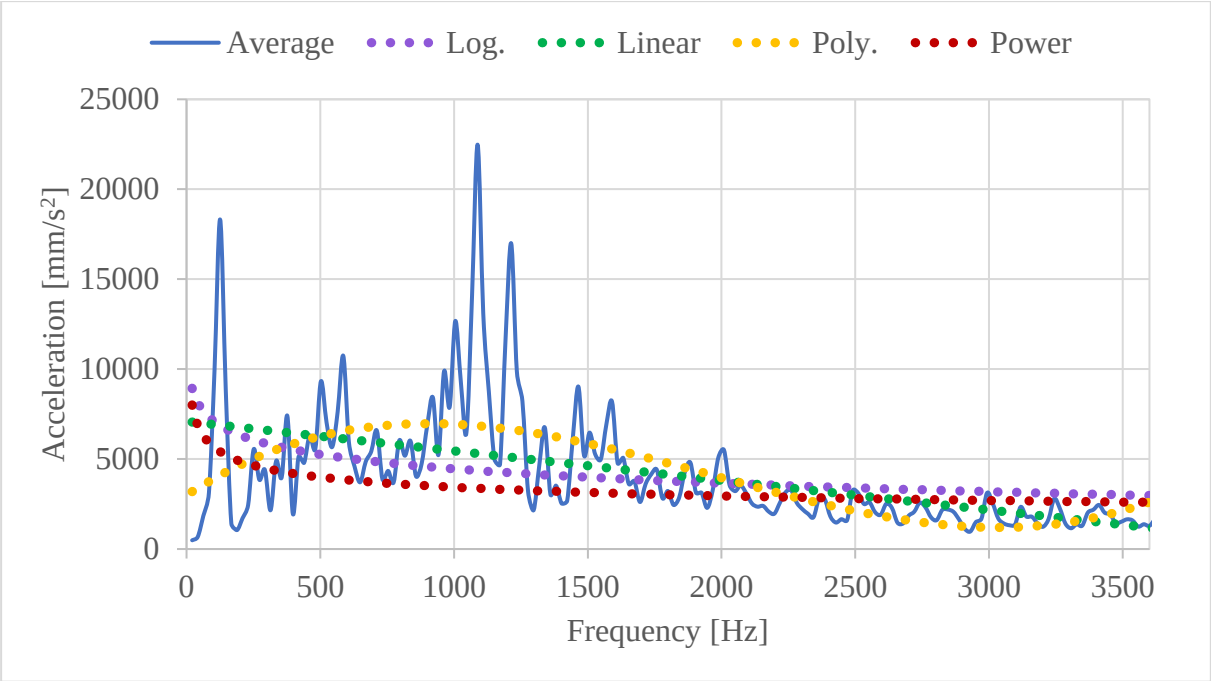

Figure 59. Averaged acceleration and trendlines in direction of DOF 2 for bolt locations 1-16

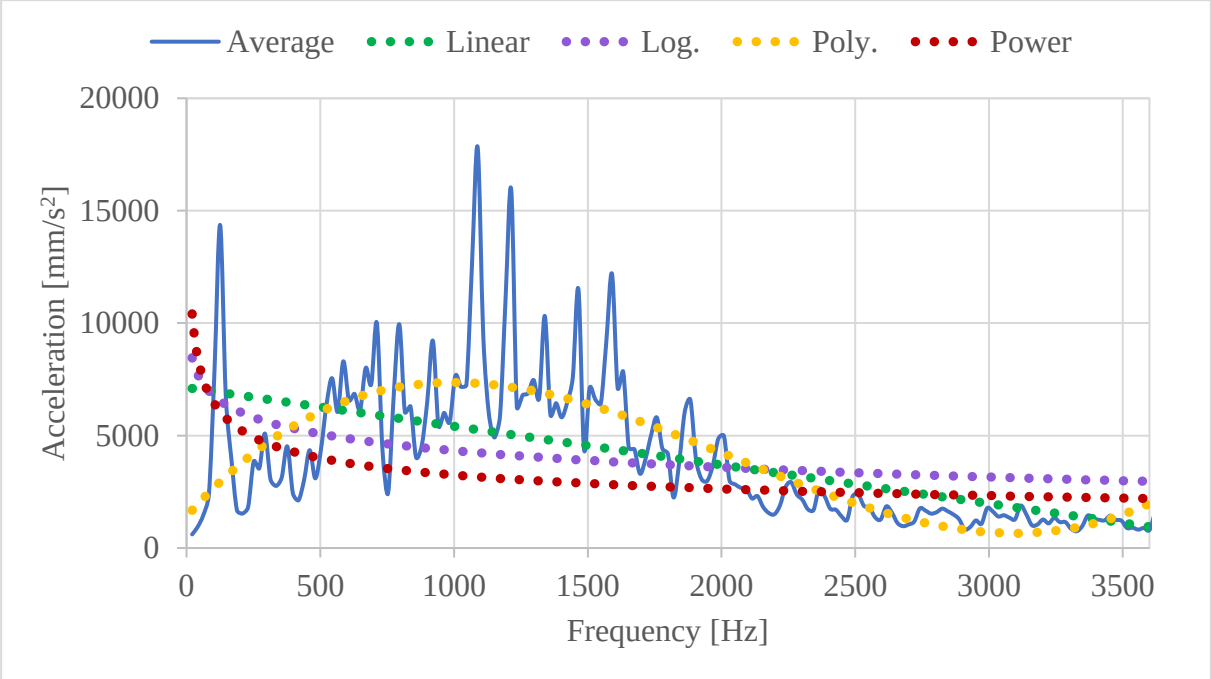

Figure 60. Averaged acceleration and trendlines in direction of DOF 3 for bolt locations 1-16

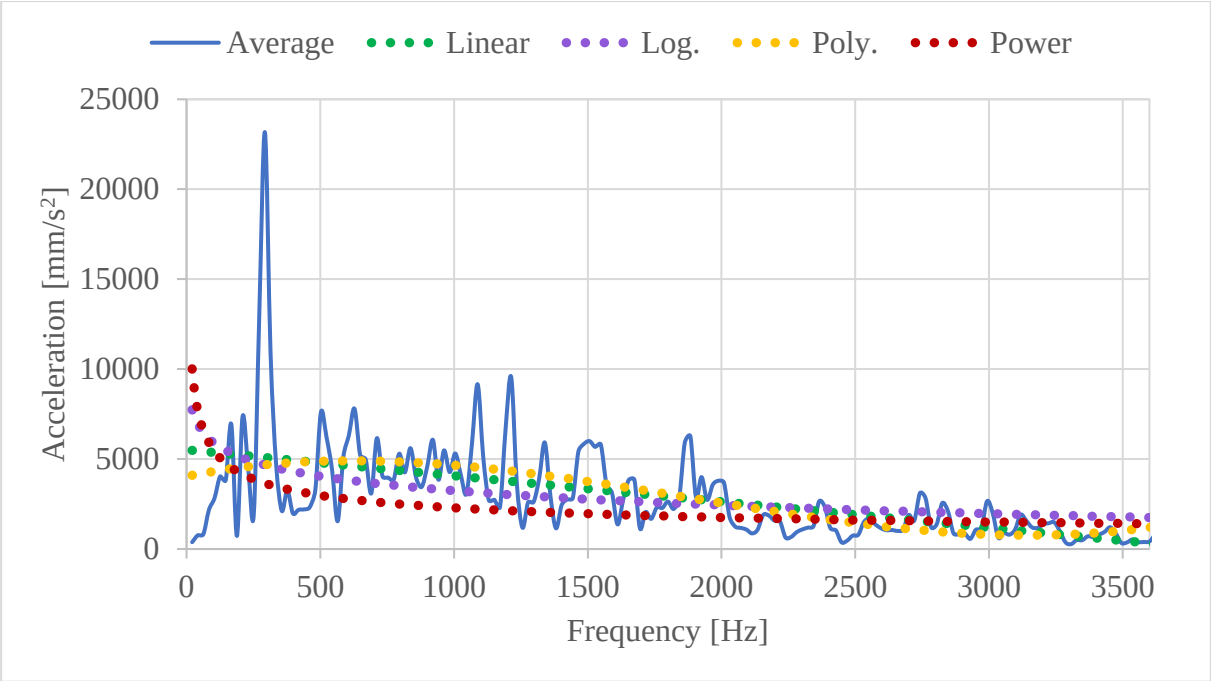

Figure 61.Averaged acceleration and trendlines in direction of DOF 1 for bolt locations 17-19

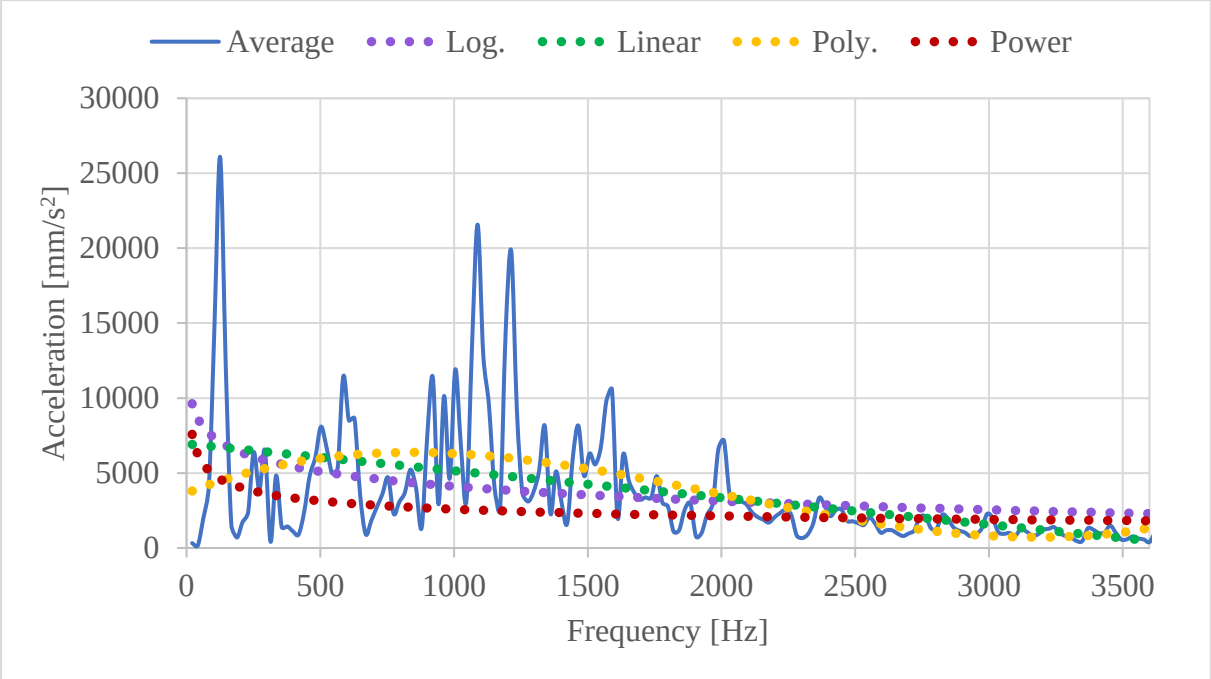

Figure 62. Averaged acceleration and trendlines in direction of DOF 2 for bolt locations 17-19

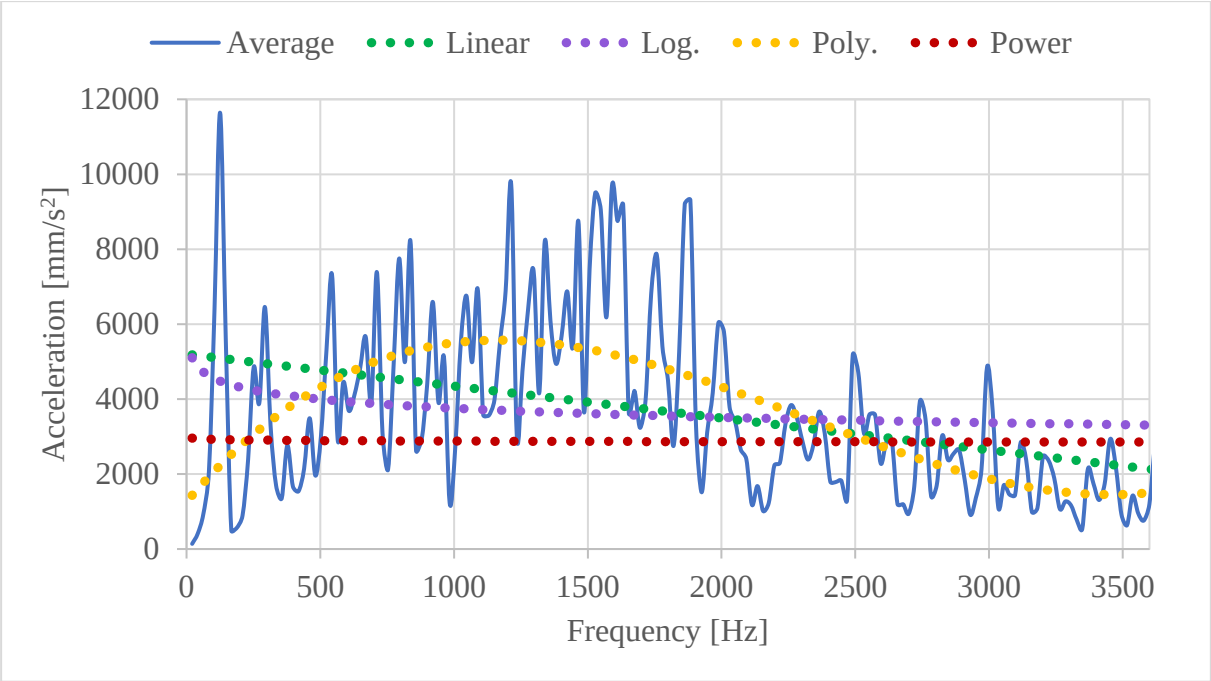

Figure 63. Averaged acceleration and trendlines in direction of DOF 3 for bolt locations 17-19

5.1.1.1. Averaged excitation

Averaged excitation represents the first step of the analysis since it is the closest to the baseline excitation. This excitation is first applied on the oil pan decoupled from the engine assembly.

Structure response to the averaged excitation and comparison with the baseline result is shown in Figure 64.

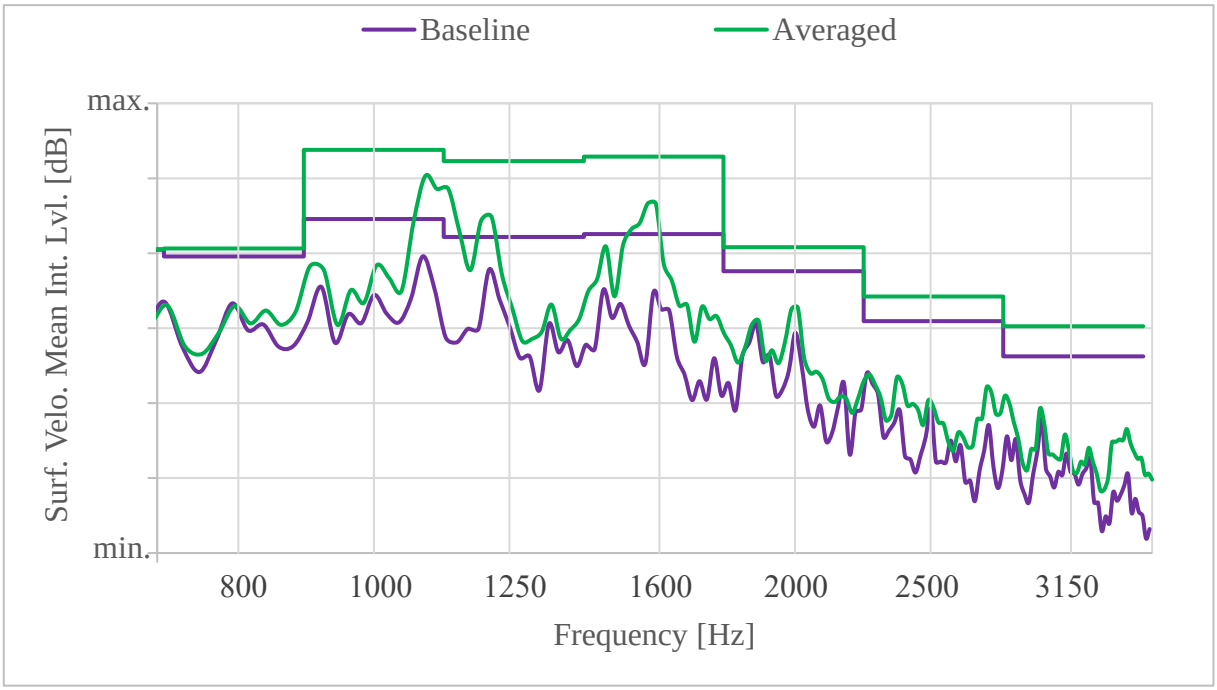

Figure 64. Structure response comparison between baseline and averaged excitation

Table 18 shows that already with the averaged excitation structural response is not acceptable.

Table 18. Absolute difference of structure response between baseline and averaged excitation

3rd octave band [Hz]	Difference in Surf. Velo. Mean Int. Lvl. [dB]
800	1.0
1000	9.2
1250	10.1
1600	10.3
2000	3.2
2500	3.3
3150	4.0

The next step was to couple the oil pan to the engine assembly in order to increase the system stiffness. This was done in a few steps, as showed in Figure 65.

MODEL 1

oil pan,
oil cooler

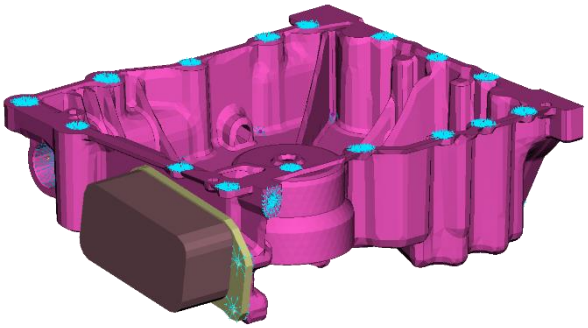

MODEL 2

oil pan, oil cooler, bedplate, cylinder block, bell housing, A/C compressor

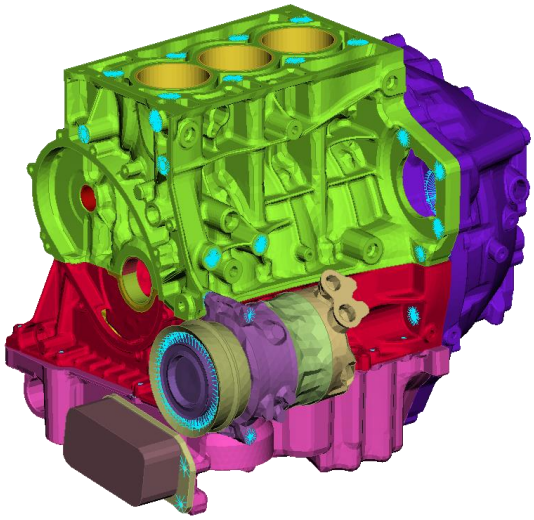

MODEL 3

oil pan, oil cooler, bedplate, cylinder block, bell housing, A/C compressor, cylinder head

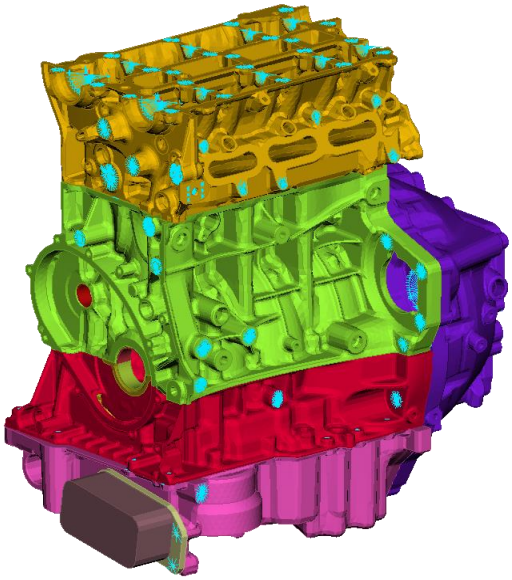

MODEL 4

full engine assembly

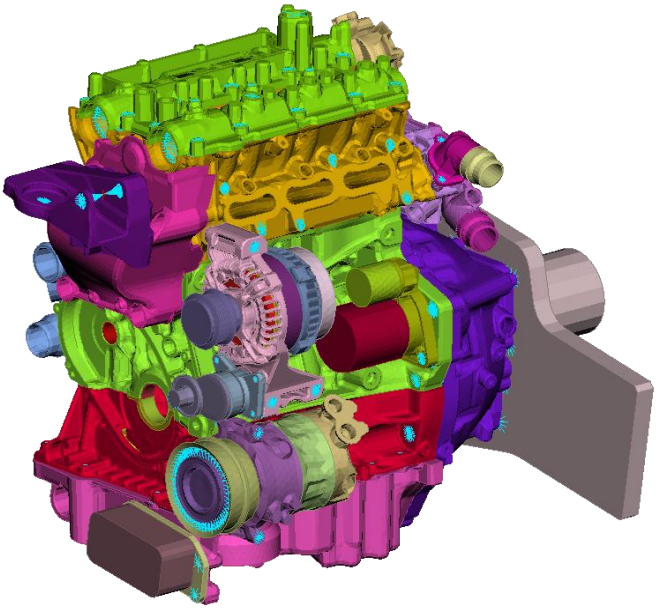

Figure 65. Model evolution

To simplify, calculation only for the full engine assembly will be presented here.

Figure 66 shows a comparison between the response to the baseline excitation and the response the averaged excitation when oil pan is coupled to the whole engine assembly.

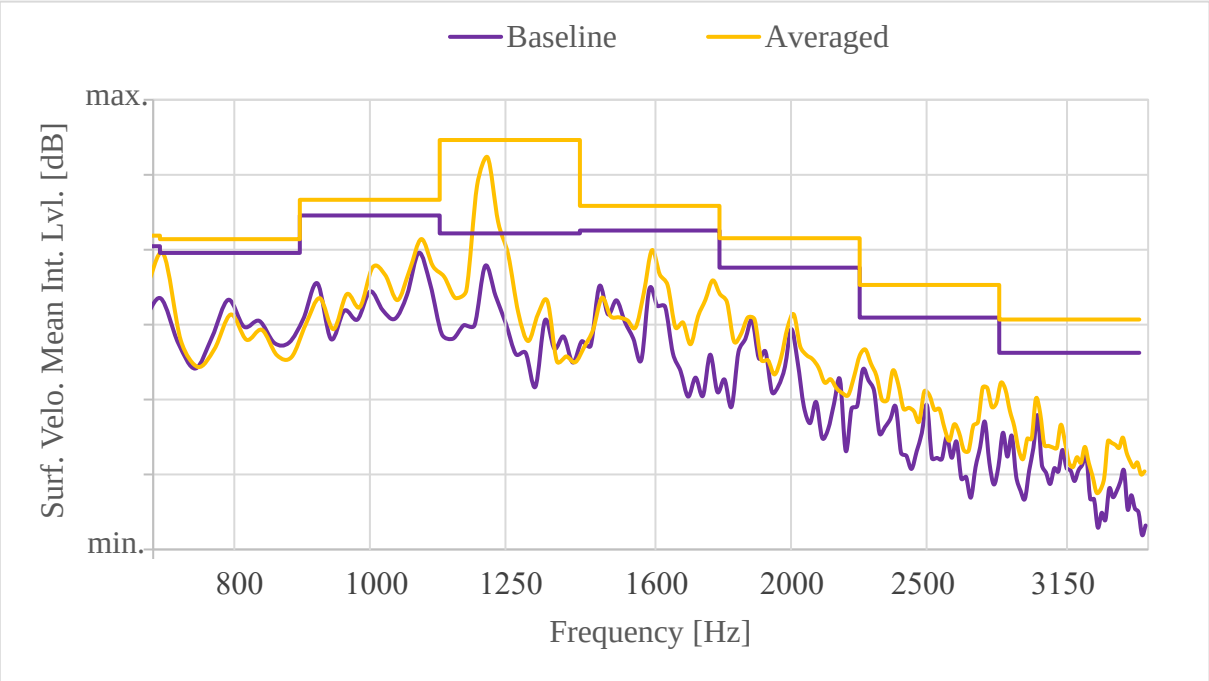

Figure 66. Structure response comparison between baseline and averaged excitation for model 4

It can be noticed that deviation levels significantly drop in the 3rd octave bands with centre frequencies 1000 Hz and 1600 Hz. Table 19 also shows that there is an increase in deviation levels in 3rd octave bands withe centre frequencies 2000, 2500 and 3150 Hz. Therefore, stiffening the analyzed system does not yield acceptable results.

Table 19. Absolute difference of structure response between baseline and averaged excitation for model 4

3^{rd} octave band [Hz]	Difference in Surf. Velo. Mean Int. Lvl. [dB]
800	1.8
1000	2.1
1250	12.5
1600	3.3
2000	3.9
2500	4.4
3150	4.4

5.1.1.2. Linear excitation

Despite the previously described unacceptable results, a calculation with the simplified excitation will be conducted. The linear excitation has lower values than the averaged excitation. In spite of that, response to a linear excitation is still much higher in some 3rd octave bands than the response to the baseline excitation. Response to the linear excitation and comparison with the baseline result is shown in Figure 67.

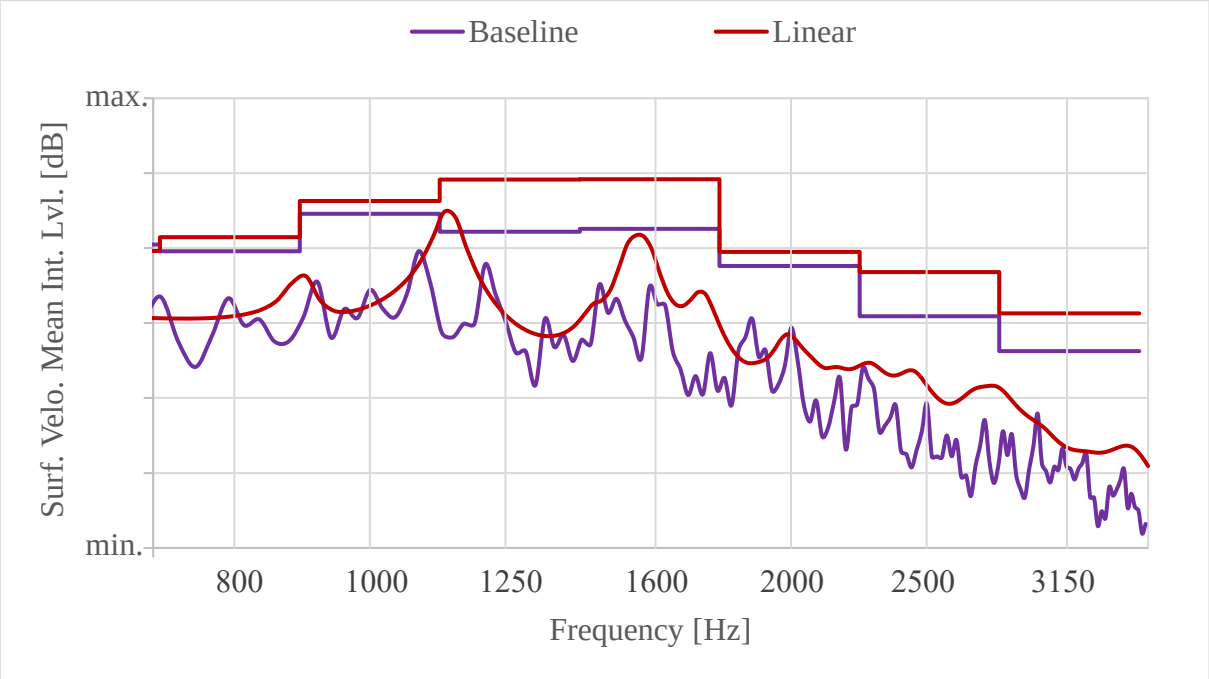

Figure 67. Structure response comparison between baseline and linear excitation for model 4

Based on the Table 20, it can be concluded that linear excitation also yields poor result. The difference occurs at the same frequencies as before.

Table 20. Absolute difference of structure response between baseline and linear excitation for model 4

3rd octave band [Hz]	Difference in Surf. Velo. Mean Int. Lvl. [dB]
800	1.9
1000	1.7
1250	7.0
1600	6.6
2000	1.9
2500	5.9
3150	5.0

5.1.1.3. Complex excitation

Since there is a problem already with the response to averaged excitation and that even lower excitation levels (linear excitation) still cause a much higher response, the next step is to take into the consideration the complex nature of the acceleration. Figure 68 and Figure 69 show averaged acceleration levels for both real and imaginary part of the acceleration.

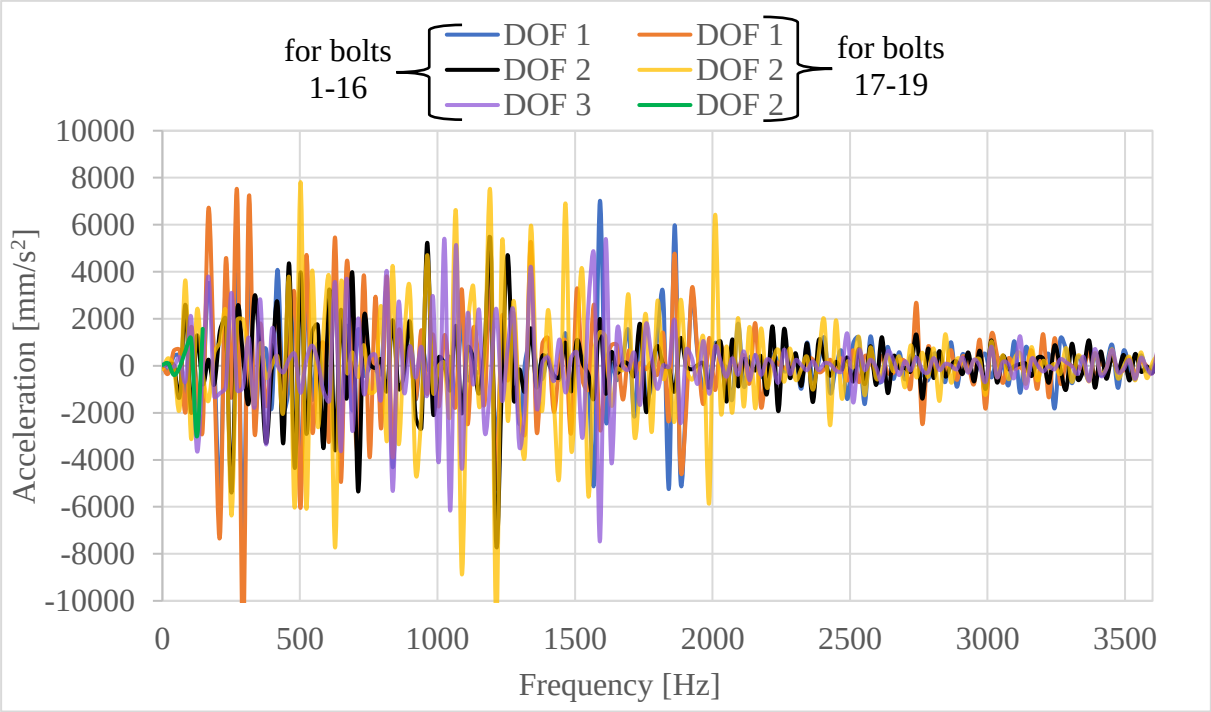

Figure 68. Real part of averaged complex excitation for all DOFs

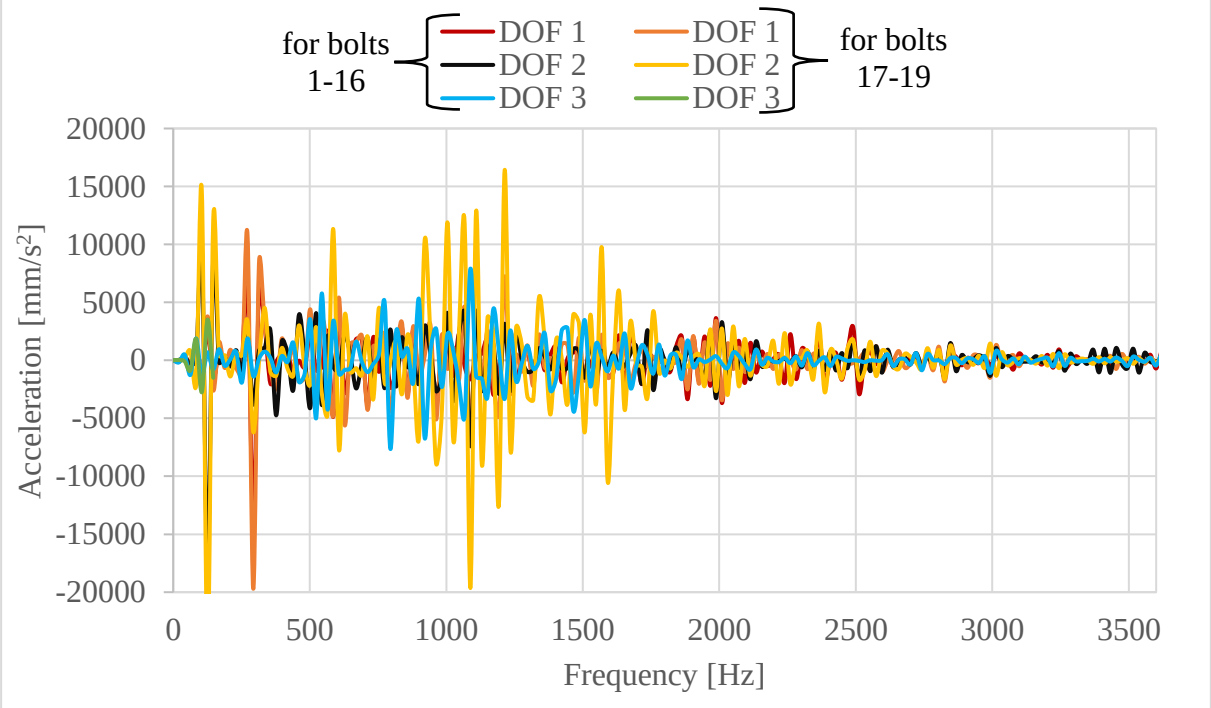

Figure 69. Imaginary part of averaged complex excitation for all DOFs

According to the Figure 70, surface velocity mean deviation level significantly drops when applying averaged complex excitation.

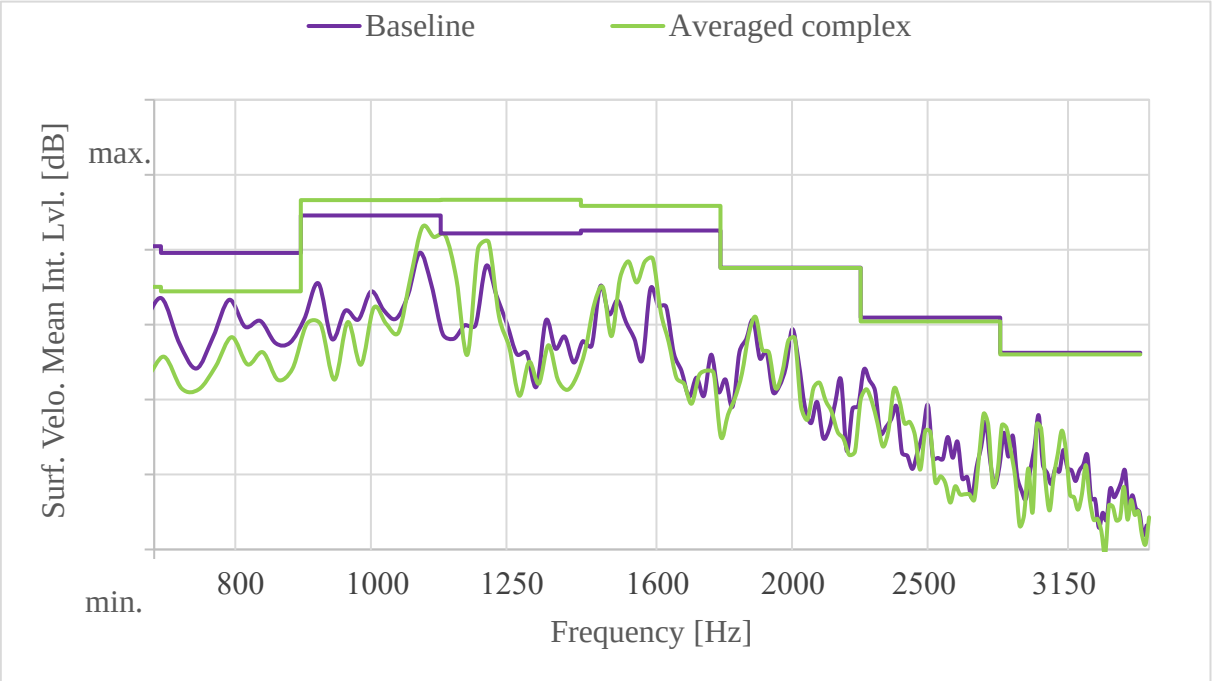

Figure 70. Structure response comparison between baseline and averaged complex excitation for model 1

There are still some inconsistencies in some 3rd octave band, as shown in the Table 21.

Table 21. Absolute difference of structure response between baseline and averaged complex excitation for model 1

3rd octave band [Hz]	Difference in Surf. Velo. Mean Int. Lvl. [dB]
800	5.2
1000	2.1
1250	4.5
1600	3.3
2000	0.1
2500	0.5
3150	0.2

Therefore, exciting the oil pan with the complex excitation improves the structure response when compared to other types of excitations. Because of its oscillating nature around x-axis, the complex excitation cannot be further simplified for the purposes of this study.

5.1.2. Surface velocity plots evaluation

Figures from Figure 71 to Figure 77 present the surface normal velocity plots in 3rd octave bands with centre frequencies from 800 Hz to 3150 Hz for different excitation types. Some areas with poor surface velocity distribution (when comparing with baseline) are marked. Besides of the previously evaluated excitations, surface velocity plots are shown also for white noise excitation. It is noticeable that the structure response is acceptable with none of the excitations. However, when all excitations compared, structure response is most acceptable with the complex excitation.

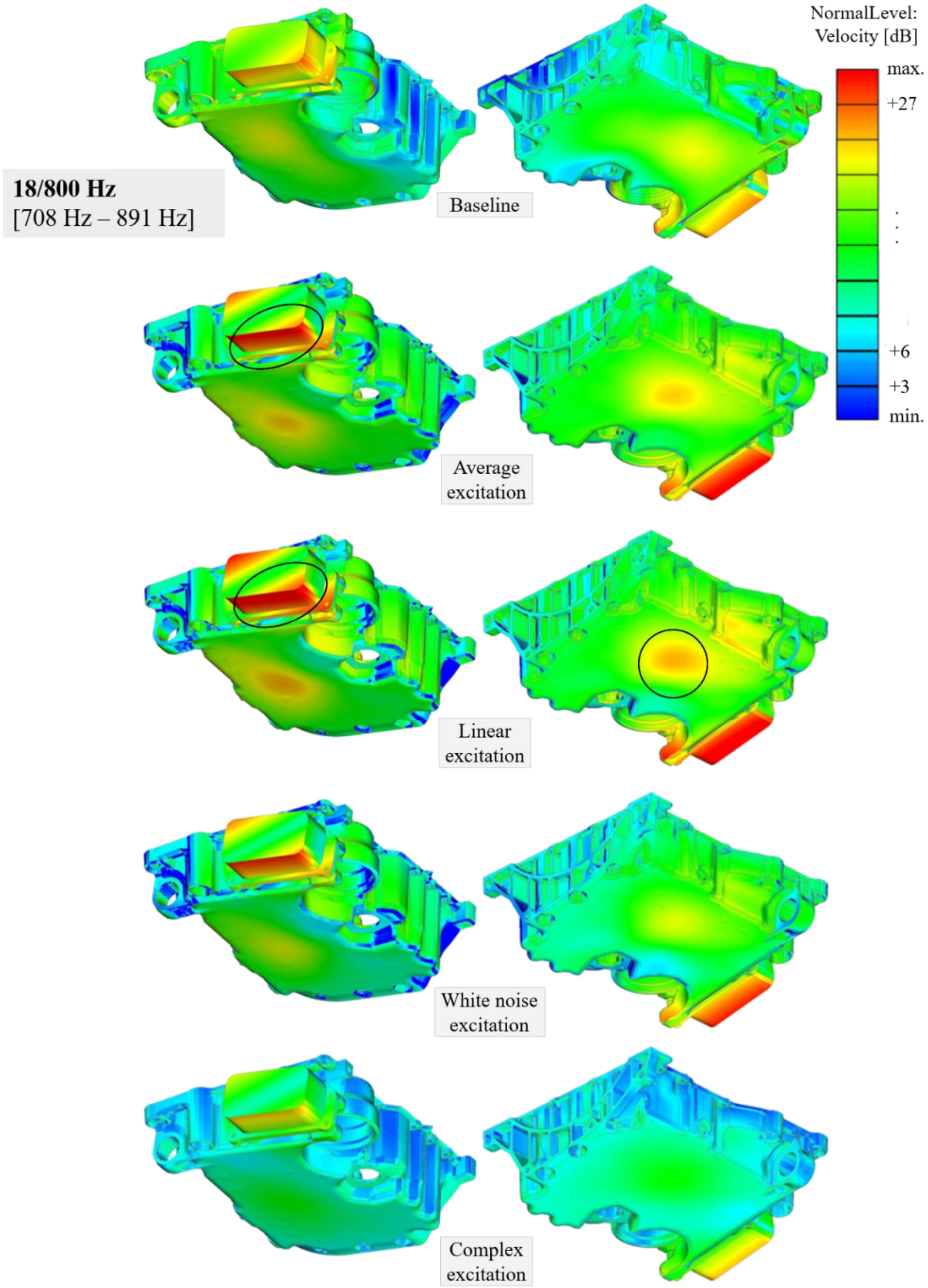

Figure 71. Structure response in form of normal velocity levels for 3rd octave band 800 Hz

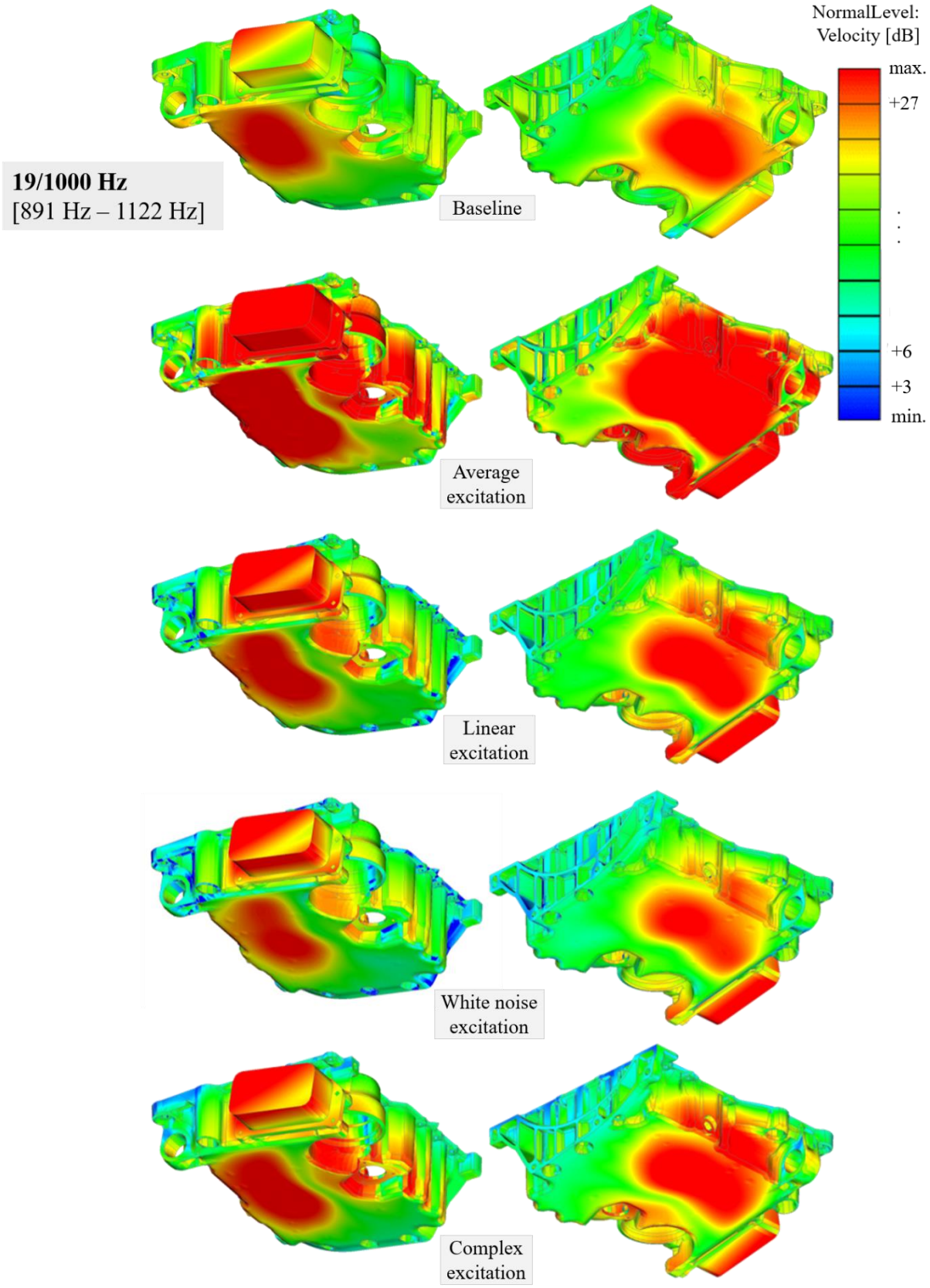

Figure 72. Structure response in form of normal velocity levels for 3rd octave band 1000 Hz

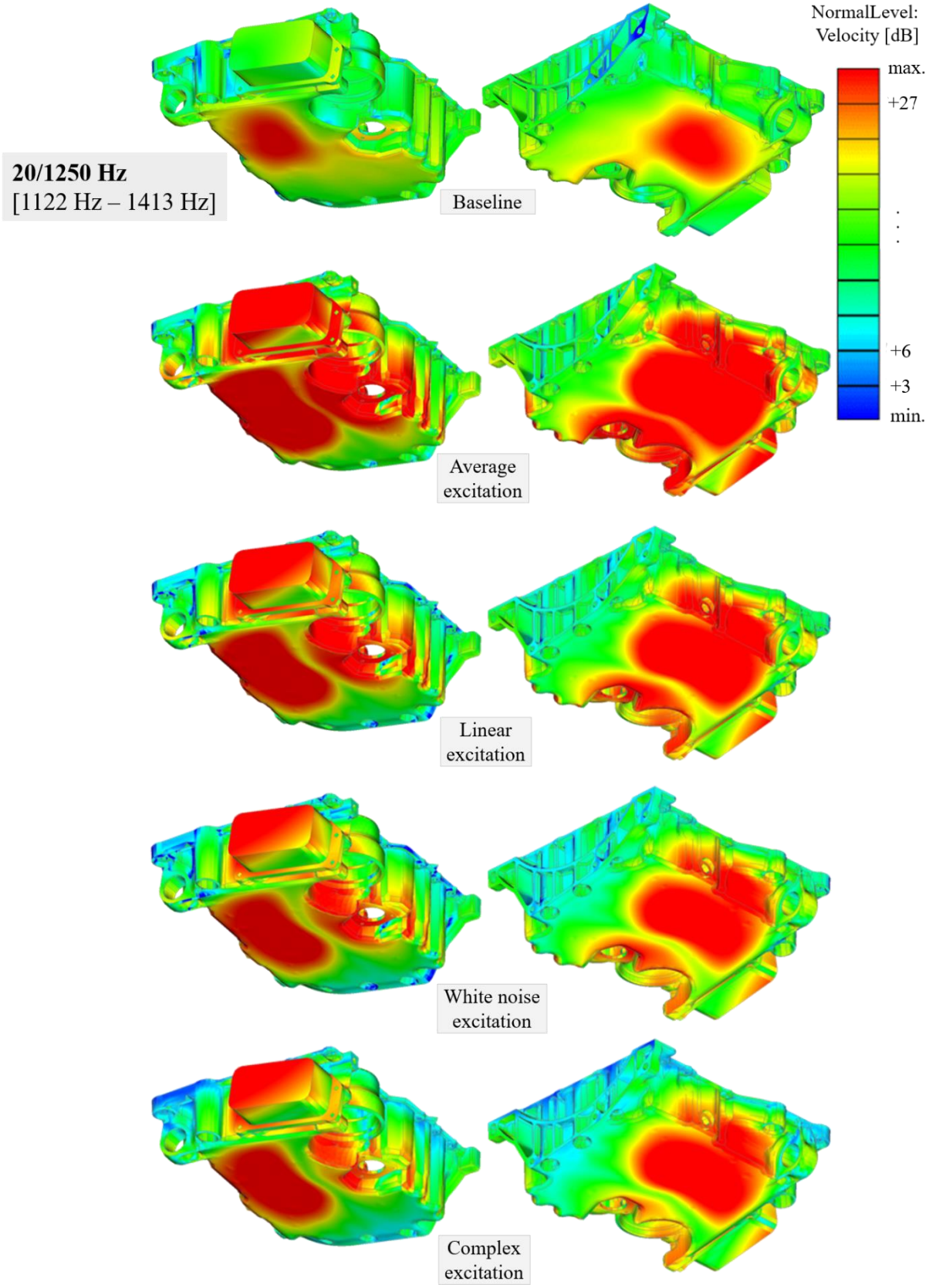

Figure 73. Structure response in form of normal velocity levels for 3rd octave band 1250 Hz

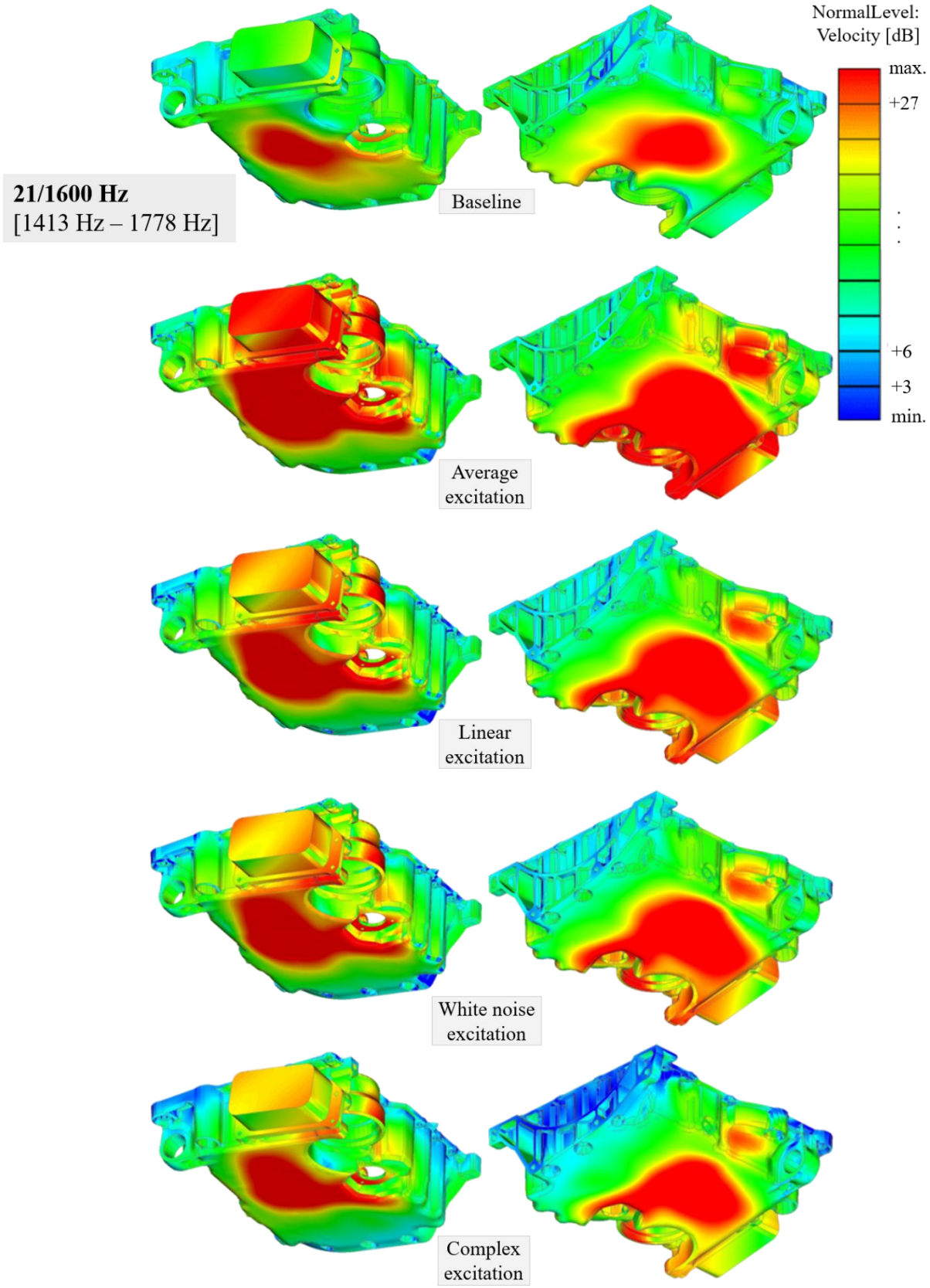

Figure 74. Structure response in form of normal velocity levels for 3rd octave band 1600 Hz

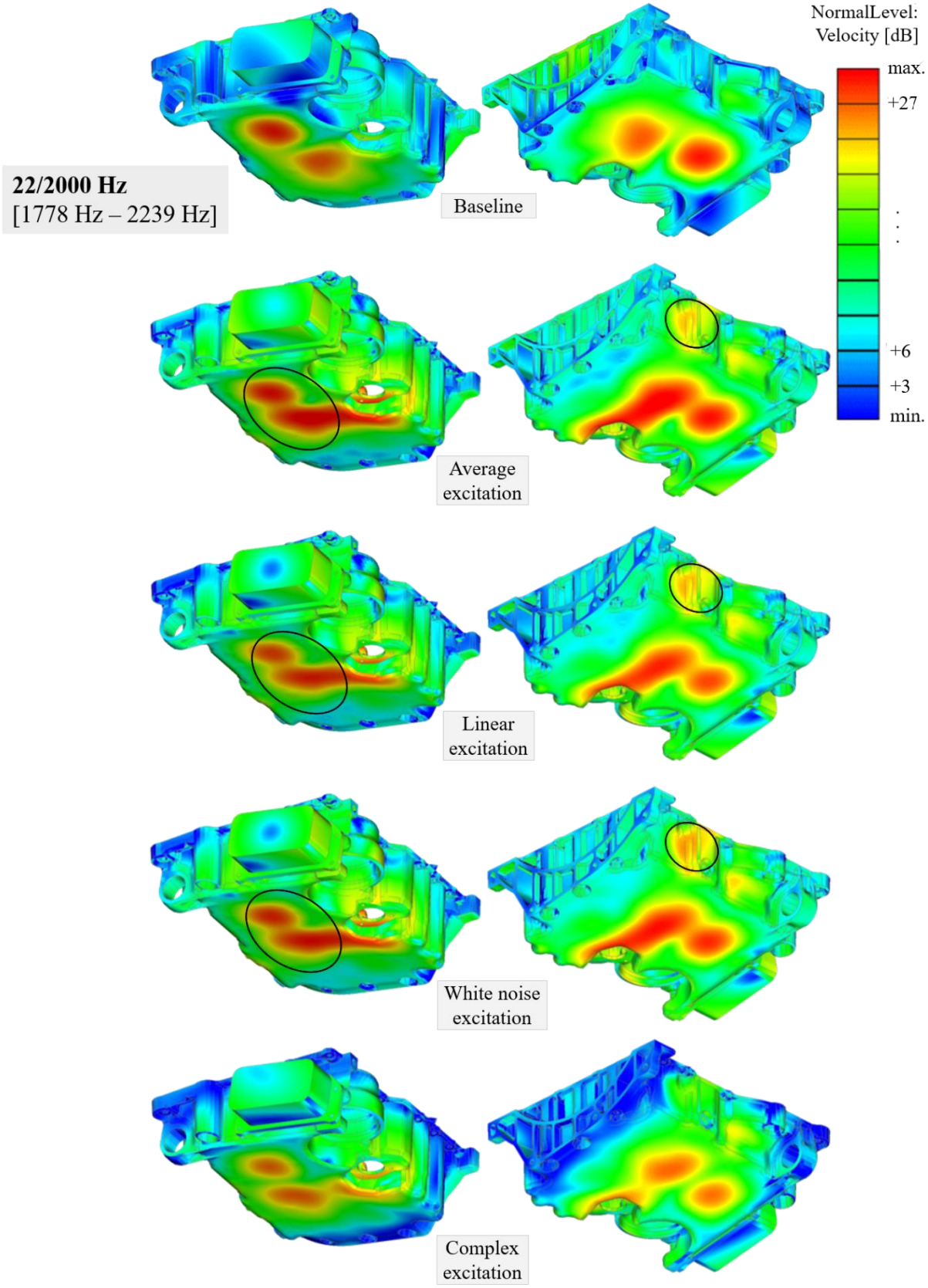

Figure 75. Structure response in form of normal velocity levels for 3rd octave band 2000 Hz

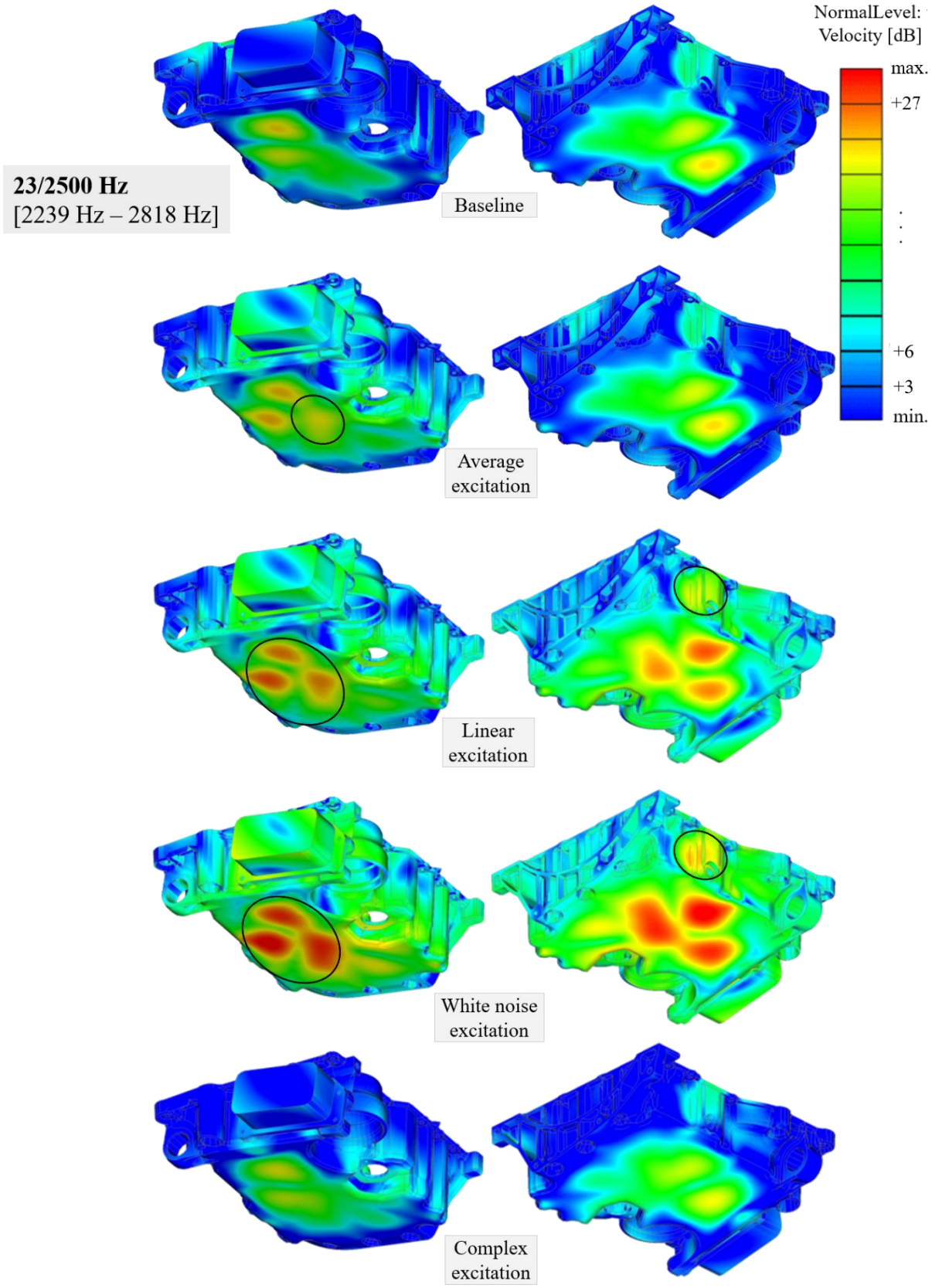

Figure 76. Structure response in form of normal velocity levels for 3rd octave band 2500 Hz

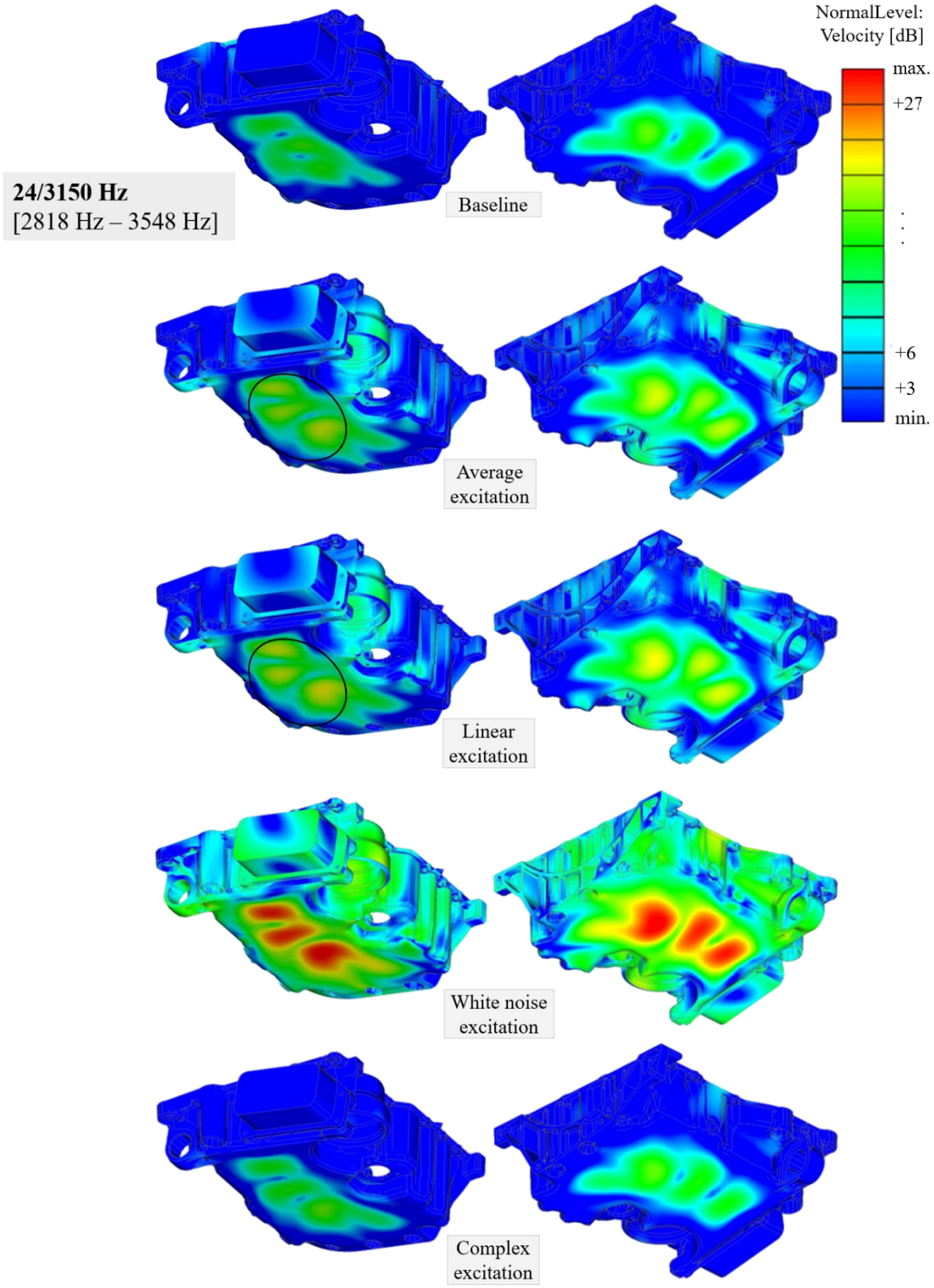

Figure 77. Structure response in form of normal velocity levels for 3rd octave band 3150 Hz

5.2. Oil pan B

The design of the oil pan B is very similar to the design of the oil pan A. Oil pan B is also coupled with 16 bolts to the bedplate and with 3 bolts to the gearbox according to Figure 78.

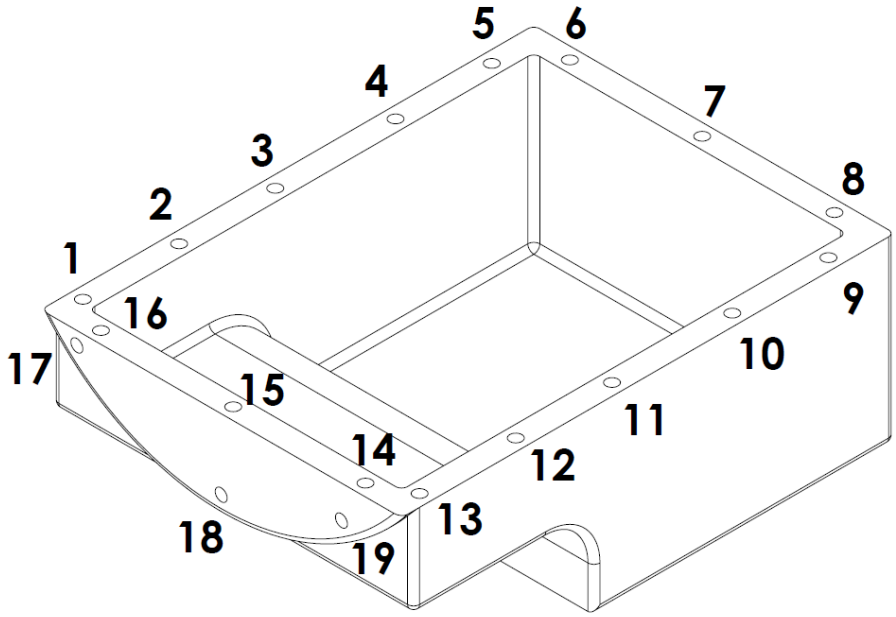

Figure 78. Schematic representation of the oil pan B

5.2.1. Simplifying of excitation

The analysis is the same as the analysis of the oil pan A. The structure response is also very similar. To simplify, only two types of simplified excitation for the single oil pan will be shown.

5.2.1.1. Averaged excitation

Response to the averaged excitation presented in Figure 79 shows high peaks at frequency around 2000 Hz.

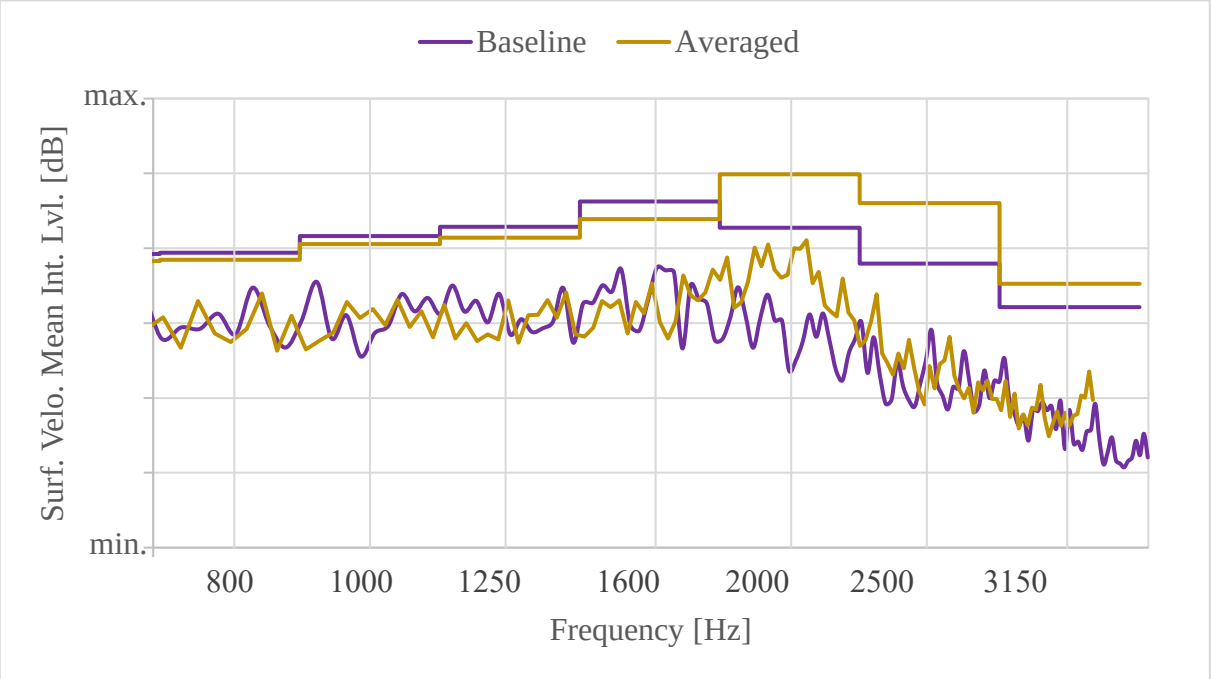

Figure 79. Structure response comparison between baseline and averaged excitation

According to the Table 22, 3rd octave bands with centre frequencies 2000 Hz and 2500 Hz have much higher structure response than baseline.

Table 22. Absolute difference of structure response between baseline and averaged excitation

3rd octave band [Hz]	Difference in Surf. Velo. Mean Int. Lvl. [dB]
800	1.0
1000	1.1
1250	1.5
1600	2.3
2000	7.1
2500	8.1
3150	3.1

5.2.1.2. Linear excitation

Figure 80 shows that the response to the linear excitation does not describe well the response to the baseline excitation.

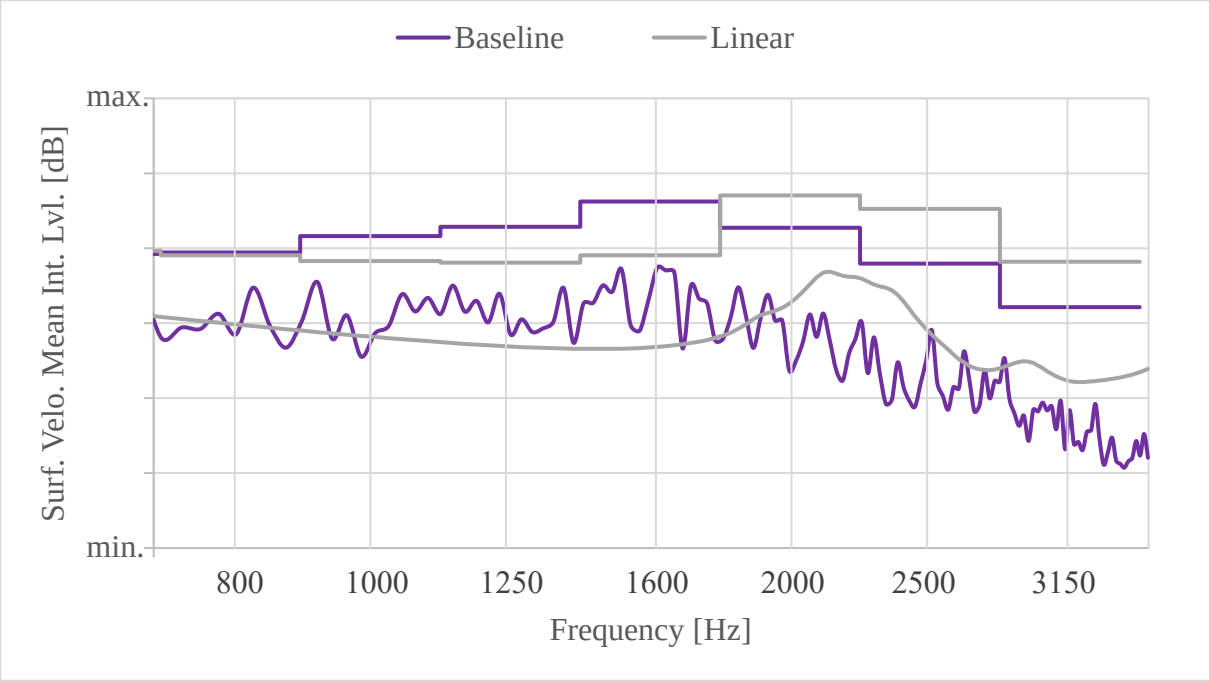

Figure 80. Structure response comparison between baseline and linear excitation

It can be noticed that the response to the linear excitation is not acceptable in almost all of the observed 3rd octave bands, as shown in Table 23.

Table 23. Absolute difference of structure response between baseline and linear excitation

3rd octave band [Hz]	Difference in Surf. Velo. Mean Int. Lvl. [dB]
800	0.4
1000	3.4
1250	4.8
1600	7.2
2000	4.3
2500	7.3
3150	6.1

5.3. Oil pan C

The design of the oil pan C does not differ significantly from the design of the oil pans A and B. However, oil pan C is attached with 16 bolts to the cylinder block and with 4 bolts to the gearbox, as shown in Figure 81.

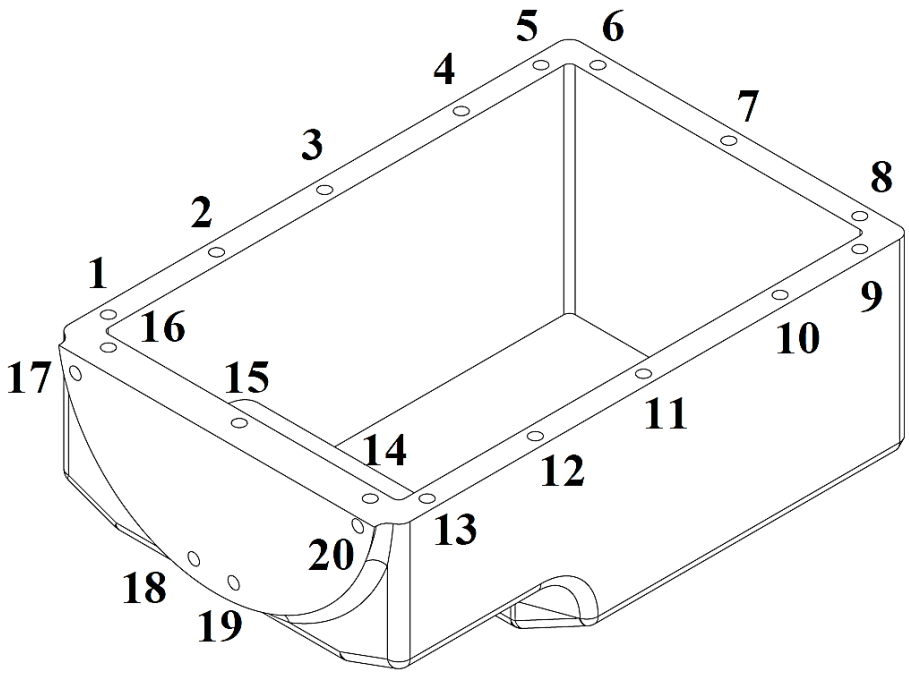

Figure 81. Schematic representation of the oil pan C

5.3.1. Simplifying of excitation

The analysis is the same as the analysis of the oil pan A. The structure response is also very similar. To simplify, only two types of simplified excitations for the single oil pan will be shown.

5.3.1.1. Averaged excitation

On the contrary to the structure response of the oil pan A and B, oil pan C has higher structure response to the averaged excitation almost throughout the whole observed frequency range. The difference in structure response between the two excitations can be noticed in Table 24.

Table 24. Absolute difference of structure response between baseline and averaged excitation

3rd octave band [Hz]	Difference in Surf. Velo. Mean Int. Lvl. [dB]
800	0.8
1000	6.9
1250	3.6
1600	1.6
2000	6.8
2500	4.4
3150	3.4

5.3.1.2. Linear excitation

Linear excitation has lower excitation levels than averaged excitation which results in more acceptable structure response in some 3rd octave bands. On the other hand, this also leads to the increase in structure response in other bands.

Table 25 shows that applying the linear excitation does not prevent the occurrence of the peaks at critical frequencies. The same was also noticed before for the oil pans A and B.

Table 25. Absolute difference of structure response between baseline and linear excitation

3rd octave band [Hz]	Difference in Surf. Velo. Mean Int. Lvl. [dB]
800	0.9
1000	3.8
1250	1.4
1600	2.7
2000	4.0
2500	5.1
3150	6.5

5.4. Conclusion

Based on the surface velocity mean integral level evaluation and surface velocity plots for oil pans A, B and C, the correct boundary conditions in the form of accelerations at the bolt locations cannot be found. It connects components at the engine bottom end, e. g. bedplate/cylinder block with the bell housing/gearbox. Since the engine bottom end is a very loaded engine area, large forces are transmitted through the bolts to the oil pan.

There are high peaks at some frequencies in the response to the averaged excitation. It could be a result of the excessive excitation levels. In addition, the same phenomenon also occurs in the response to the lower linear excitation. Therefore, this method is marked as not acceptable.

When taking the complex nature of the acceleration into account, there is a significant improvement in the structure response. Excitation in the form of a complex number takes into the consideration real motion of the oil pan. In other words, it includes back and forth motion that is not considered when only magnitude is applied.

Therefore, it can be observed that the motion of the oil pan cannot be simplified and that the phase, that indicates the direction of the movement, should be considered.

On the other hand, the main drawback of the complex excitation is that it cannot be simplified. As seen before, both real and imaginary parts oscillate around x-axis. Any simplification results in extremely low unreal excitation levels.

Surface velocity plots show that misleading monopole sources are being generated at side walls as a result of the insufficient stiffness. This is improved when oil pan is attached to the rest of the engine structure.

Altogether, an efficient method for assuming the NVH behavior of the oil pan cannot be developed. Forces acting on the oil pan are very complicated and unpredictable.

6. CAM COVER ANALYSIS

Two different intake manifolds are analyzed in this study. The basic properties of the observed components are shown in Table 26.

Table 26. Characteristics of cam covers

			Material properties		
		Bolt No.	**Density** [kg/m^3]	**Young's modulus** [MPa]	**Poisson's ratio** [-]
Engine A	**Cam cover A**	23	2750	75000	0.33
Engine B	**Cam cover B**	15	1400	8500	0.42
Engine C	**Cam cover C**	13	1480	7200	0.42

6.1. Cam cover A

Cam cover A is shown in Figure 82. It is made of aluminium alloy and has integrated camshaft bearing support (marked red). Therefore, it will not be further analyzed.

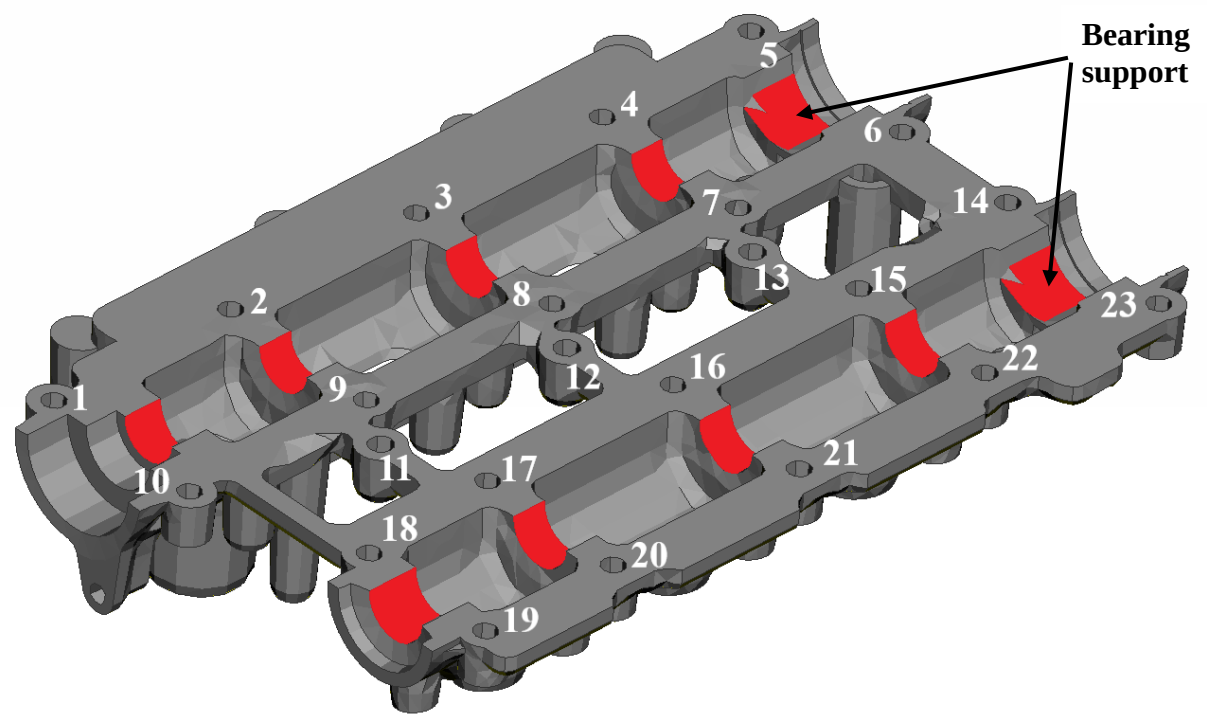

Figure 82. Cam cover A bolt locations and bearing support

6.2. Cam cover B

Cam cover B is connected with 15 bolts to the cylinder head.

6.2.1. Simplifying of excitation

After averaging the acceleration levels at all bolt locations, simplified excitations can be defined. Averaged accelerations and their trendlines in direction of three translational DOFs are shown in Figure 83, Figure 84 and Figure 85.

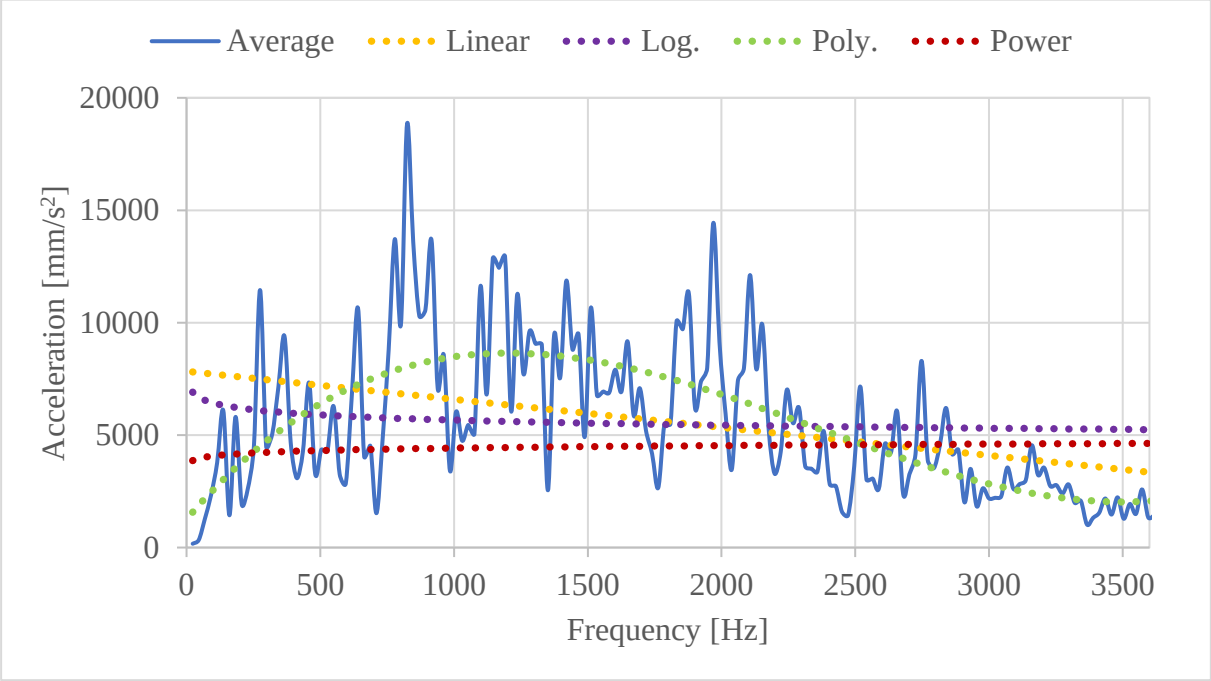

Figure 83. Averaged acceleration and trendlines in direction of DOF 1

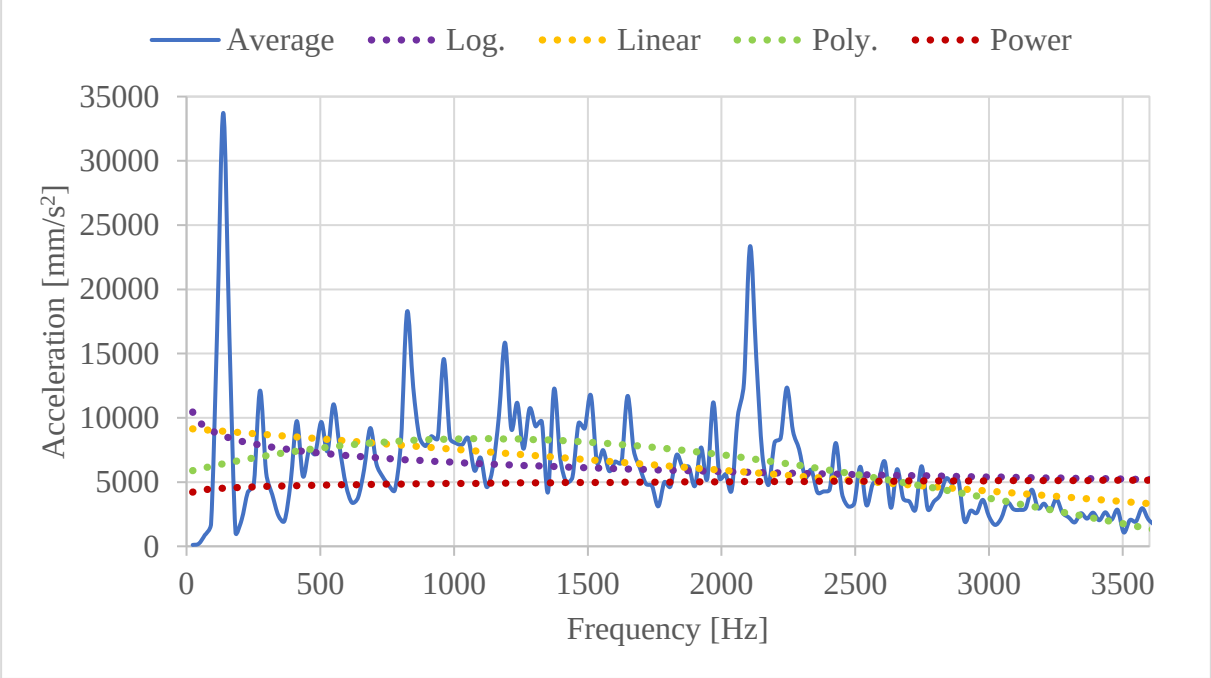

Figure 84. Averaged acceleration and trendlines in direction of DOF 2

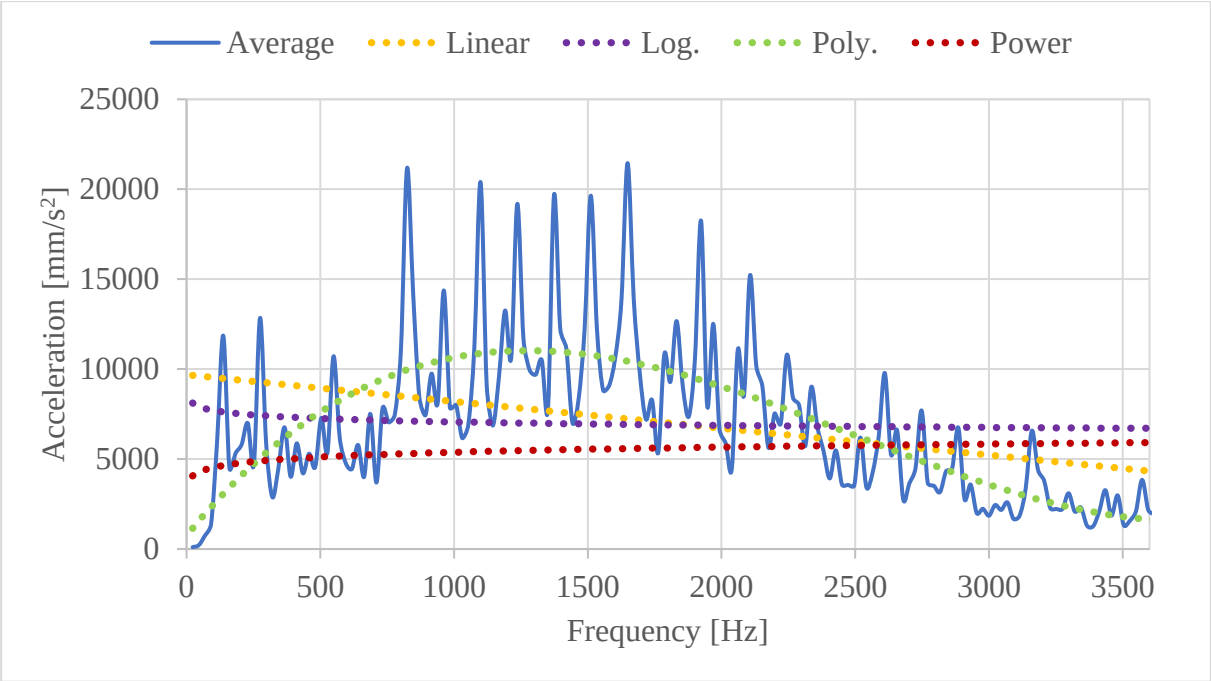

Figure 85. Averaged acceleration and trendlines in direction of DOF 3

6.2.1.1. Averaged excitation

As before, the first step is to excite the cam cover with the averaged excitation. Response to the averaged excitation shows acceptable results in all 3rd octave bands according to Figure 86 and Table 27.

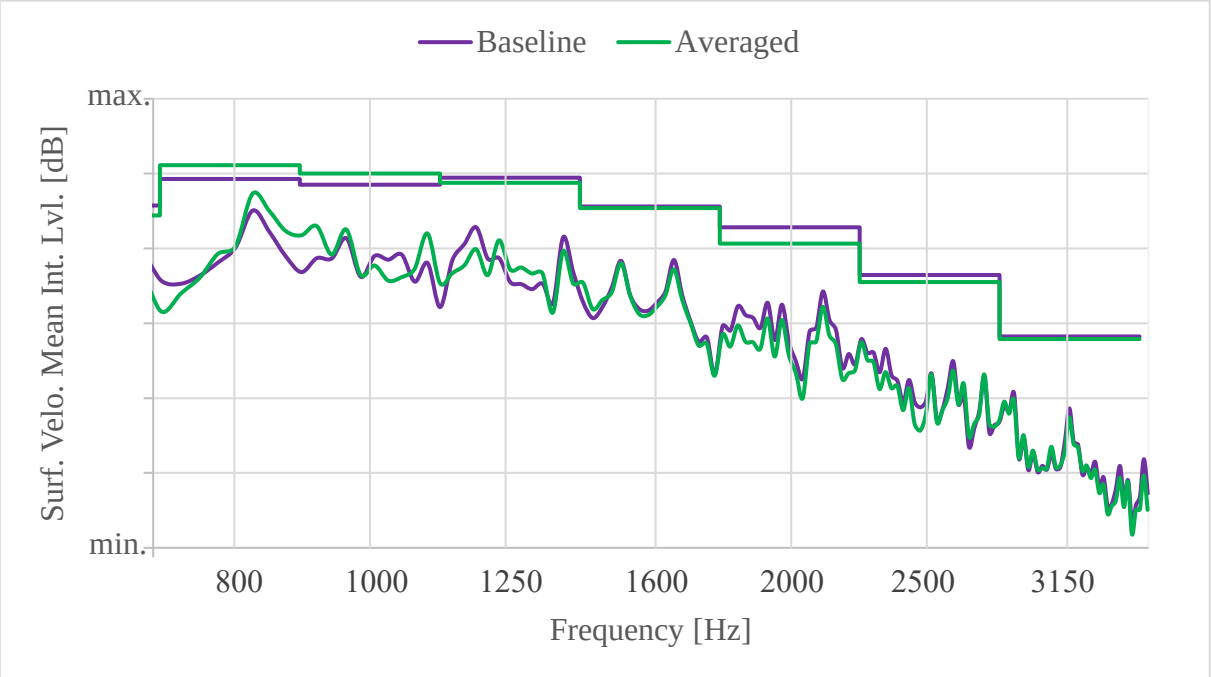

Figure 86. Structure response comparison between baseline and averaged excitation

Table 27. Absolute difference of structure response between baseline and averaged excitation

3rd octave band [Hz]	Difference in Surf. Velo. Mean Int. Lvl. [dB]
800	1.9
1000	1.5
1250	0.7
1600	0.2
2000	2.2
2500	0.9
3150	0.3

6.2.1.2. Linear excitation

Figure 87 shows that response to the linear excitation is lower in some 3rd octave bands than the baseline.

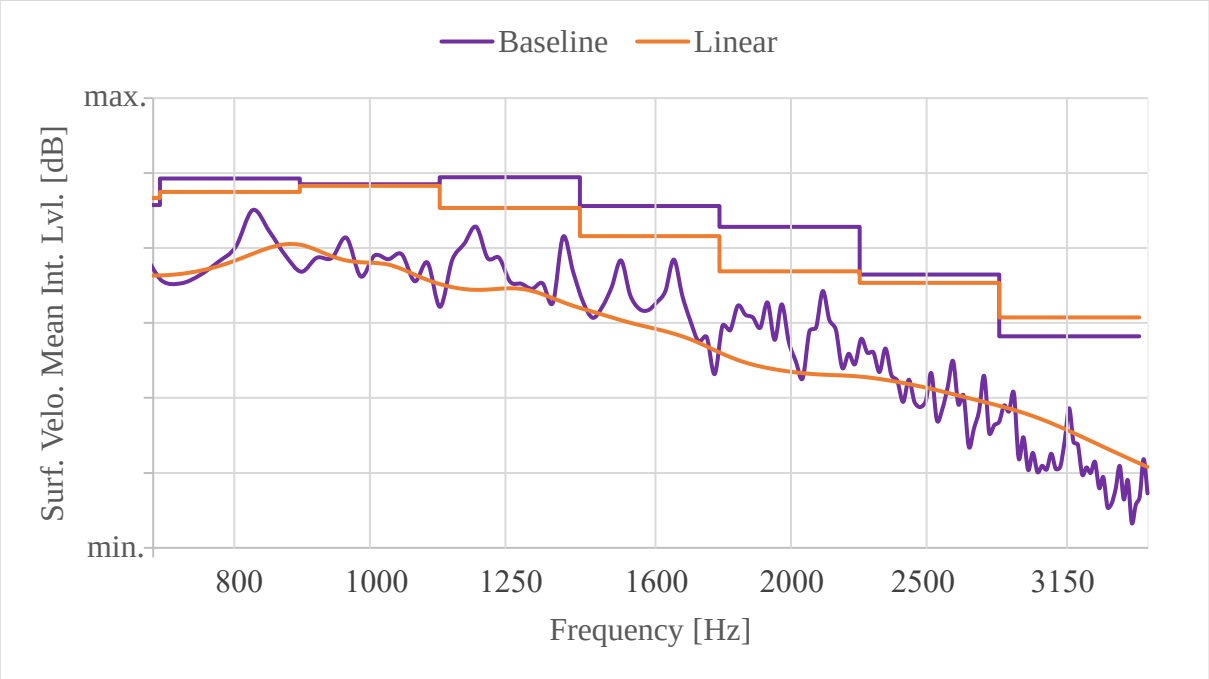

Figure 87. Structure response comparison between baseline and linear excitation

According to Table 28, structure response in one 3rd octave band is marked as not acceptable and in two as borderline. This is the result of the poor linearization, the same as with the component intake manifold C. Based on the Figure 83, Figure 84 and Figure 85, one can see that linear trendline does not describe well the averaged excitation in DOFs 1 and 3.

Table 28. Absolute difference of structure response between baseline and linear excitation

3rd octave band [Hz]	Difference in Surf. Velo. Mean Int. Lvl. [dB]
800	1.8
1000	0.2
1250	4.1
1600	4.0
2000	5.9
2500	1.1
3150	2.5

6.3. Cam cover C

Cam cover C is characterized by the similar design as the cam cover B, but it is connected to the cylinder head with 13 bolts.

6.3.1. Simplifying of excitation

6.3.1.1. Averaged excitation

According to the Table 29, there is almost zero difference in structure response in form of surface velocity mean integral level between baseline and averaged excitation at higher frequencies.

Table 29. Absolute difference of structure response between baseline and averaged excitation

3rd octave band [Hz]	Difference in Surf. Velo. Mean Int. Lvl. [dB]
800	2.7
1000	2.3
1250	0.1
1600	0.2
2000	0.2
2500	0.2
3150	0.2

6.3.1.2. Linear excitation

Structure response to the linear excitation is mostly acceptable in observed 3rd octave bands, it is only marked as borderline in 3rd octave band 1600 Hz, as shown in the Table 30.

Table 30. Absolute difference of structure response between baseline and linear excitation

3rd octave band [Hz]	Difference in Surf. Velo. Mean Int. Lvl. [dB]
800	2.6
1000	0.4
1250	3.3
1600	4.1
2000	3.0
2500	0.1
3150	3.5

6.4. Conclusion

Based on the surface velocity mean integral level evaluation, it can be concluded that with the proper simplification of the averaged excitation, structure response could be acceptable. Cam cover B has a problem with the poor linearization of the averaged excitation curve. When examined averaged excitation curve, one can notice that there could be defined trendlines better than linear.

Based on the surface velocity plots (cannot be shown) it can be concluded that cam cover should be attached to the cylinder head to correctly describe the structure response. Furthermore, cam cover is characterized by the large flat surfaces which could have tendency to generate monopole sources. This results in higher noise radiation. Uncertainties can especially occur at the side walls. Misleading monopole sources appear there causing the wrong impression. By attaching the cam cover to the cylinder head, misleading monopole sources weaken and the overall result is better.

7. CONCLUSION

The objective of this Thesis was to find a method to predict the NVH behaviour of the engine components at the very early stage of the engine development to reduce development time and costs.

The study was conducted for three engines (engines A, B and C) with the same configuration - inline 3-cylinder turbocharged gasoline engines. Three engine components (intake, oil pan and cam cover) were analyzed in mid and high frequency domain that includes frequencies from 708 Hz to 3548 Hz (from 3rd octave band 800 Hz to 3rd octave band 3150 Hz). There was a difference in engine core design and characteristics, but also in bolt number, bolt location and design between the studied components.

The mentioned boundary conditions used in this Thesis were in form of an enforced motion, i. e. acceleration. Therefore, the accelerations in frequency domain were applied as an excitation at the bolt locations of the studied components in the forced frequency response analysis (Nastran SOL 111). The applied accelerations represented the response at the bolt locations in *Excite Power Unit* simulation when gas pressure, inertia, timing drive and valve train forces were acting.

Although the three very similar engines were studied, it was noticed that the acceleration levels, generated at the bolt locations of the studied components, vary a lot from engine to engine. That was the consequence of the difference in the gas cylinder pressure forces, the unbalanced bending moments (due to inertia forces) because of different engine design and observed rated speed. When comparing the three studied engines, there was also the inconsistency in the behaviour of the engine A due to its testbed configuration (no transmission). Furthermore, engine C has higher gas cylinder pressure forces, inertia forces and rated speed, and consequently higher acceleration levels at the bolt locations than the engine B.

Timing drive and valve train forces significantly contributed to the overall response at higher frequencies (>2000 Hz) as well. Therefore, the difference in timing drive and valve train design should be kept in mind.

The first step of the analysis was to excite the studied components with the average value of the acceleration (only magnitude) at all bolt locations in direction of translational degrees of freedom. The next step was to generate simplified excitations from averaged acceleration values. After that, obtained simplified excitations were applied on the observed components and the structure response was evaluated. Finally, considering the accuracy of the results and the complexity of the curve, a linear excitation was specified as the most acceptable.

All the following calculations were conducted with the linear excitation. At the end, a comparison between linear and white noise excitation was examined.

Before the results evaluation, a difference in linear excitation levels must be understood. Figures 88, 89 and 90 show the difference in excitation levels between studied components. It can be observed that excitation levels significantly depend on the engine. As mentioned before, engine C components have higher excitation levels at the bolt locations than engine B components.

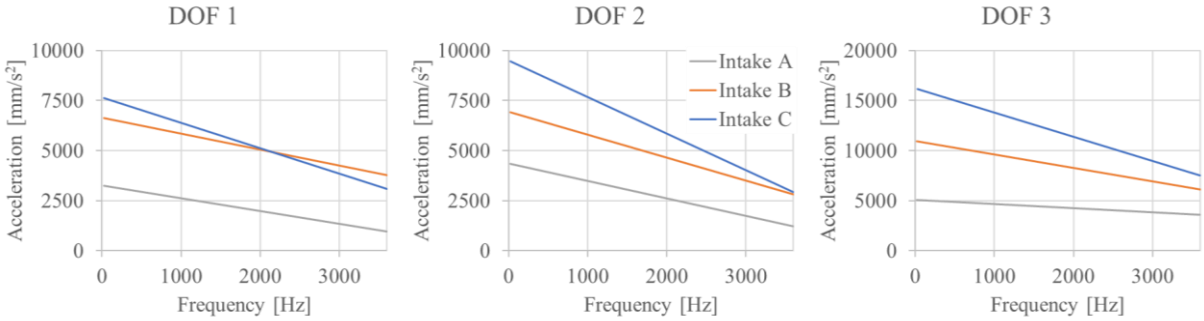

Figure 88. Difference in excitation levels between intake manifolds

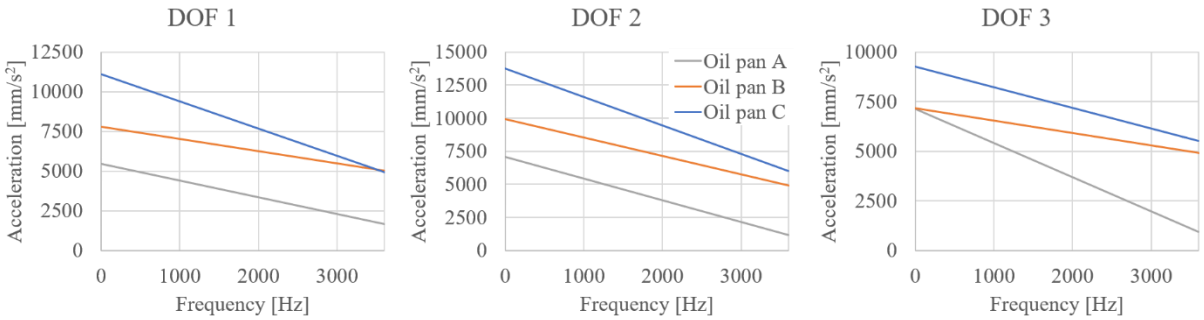

Figure 89. Difference in excitation levels between oil pans

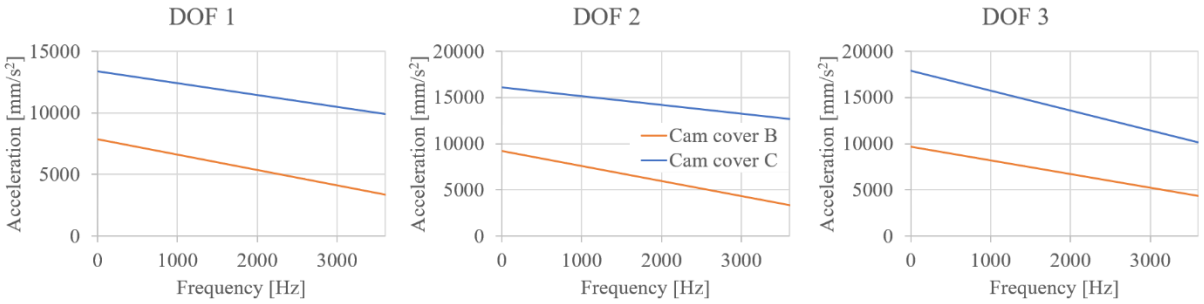

Figure 90. Difference in excitation levels between cam covers

There are three different conclusions for the three studied components:

- First studied component was intake manifold A. When examining the averaged excitation, it was noticed that it varies with more or less constant amplitude. Therefore, a linearization of the complex excitation curve could be successfully conducted. This study showed that it is possible to excite a component with a simple excitation, but still obtain an acceptable result. On the other hand, structure response of the intake manifold B to the simplified linear excitation was defined as not acceptable. Since the structure response to the averaged excitation was not acceptable as well, it could be concluded that the structure response of the intake manifold B, could not be assumed. The reason for that was the design of the intake manifold B and location of the bolts. Design of the intake manifold C was similar to the design of the intake manifold A and structure response was acceptable with the averaged excitation. However, the linearization of the averaged excitation could not be successfully conducted because averaged excitation had high peaks over the part of the frequency range. Consequently, linear trendline did not cover that range well and an underestimated excitation was generated.
  Therefore, the established method was not successful for the intake analysis in general. However, the study has shown that it depends on the excitation curve behaviour and a component design. With the right combination of the mentioned parameters, this method would be efficient. In order to find the corresponding limitations, further analysis should be carried out.

- Oil pans A, B and C are very important structural parts of the engine since they are connected to the engine bottom end and bell housing (gearbox). Furthermore, forces are well transmitted through the bolts to the oil pan. NVH performance of the oil pans A, B and C was very similar. When studying the acceleration magnitude levels at the bolt locations, it was revealed that there is a big difference in the acceleration magnitude from bolt to bolt. Oil pan was first excited with a simple linear excitation (linear approximation of the average acceleration magnitude levels at bolt locations in each DOF), but it did not yield an acceptable deviation level. Attaching the oil pan to the full engine assembly, in order to increase the stiffness, also did not result in significant improvements. Once the excitation in the form of a complex number was applied, the results significantly improved. In so defined excitation, phase of the excitation was included. When phase was included, directions of the applied load were correctly

described which resulted in more accurate structure response. This type of excitation could not be simplified since it oscillates around x-axis. Therefore, it is not possible to find a simple excitation to predict the NVH behaviour of the oil pan.

- Cam cover analysis was carried out only for cam covers B and C. Due to the difference in material and design, cam cover A was not analyzed. To be specific, cam cover A is a structural part due to integrated camshaft bearing support.

  As well as before, the structure response of a cam cover to an averaged and linear excitation was observed. Both studied cam covers (B and C) showed similar NVH behaviour. Misleading monopole sources were generated at the side walls. Consequently, shape of the vibrations was significantly different when compared with the baseline model. Once the cam covers were coupled to the cylinder head, the misleading monopole were eliminated and the structure response deviation level decreased. Furthermore, it was noticed that linear excitation could not generate acceptable results in all observed 3rd octave bands due to the poor linearization of the averaged excitation. Since the structural response was acceptable with the averaged excitation, it could be expected that with better description of the averaged curve, more acceptable results could be obtained. This could be probably achieved with the polynomial curve.

  Therefore, this method could successfully determine the NVH behaviour of the cam cover at the beginning of the development, but different excitation curves should be used.

As mentioned before, the final step of this study was to compare the observed excitations with the white noise excitation. As expected, the white noise excitation generated higher deviation levels of the structure response than other studied excitation types for all observed components. White noise excitation is characterized with the constant excitation level over the whole frequency range, i.e. it is not frequency dependent. All other excitation types consider the change of the dynamic excitation level with frequency hence generating more realistic results.

All things considered, the established method could not correctly describe the NVH behaviour of engine components in advance. The study has shown that it could work with plastic components which are coupled to a stiff engine area, but not with the structural

components like the oil pan. Although, it should be always taken with caution because even very similar engines could have a great difference in the NVH performance.

At the end, recommendations for the future studies will be shortly given for each studied component separately. First, it should be noticed that this study was conducted only for three-cylinder engines. Therefore, the first step should be to extend this study to the four-cylinder engines to see the impact of engine configuration on the NVH behaviour of the engine components.

Analysis of the intake manifold should be focused on very similar design of the intake manifolds and different excitation types (polynomial excitation) should be considered as well.

On the other hand, there are no further recommendations for the analysis of the oil pan since it is not possible to obtain acceptable results by simplifying the excitations.

Finally, cam cover could be characterized as the most promising component for the assessment of the NVH behaviour at the early stages of design. Therefore, different excitation types (polynomial excitation) should be considered to achieve more acceptable results.

LITERATURE

[1] Beloiu, D., "Modeling and Analysis of Powertrain NVH", SAE Technical Paper, 2012.

[2] Lee, N., Park, W., Ruotolo, R., and Trombley, D., " NVH Development of EU5 2.0L and 2.2L Diesel Engine", SAE Technical Paper, 2011.

[3] Wang, X., "Target setting and benchmarking for vehicle noise and vibration refinement", *Vehicle Noise and Vibration Refinement*, Woodhead Publishing Limited, 2010, pp. 18–29.

[4] Xin, Q., "Noise, vibration, and harshness (NVH) in diesel engine system design", *Diesel Engine System Design*, Woodhead Publishing Limited, 2013, pp. 759–821.

[5] Barton, D. C., and Fieldhouse, J., D., *Automotive Chassis Engineering*, Springer International Publishing, 2018

[6] Querengässer, J., Meyer, J., Wolschendorf, J., and Nehl, J., "NVH Optimization of an In-Line 4-Cylinder Powertrain", SAE Technical Paper, 1995.

[7] Vorwerk C., Busch G., Kaiser H.-J., Wilhelm M., "Influence of Bottom End Design on Engine Noise and Vibration Behavior of 4-Cylinder Inline Gasoline Engines", SAE Technical Paper, 1993.

[8] Brandl, S., Graf, B., and Rust, A., "NVH Challenges and Solutions for Vehicles with Low CO_2 Emission", SAE Int. J. Passeng. Cars - Mech. Syst., 2012.

[9] Baillie, D. C., "Noise and vibration refinement of powertrain systems in vehicles", *Vehicle Noise and Vibration Refinement*, Woodhead Publishing Limited, 2010, pp. 252–285.

[10] Hoag, K., and Dondlinger, B., "Block and Head Development", *Vehicular Engine Design*, Springer Vienna, 2016, pp. 177-191

[11] Mahalec, I., Lulić, Z. and Kozarac, D., "Konstrukcije motora", interna skripta, FSB Zagreb, 2015.

[12] Hoag, K., and Dondlinger, B., "Engine Configuration and Balance", *Vehicular Engine Design*, Springer Viena, 2016, pp. 69-95.

[13] Sandalci, T., "Balancing of Masses in the Reciprocating-Piston Engine", Yildiz Technical University, 2002.

[14] Küntscher, V., "Kraftzeugmotoren – Auslegung und Konstruktion", Berlin, 1987.

[15] Harrison, Matthew, *Vehicle Refinement: controlling noise and vibration in road vehicles*, 2004.

[16] Yerges, L. F., "Acoustical materials", Academic Press, 1970.

[17] Saha, P., "Developing Vehicle Sound Packages", SAE Technical Paper, 2011.

[18] https://www.eea.europa.eu/data-and-maps/indicators/transport-emissions-of-greenhouse-gases/transport-emissions-of-greenhouse-gases-11, European Environment Agency, page visited on April 3rd, 2019.

[19] Downsizing Powertrains – webinar, Siemens AG, 2017

[20] *MSC Nastran*, User's Guide

APPENDIX 1

MSC Nastran Input File for performing Forced Frequency Response Analysis

```
SOL 111
$
CEND
$
TITLE=Excite FEA Dynamic Response Analysis
SUBTITLE=Job: intake_analysis
$
METHOD=103
DLOAD=111
FREQUENCY=122
SDAMPING=144
SPC=777
VELOCITY(SORT1,PLOT,PHASE)=ALL
$
BEGIN BULK
$
PARAM,DDRMM,-1
PARAM,POST,-1
PARAM,GRDPNT,0
PARAM,PRGPST,NO
PARAM,MAXRATIO,1.E8
$
INCLUDE 'mesh_intake.bdf'
$
SPC1        100  123456 5000401
SPC1        100  123456 5000402
SPC1        100  123456 5000403
SPC1        100  123456 5000404
SPC1        100  123456 5000405
SPC1        100  123456 5000406
$Anonymous LOAD SET
SPCD        1001 5000401      1     1.
SPCD        1001 5000402      1     1.
SPCD        1001 5000403      1     1.
SPCD        1001 5000404      1     1.
SPCD        1001 5000405      1     1.
SPCD        1001 5000406      1     1.
$Anonymous LOAD SET
SPCD        1002 5000401      2     1.
SPCD        1002 5000402      2     1.
SPCD        1002 5000403      2     1.
SPCD        1002 5000404      2     1.
SPCD        1002 5000405      2     1.
SPCD        1002 5000406      2     1.
$Anonymous LOAD SET
SPCD        1003 5000401      3     1.
```

```
SPCD       1003 5000402      3     1.
SPCD       1003 5000403      3     1.
SPCD       1003 5000404      3     1.
SPCD       1003 5000405      3     1.
SPCD       1003 5000406      3     1.
$
$Anonymous SPC SET
SPCADD      777     100
$
$Anonymous DLOAD SET
DLOAD       111     1.     1.    1001     1.    1002     1.    1003
$
$Anonymous DLOAD SET
RLOAD1      1001    1001                1            3
$Anonymous DLOAD SET
RLOAD1      1002    1002                2            3
$Anonymous DLOAD SET
RLOAD1      1003    1003                3            3
$
$TABLED  Card
TABLED1       1LINEAR  LINEAR
+           0.   2115.  10000.   2115.ENDT
$
$TABLED  Card
TABLED1       2LINEAR  LINEAR
+           0.   2769.  10000.   2769.ENDT
$
$TABLED  Card
TABLED1       3LINEAR  LINEAR
+           0.   4317.  10000.   4317.ENDT
$
$ Modal Damping:
TABDMP1      144CRIT
+           40.   0.193     50.   0.155    100.   0.079    150.   0.055
+          200.   0.043    250.   0.037    300.   0.033    350.    0.03
+          400.   0.028    450.   0.027    500.   0.027    650.   0.027
+          800.   0.028   1000.   0.031   1250.   0.035   1500.    0.04
+         1750.   0.045   2000.    0.05   2500.   0.061   3000.   0.072
+         3150.   0.075   3300.   0.078   3600.    0.08ENDT
$
FREQ        122 20.93   1506.88 3557.91
$METHOD  Card
EIGRL       103          4000.             0              MASS
ENDDATA
```

APPENDIX 2

I. CD – R disc